MAR 20070005: OLD FORT BAY

Received date: Mar 26, 2007

Public release date: Jun 03, 2008

DISCLAIMER

By accessing and using the Alberta Energy website to download or otherwise obtain a scanned mineral assessment report, you (“User”) agree to be bound by the following terms and conditions:

a) Each scanned mineral assessment report that is downloaded or otherwise obtained from Alberta Energy is provided “AS IS”, with no warranties or representations of any kind whatsoever from Her Majesty the Queen in Right of Alberta, as represented by the Minister of Energy (“Minister”), expressed or implied, including, but not limited to, no warranties or other representations from the Minister, regarding the content, accuracy, reliability, use or results from the use of or the integrity, completeness, quality or legibility of each such scanned mineral assessment report;

b) To the fullest extent permitted by applicable laws, the Minister hereby expressly disclaims, and is released from, liability and responsibility for all warranties and conditions, expressed or implied, in relation to each scanned mineral assessment report shown or displayed on the Alberta Energy website including but not limited to warranties as to the satisfactory quality of or the fitness of the scanned mineral assessment report for a particular purpose and warranties as to the non-infringement or other non-violation of the proprietary rights held by any third party in respect of the scanned mineral assessment report;

c) To the fullest extent permitted by applicable law, the Minister, and the Minister’s employees and agents, exclude and disclaim liability to the User for losses and damages of whatsoever nature and howsoever arising including, without limitation, any direct, indirect, special, consequential, punitive or incidental damages, loss of use, loss of data, loss caused by a virus, loss of income or profit, claims of third parties, even if Alberta Energy have been advised of the possibility of such damages or losses, arising out of or in connection with the use of the Alberta Energy website, including the accessing or downloading of the scanned mineral assessment report and the use for any purpose of the scanned mineral assessment report so downloaded or retrieved.

d) User agrees to indemnify and hold harmless the Minister, and the Minister’s employees and agents against and from any and all third party claims, losses, liabilities, demands, actions or proceedings related to the downloading, distribution, transmissions, storage, redistribution, reproduction or exploitation of each scanned mineral assessment report obtained by the User from Alberta Energy.

Alberta Mineral Assessment Reporting System

MAR 26 2007
20070005

PART B
(TECHNICAL INFORMATION)

AND

PART C
(SUPPORTING APPENDICES)

ASSESSMENT REPORT

OLD FORT BAY PROPERTY
ALBERTA

TRIEX MINERALS CORP., ROUGHRIDER URANIUM CORP. & BROCKINGTON
Metallic and Industrial Minerals Permit Nos. 9305010842 to 9305010851

Prepared for
TRIEX MINERALS CORPORATION

Submitted by
Ross McElroy, B.Sc., P. Geol

March 22, 2007

TABLE OF CONTENTS

PART B – TECHNICAL INFORMATION

Page

1. SUMMARY 1

2. INTRODUCTION 4

3. BREAKDOWN STATEMENT OF PROJECT WORK 5

4. PROPERTY LOCATION AND ACCESS 6

5. REGIONAL GEOLOGY 6

6. EXPLORATION HISTORY 7

7. 2004 EXPLORATION PROGRAM 8
   7.1 Airborne Magnetic and Electromagnetic Survey 8
   7.2 Processing of MEGATEM Data 11

8. CONCLUSIONS AND RECCOMENDATIONS 11

9. QUALIFICATIONS 12

10. REFERENCES 13

List of Tables

Table 1: Airborne Survey Line-Kilometers and Cost Breakdown per Permit 9

List of Figures

Figure 1: Old Fort Bay Property – Regional Location Map 2

Figure 2: Old Fort Bay Property – Property Scale Location Map 3

Figure 3: Old Fort Bay Property – Regional Geology Map 7

Figure 4: Old Fort Bay Property – Airborne MEGATEM Flight Lines 10

PART C – SUPPORTING APPENDICES

List of Appendices

Appendix 1	List of Field Contractors
Appendix 2	Logistics and Processing Report, Airborne Magnetic and MEGATEM Survey, Old Fort Bay Property, Fort McMurray, Alberta Job No. 00430, Triex Minerals Corp. and Roughrider Uranium Corp.
Appendix 3	1:50,000 Scale Maps From Airborne Magnetic and MEGATEM Survey: Map 1 – Flight Path Map 2 – Residual Magnetic Intensity Map 3 – First Vertical Derivative of the Residual Magnetic Intensity Map 4 – Apparent Conductance derived from dB/dt X and Z Coils Map 5 – 3rd Order Moment derived from B Field X and Z Coils Map 6 – Decay Constant (Tau) derived from B Field Z Coil Channels 12-20 Map 7 – Basic EM Interpretation Map
Appendix 4	Report on Processing of MEGATEM II 90 Hz Data, Old Fort Bay Property, NE Alberta, Triex Minerals Corporation, April 2006
Appendix 5	1:50,000 Scale Maps From Processing of MEGATEM II 90 Hz Data: Map 8 – TMI Map 9 – 1st Vertical Derivative of TMI Map 10 – EM Bfield Z Ch 8 amplitude Map 11 – AdTau Bfield Z (cut-off 1,000 fT) Map 12 – DTM
Appendix 6	Summary Interpretation of Time Domain Electromagnetic Data from a Fugro MEGATEM Survey Carried Out During the Period October 20 and November 12, 2004 on Permits 9305010842 through 9305010851 in the Western Athabasca Basin Region, Saskatchewan NTS 74 L/9, & 16
Appendix 7	1:50,000 Scale Maps from Interpretex Resources Ltd. Map 13 - Stacked Fugro Conductivity Depth Transforms Map 14 - Residual Magnetic Intensity Contours & Interpretation Map 15 - First Vertical Derivative of Residual Magnetic Intensity Map 16 - Tilt Derivative of RMI & Interpretation Map 17 - Flight Path, Permits and Interpretation Map

1. SUMMARY

The Old Fort Bay property is located in the NE region of the province of Alberta, Canada, located approximately 250 km NNE of the city of Fort McMurray, Alberta (see Figure 1). The permits falls on NTS map sheet 74L/9 and 74L/16. The property consists of 10 contiguous prospecting permits with an area of 87,040 hectares (see Figure 2). Under a joint venture agreement, Triex Minerals Corp. holds 51% interest and Roughrider Uranium Corp. holds 25% interest in the property and 24% is held by a private investor. Triex is the operator of the project and the permit title holder.

The occurrences of the Maybelle River uranium deposit approximately 50 km to the southwest in Alberta and the Cluff Lake uranium mine (former producer) 35 km to the south-east in Saskatchewan, has promoted interest in exploring for uranium on the Old Fort Bay property.

A property scale airborne magnetic and electromagnetic (EM) survey conducted by Fugro Airborne Surveys was flown in the fall of 2004. The purpose of the survey was to obtain information about the subsurface magnetic and conductive environment within the permits, that may reflect zones of significant alteration and mineralization within bedrock at or near the basement rock interface. A total of 2,924 line-kilometers of data were collected using a Dash 7 modified aircraft. Flight lines were flown to just beyond the permit boundaries, thus a total of 2,572.4 line-kilometers were flown within the permit boundaries. Assessment work and costs reported reflects the cost of 2,572.4 line-kilometers of survey. In the "Statement of Intent to File" submitted on January 23, 2007 it was stated that the total airborne survey represented 3,062 line-kilometers of data with 2,572.4 line-kilometres within the permit boundaries, but Fugro Airborne Surveys report states that the total line-kilometers is 2,924. This correction is reflected in this assessment report.

Details of the logistics and processing of data of the airborne magnetic and electromagnetic survey can be found in Section 7.1 - Airborne Magnetic and Electromagnetic Survey and in Appendix 2 (back of report). Folded 1:50,000 scale maps of results can be found in Appendix 3 (back of report).

In April of 2006, further processing of selected portions of the airborne EM survey was conducted by Condor Consulting Inc. A total of 911 line-km including 29 EW traverse lines and 7 NS tie lines were processed. Details of the processing of EM data can be found in Section 7.2 - Processing of MEGATEM Data and in Appendix 4 (back of report). Folded 1:50,000 scale maps of results can be found in Appendix 5 (back of report).

A synthesis of the interpretation of results authored by Edwin Rockel (Interpretex Resources Ltd.) for both the Fugro and Condor processing of the airborne data, can be found in Appendix 6 (back of report). Folded 1:50,000 scale maps of results can be found in Appendix 7 (back of report).

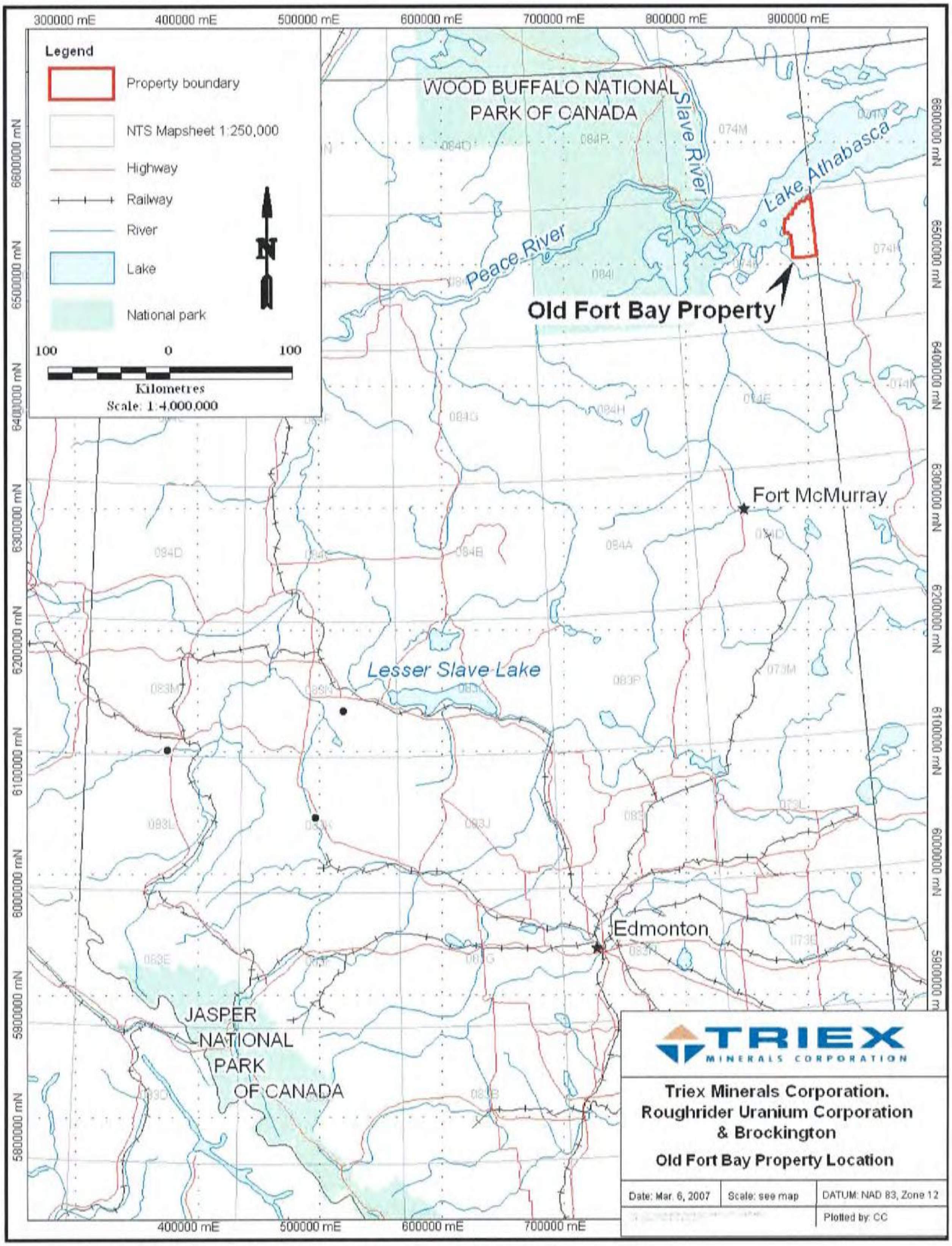

Figure 1: Old Fort Bay Property – Regional Location Map

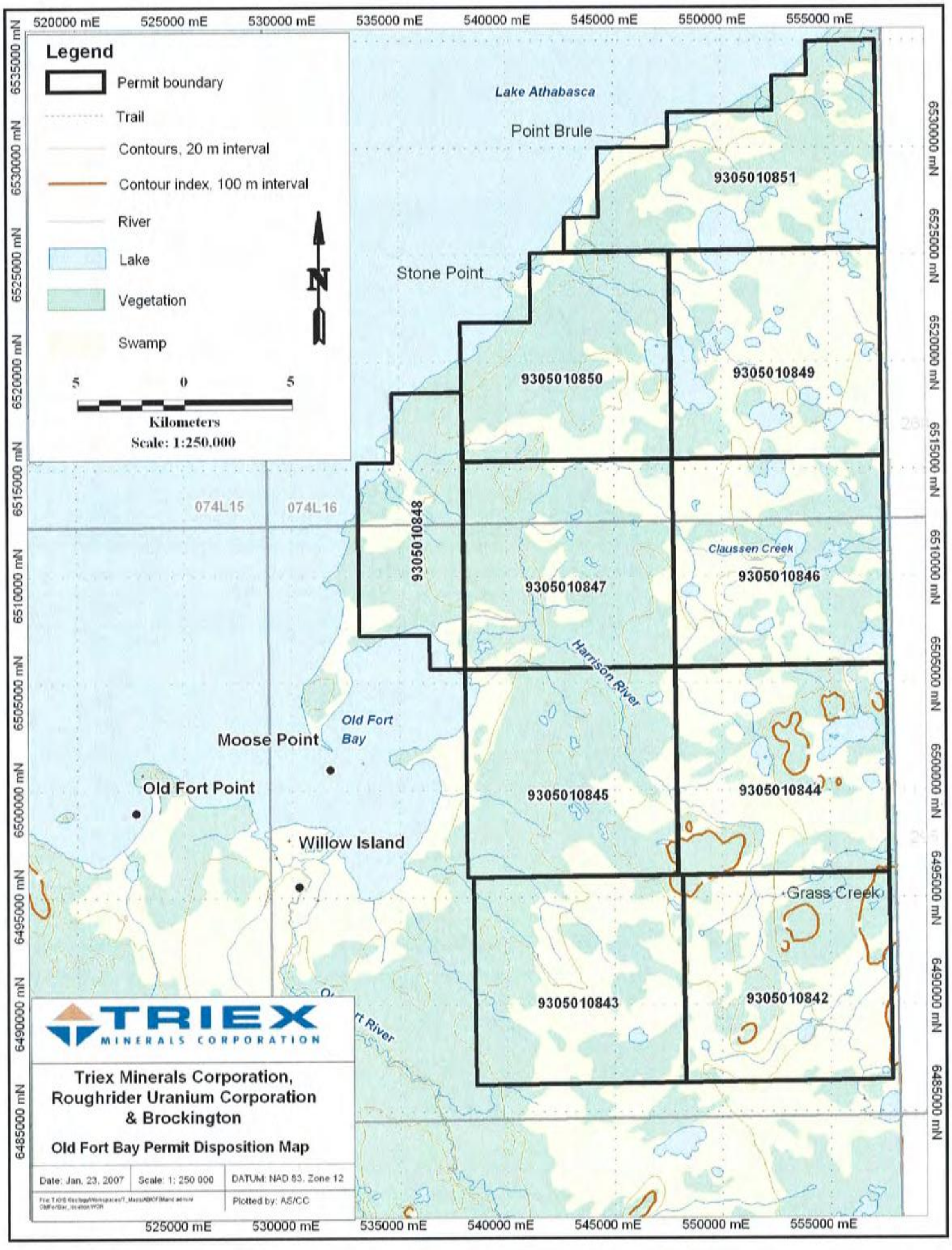

Figure 2: Old Fort Bay Property – Property Scale Location Map

2. INTRODUCTION

This report is a summary of the 2004 airborne magnetic and electromagnetic survey flown by Fugro Airborne Surveys and the subsequent processing of portions of the electromagnetic data by Condor Consulting Inc. that were conducted on the Old Fort Bay property on behalf of the Triex Minerals Corp., Roughrider Uranium Corporation and Brockington joint venture. Triex Minerals Corp. is the operator of the joint venture. The 2004 survey was conducted between October 20 and November 12, 2004. The data processing work by Condor Consulting Inc. was carried out during April 2006. Interpretation of the results of the airborne survey has been done by Edwin Rockel of Interpretex Resources Ltd.

The Fugro Airborne Survey's trademark name for the type of magnetic and EM survey conducted with this particular equipment is referred to as MEGATEM or MEGATEM II. This equipment is a time domain EM system. Under ideal circumstances, Fugro claims MEGATEM to be capable of measuring the magnetic and electromagnetic signatures of rocks that are buried at depths up to at least 1000m. This significantly deep penetrating system is well suited for properties such as Old Fort Bay, where the depth to basement rocks are overlain by > 800m glacial overburden and Athabasca Formation sediment.

The general target for searching for uranium mineralization in the Athabasca basin is at or near the unconformity between the Athabasca Formation sediment, and the underlying basement rocks. It is the complex relationship of differing chemistry between the different rock groups at the unconformity, and fluid flow control mechanisms (pathways and traps) that are responsible for the precipitation and accumulation of uranium at or near the unconformity interface. In order to look for targets of potential mineralization, it is an important step to map out the geology by means of magnetics and electromagnetic surveys. These surveys help to identify the nature of the hidden geology with respect to lithology, alteration and structure. The purpose of the survey was to obtain information about the subsurface magnetic and conductive environment within the permits, that may reflect zones of significant alteration and mineralization within bedrock at or near the basement rock interface.

3. BREAKDOWN STATEMENT OF PROJECT WORK

	Amount Spent
1. Prospecting	$
2. Geological Mapping & Petrography	$
3. Geophysical Surveys	
a. Airborne	$ 392,150.28
b. Ground	$
4. Geochemical Surveys	$
5. Trenching and Stripping	$
6. Drilling	$
7. Assaying and Whole Rock Analysis	$
8. Other Work	$
Subtotal	$ 392,150.28
9. Administration (10% of subtotal)	$ 40,693.43
Total	$ 432,843.71
[redacted]	Mar 22, 2007
SIGNATURE	**DATE**
Ross McElroy	
PRINT NAME	

4. PROPERTY LOCATION AND ACCESS

The Old Fort Bay property is located in the NE of Alberta, Canada. The property is centered approximately 250 km NE of the city of Fort McMurray, AB and 600km NE of ? the city of Alberta, AB (Figure 1). The Metallic and Industrial Minerals Permits Nos. 9305010842 to 9305010851 which constitute the property are located on NTS map 74/L. The property is centered approximately 50km northeast of the Maybelle River uranium deposit of Alberta and approximately 35km northwest of the Cluff Lake uranium mine (past producer) in Saskatchewan.

The Old Fort Bay property is accessible year-round by float and/or ski-equipped aircraft from Fort McMurray, Alberta. Fuel and supplies can be transported by air from Fort McMurray directly to the property. To date, Triex has not operated a program which necessitated transporting supplies to the Old Fort Bay property. The 2004 airborne magnetic and EM survey was operated out of Fort McMurray. The aircraft flew from Fort McMurray to the property daily, and returned at the end of each survey day. Figure 2 shows the Old Fort Bay Property with individual permit boundaries at 1:250,000 scale.

5. REGIONAL GEOLOGY

The Old Fort Bay property is situated in the north-west region of the Athabasca sedimentary basin. The Athabasca basin is dated as late Proterozoic in age and is comprised of sedimentary rocks; dominantly sandstones, with occasional silt and mudstones intervals. The sedimentary rocks which comprise the Athabasca basin in the Old Fort Bay project area are generally low angle to horizontally layered stratigraphy which unconformably overlies older, steeply dipping metamorphic rocks of the Rae Province. It is believed that the western continuation of the Grease River Shear Zone, a crustal-scale structural splay off the Snowbird Tectonic Zone in northern Saskatchewan, continues on to the Old Fort Bay property (see Figure 3).

It is the relationship at or near the interface between the Athabasca sediments and the underlying basement rocks that are considered to be important in creating a structural and geochemical trap which focuses the uranium mineralization as observed in most of the major uranium deposits of the Athabasca basin. Such is the case at the Maybelle River uranium deposit where the Maybelle River basement conductor is related to the graphitic mylonite that transects the granitoid gneiss along the east side of the Maybelle River mineralized trend, and also includes brittle structures (Jefferson et. al., 2002).

Generally, the sedimentary rocks of the Athabasca formations are clean, quartz-rich meta-arkoses and lesser amounts of siltstone and mudstone layers of varying thickness. Rocks of the Athabasca Formation group in the Old Fort bay area consist of the Wolverine Point Formation and the Manitou Falls Formations (MFd, MFc, MFb and MFa). The Wolverine Point Formation is a very well sorted, clay-rich, fine to medium grained sandstone with minor siltstone and mudstone (*Yeo, Jeffereson and Ramaekers,* *2002*), which can reach thickness >50m. Rocks of the Manitou Falls Formations randge from fine grained to very coarse grained and pebbly and conglomeratic sandstone. Airborne magnetic and EM surveys such as the MEGATEM survey flown over the Old Fort Bay property can be used to effectively interpret and map the underlying lithology and structural features.

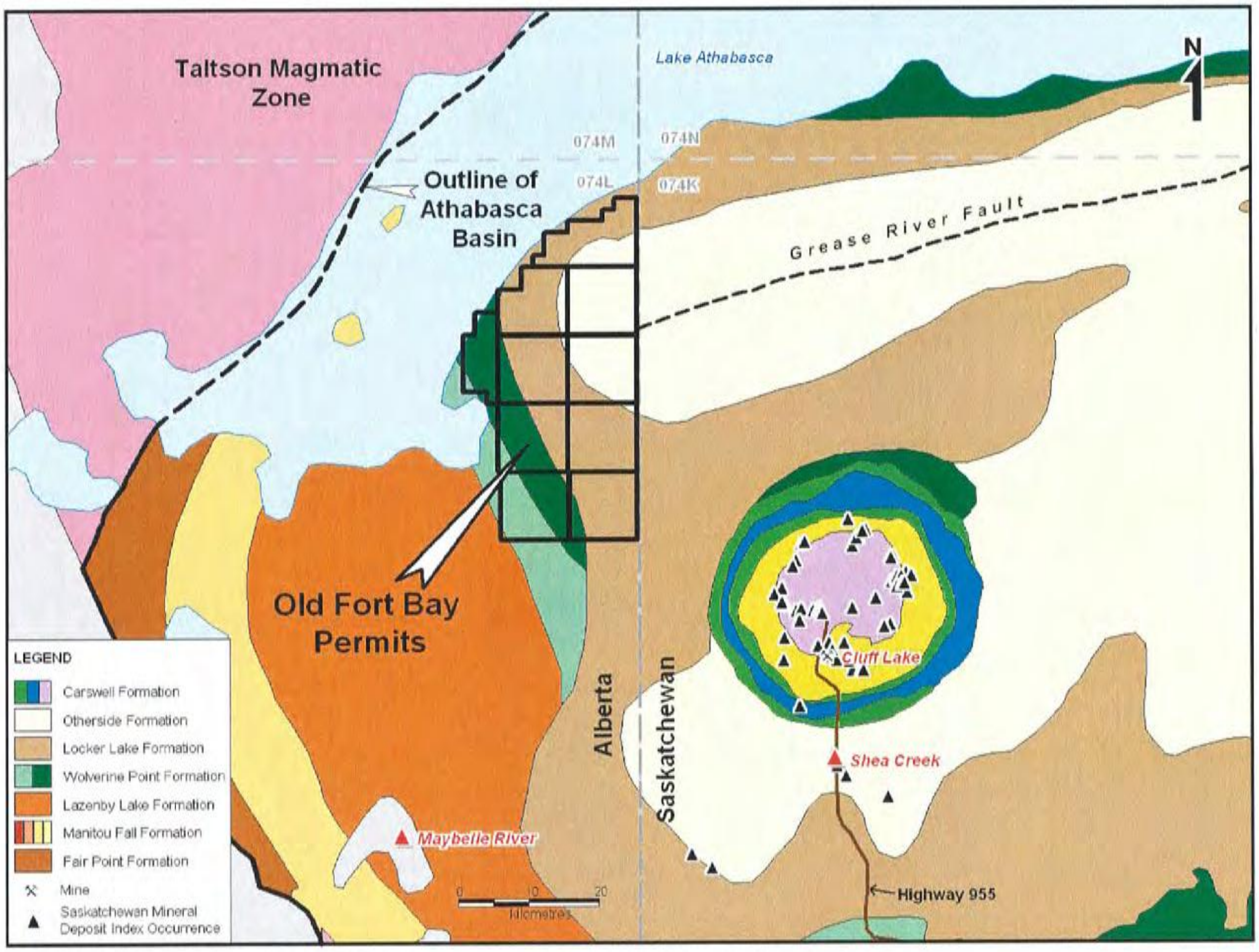

Figure 3: Old Fort Bay Property – Regional Geology Map

6. EXPLORATION HISTORY

Several companies, including Esso Minerals, explored the property in the 1970's. Reconnaissance-style lake water and lake sediment surveys, soil samples, and seismic and gravity surveys were completed in 1977. Data was integrated with regional airborne magnetic data to identify targets. A total of nine drill holes were completed in successive programs in 1978 and 1979; designated as AGS ID (Alberta Geological Survey) FC-002 to FC-008 inclusive and FC-068 and FC-069. A cluster of 5 holes were drilled in the northeast area of the property (FC-002, 003, 004, 005 and 006). Holes FC-007 and FC-008 were drilled in the northwest area of the property. Hole FC-068 was drilled in the south-west area of the property and FC-069 was drilled in the east-central east area of the property. The collar locations of the historic drill holes are shown on the 1:50,000 scale maps included in Appendix 7. The historic holes mentioned in Condor Consulting Inc's. report (Appendix 4, pp. 3 and 4) refers to drill holes with a different ID, but apparently similar geographical locations. With respect to the holes mentioned in Condor's report, an assumption is made by this author, that the northern holes 78-ALJV-002 and 004 are part of the cluster of holes with AGS ID from FC-001 through 006 (at the northern area boundary) and that hole 08-78-2 is the same as AGS hole FC-069. Hole 08-78-2 (i.e. FC-069) is in the east-central part of the current property holding and was terminated prior to reaching the unconformity because of excessive caving. It targets a strong east-west feature on both magnetic and gravity maps which is believed to be the western terminus of the Grease River Shear Zone. Holes 78-LAJV-002 and 004 (i.e. part of the cluster of holes with AGS ID of FC-002 to FC-006) are at the north end of the current property, near the south shore of Lake Athabasca, and are believed to have intersected the south-western extent of the Black Bay Shear Zone (Mineral Assessment Report 19780006), a major crustal feature that anchors mineral deposits in the Uranium City camp on the north shore of the lake. Core in Hole 004 is heavily fractured, and there is an east-west, multi-element soil anomaly associated with the surface projection of the fault. Basement samples from Hole 002 at the unconformity are graphitic, chlorite-altered, and strongly sheared. Regolith at the unconformity is up to 6 meters thick and strongly hematitic. Core assays contain up to 292 ppm uranium and 0.08 oz/ton gold, as well as being enriched in nickel, zinc and silver. A 1982 publication by the Geological Survey of Canada (paper 81-20) discusses the positive mineral potential of the area based on the results from this historical drilling. In all holes drilled in this area, a thick, horizontal stratified sequence of silt and mudstone was encountered. This silt-mudstone is likely part of the Wolverine Formation within the Athabasca group stratigraphy.

7. 2004 EXPLORATION PROGRAM

Exploration efforts by Triex Minerals, since the granting of the permits in late 2004, have focussed on indirectly mapping the geology by way of geophysical surveys. These surveys measure the magnetic characteristics of the geology and allow for the recognition of EM conductors, potentially associated with uranium, on the property. The work that has been performed thus far on the Old Fort Bay property includes an airborne magnetic and electromagnetic survey (Fugro Airborne Surveys) and processing of the data (Fugro and Condor Consulting Inc.) and an interpretation of the data (Interpretex Resources Ltd).

7.1 Airborne Magnetic and Electromagnetic Survey

From October 20th to November 12th, 2004 Fugro Airborne Surveys conducted a MEGATEM electromagnetic and magnetic survey of the Old Fort Bay property on behalf of Triex Minerals Corp. A total of 2,924 line-kilometres of data were collected using a Dash 7 modified aircraft. A total of 123 traverse lines at 400m line-spacing were flown on east-west oriented lines, and 12 north-south oriented tie-lines were flown at 2000m line-spacing (see Figure 4). The survey covered the entire property. As the traverse and tie lines extended slightly beyond the permit boundaries, a total of 2,572.4 of the 2,924 line-kilometres flown, can be attributed to the assessment spending on the permits. Table 1 shows the breakdown of line-kilometers flown on each permit.

Table 1: Airborne Survey Line-Kilometers and Cost Breakdown per Permit

Old Fort Bay - MEGATEM Survey

Permit	Line km	% of Survey Cost	Reportable Expenditure	% for Permit Costs
9305010842	271	9.3%	$ 39,996.63	10.5%
9305010843	274.9	9.4%	$ 40,572.23	10.7%
9305010844	273.2	9.3%	$ 40,321.33	10.6%
9305010845	278.3	9.5%	$ 41,074.03	10.8%
9305010846	262.7	9.0%	$ 38,771.65	10.2%
9305010847	282.6	9.7%	$ 41,708.67	11.0%
9305010848	124.2	4.2%	$ 18,330.56	4.8%
9305010849	280.2	9.6%	$ 41,354.45	10.9%
9305010850	251.5	8.6%	$ 37,118.65	9.8%
9305010851	273.8	9.4%	$ 40,409.88	10.6%
Total Line km inside permits	**2572.4**	**88.0%**	**$ 379,658.09**	**100.0%**
Total Line km outside permits	**351.6**	**12.0%**	**$ 51,892.31**	
Total Survey	**2924.0**	**100.0%**	**$ 431,550.40**	
Total Survey Cost	$ 431,550.40			

The purpose of the survey was to obtain information about the subsurface magnetic and conductive environment within the permits, that may reflect zones of significant alteration and mineralization within bedrock at or near the basement rock interface. The MEGATEM system is a time-domain towed-bird electromagnetic system incorporating a high-speed digital EM receiver. The operation of a towed-bird time-domain electromagnetic system involves the measurement of decaying secondary electromagnetic fields induced by a series of sort current pulses generated from an aircraft mounted transmitter. Variations in the decay characteristics of the secondary field are analyzed and interpreted to provide information about the subsurface geology. Such a system can provide excellent sensitivity for mapping very resistive features and very conductive features, and thus mapping geology. This method also offers very good discrimination of conductor geometry. Refer to Appendix 2, Section – Appendix A of the Fugro Airborne Surveys report for more detailed information about the MEGATEM system.

A detailed report of the logistics and processing of the airborne survey is included in Appendix 2. A series of seven 1:50,000 scale maps were produced by Fugro Airborne Surveys based on the results of the survey. These maps are folded and are included in Appendix 3 of this report.

Interpretex Resources Ltd. (Edwin Rockel) has provided a report on the Summary Interpretation of Time Domain Electromagnetic Data from the airborne survey and is included in Appendix 6. A series of five 1:50,000 scale maps were produced by Interpretex based on interpretation of the airborne survey data. These maps are folded and are included in Appendix 7 of this report.

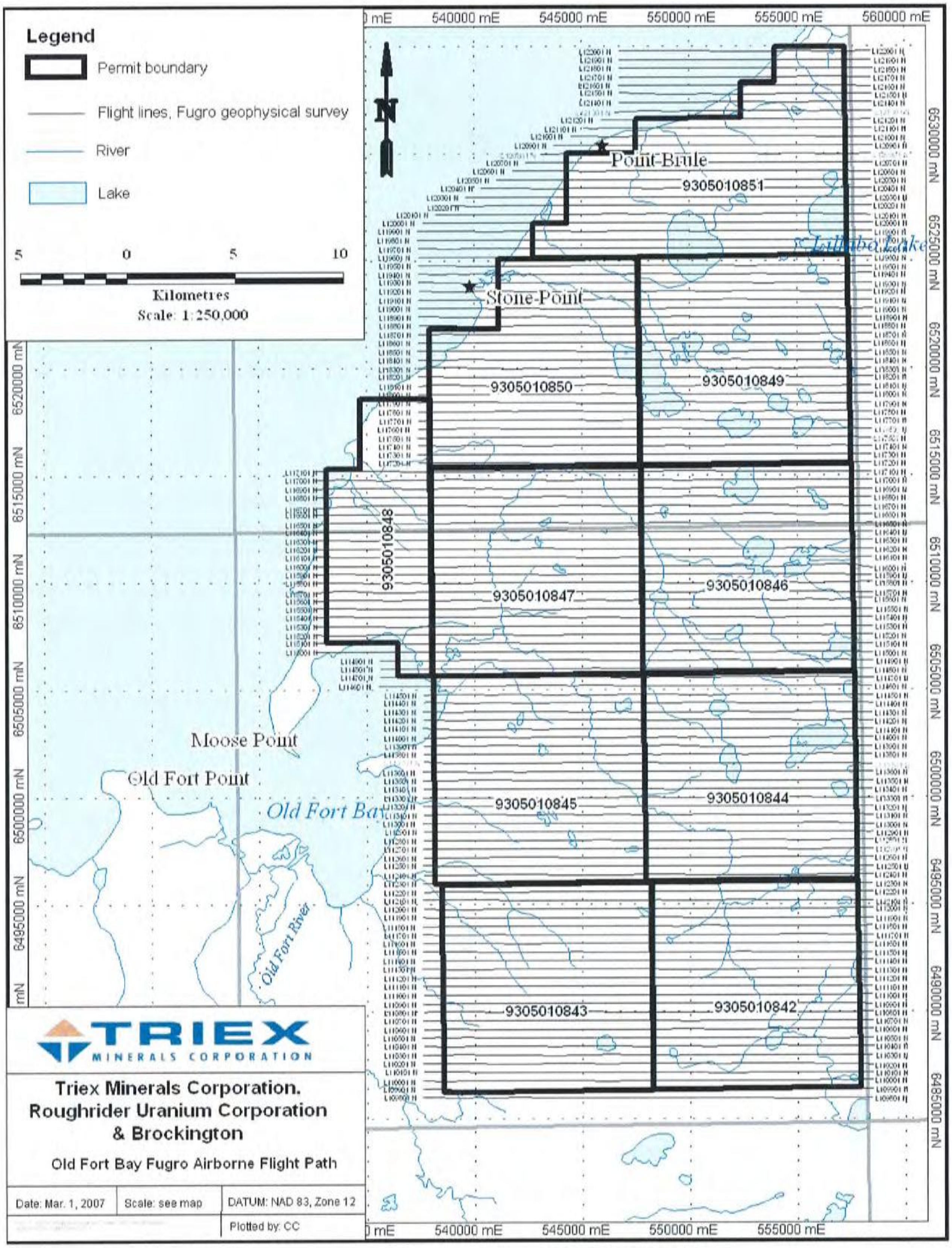

Figure 4: Old Fort Bay Property – Airborne MEGATEM Flight Lines

7.2 Processing of MEGATEM Data

In an effort to extract more information out of the data using a different point of view, Condor Consultants Inc. were contracted to re-process some of the 2004 airborne survey data, however no interpretation of the results was provided. Results of the Condor re-processing were similar to Fugro's work. A total of 911 line-km including 29 EW traverse lines and 7 NS tie lines were re-processed.

A report on the processing of the electromagnetic data by Condor Consultants Inc. is included in Appendix 4 at the back of this report. A series of five 1:50,000 scale maps were produced based on the lines that were examined. These maps are folded and are included in Appendix 5 at the back of this report.

8. CONCLUSIONS AND RECCOMENDATIONS

Based on historical drilling three conclusions can be suggested: 1) a "strong east-west magnetic feature" (central-east part of the area) remains unexplained. 2) the graphite, alteration and uranium mineralization which all occur at the bottom of deep hole 78-LAJV-002 (cluster of holes with AGS ID FC-002 to FC-006) near the northern area boundary are apparently associated with faults or shear zones and 3) the multi-element soil anomaly associated with the surface projection of the fault suggests that some faults may continue to near surface and may have a near surface geochemical and then perhaps a geophysical signature. Thus the "strong east-west magnetic feature", possibly related to the extension of the deep Grease River Fault structure, is still prospective and if other structural features can be predicted, they may also be targets for deep exploration for uranium mineralization.

Neither Fugro's nor Condor's manipulations of the 2004 airborne magnetic and electromagnetic survey data resulted in specific conductors being defined that were considered to be related to deep basement graphitic faults. However, it is suspected that the thick sequence of silt and clay-stones encountered in these historic drill holes (probably relating to the Wolverine Point Formation) significantly constrained the ability of the electromagnetic survey to penetrate >800m to reach the basement. The inability of the EM survey to see through to the basement does not lessen the potential for this area to host an accumulation of uranium.

Based on the previously flown MEGATEM airborne geophysical electromagnetic survey flown in 2004, further work is warranted on the Old Fort Bay Property. Future work here will likely include deep penetrating ground geophysical surveys such as a magnetotelluric (MT) survey over areas deemed strategically important, such as the possible extension of the Grease River Shear Zone. It is expected that a MT survey would be able to "see through" the thick Wolverine Point Formation siltstone, and thus help to evaluate the basement geology and provide guidance for targeting future drill holes.

To advance the property, it is recommended that a ground magnetotelluric geophysical survey be conducted in 2007. A drill program targeting high priority areas such as those along the Grease River Fault trend in the central part of the property, and around the interesting geochemical anomalies identified in the north end of the property, should be considered for 2008.

9. QUALIFICATIONS

STATEMENT OF QUALIFICATIONS – ROSS E. MCELROY

I, Ross E. McElroy, of P.O. Box 11584, 1410 – 640 West Georgia St., Vancouver, V6B 4N8 in the Province of British Columbia, do hereby certify:

a) I am presently employed as Exploration Manager by Triex Minerals Corp., 1410 – 650 West Georgia St., Vancouver, BC, V6B 4N8

b) I am a graduate of the University of Alberta, Edmonton, Alberta, with a B.Sc. in Geology (1987). I have been employed in the mineral exploration and mining industry since 1987 and have practiced my profession since graduation. I am a registered licensee with the Association of Professional Engineers and Geoscientists of Saskatchewan, the Association of Professional Engineers, Geologists and Geophysicists of the Northwest Territories and the Association of Professional Engineers, Geologists and Geophysicists of Alberta.

c) I have not visited the subject property

d) I am responsible for the presentation and compilation of all sections of this report

e) I have been involved with the property since 2005

ROSS E. McELROY

Dated "March 22, 2007"
R.E. McElroy, P. Geol

Signed "*Ross McElroy*"

10. REFERENCES

Jefferson, C.W., Delaney, G., Olson, R.A., 2002; *EXTECH IV Athabasca Uranium Multidisciplinary Study: Mid-year 2002-03 Overview and Impact Analysis;* Saskatchewan Geological Survey, Summary of Investigations 2002, Volume 2: pp. 1-7.

Nelson, W.E., 1978; *Mineral Assessment Report 19780006 Report on the Lake Athabasca Joint Venture Diamond Drilling, Geophysics and Geochemistry Program, June to October 1978, Permits 219-233;* Golden Eagle Oil and Gas Ltd.

Tremblay, L.P., 1982; *Geology of the Uranium Deposit Related to the Sub-Athabasca Unconformity, Saskatchewan;* Geological Survey of Canada, Paper 81-20.

Yeo, G., Jefferson, C.W., Ramaekers, P.,; *A Preliminary Comparison of Manitou Falls Formation Stratigraphy in Four Athabasca Basin Deposystems;* Saskatchewan Geological Survey, Summary of Investigations 2002, Volume 2

PART C
(SUPPORTING APPENDICES)

APPENDIX 1

List of Field Contractors

OLD FORT BAY PROPERTY, ALBERTA

PROJECT NAME:	Old Fort Bay
LOCATION:	South-West Lake Athabasca Area, Alberta (Metallic and Industrial Minerals Permit Nos. 9305010842 to 9305010851)
FIELD WORK:	October 20th to November 12th, 2004
ACCOMMODATIONS:	Fort McMurray, Alberta
TRANSPORTATION:	Dash 7 modified aircraft

LIST OF CONTRACTORS

Fugro Airborne Surveys
2060 Walkley Road
Ottawa, ON
K1G 3P5
- Airborne Magnetic and MEGATEM Survey

Condor Consulting
Lakewood, CO
USA
- Processing of MEGATEM II 90 Hz Data

Interpretex Resources Ltd.
13000 54A Avenue
Surrey, BC
- Interpretation of Results of MEGATEM Survey and Condor Consulting's Processing of Data

APPENDIX 2

Logistics and Processing Report, Airborne Magnetic and MEGATEM Survey, Old Fort Bay Property, Fort McMurray, Alberta Job No. 00430, Triex Minerals Corp. and Roughrider Uranium Corp.

Fugro Airborne Surveys

LOGISTICS AND PROCESSING REPORT

Airborne Magnetic and MEGATEM® Survey

Old Fort Bay Property

Fort McMurray, Alberta

Job No. 04430

Triex Minerals Corp. and Roughrider Uranium Corp.

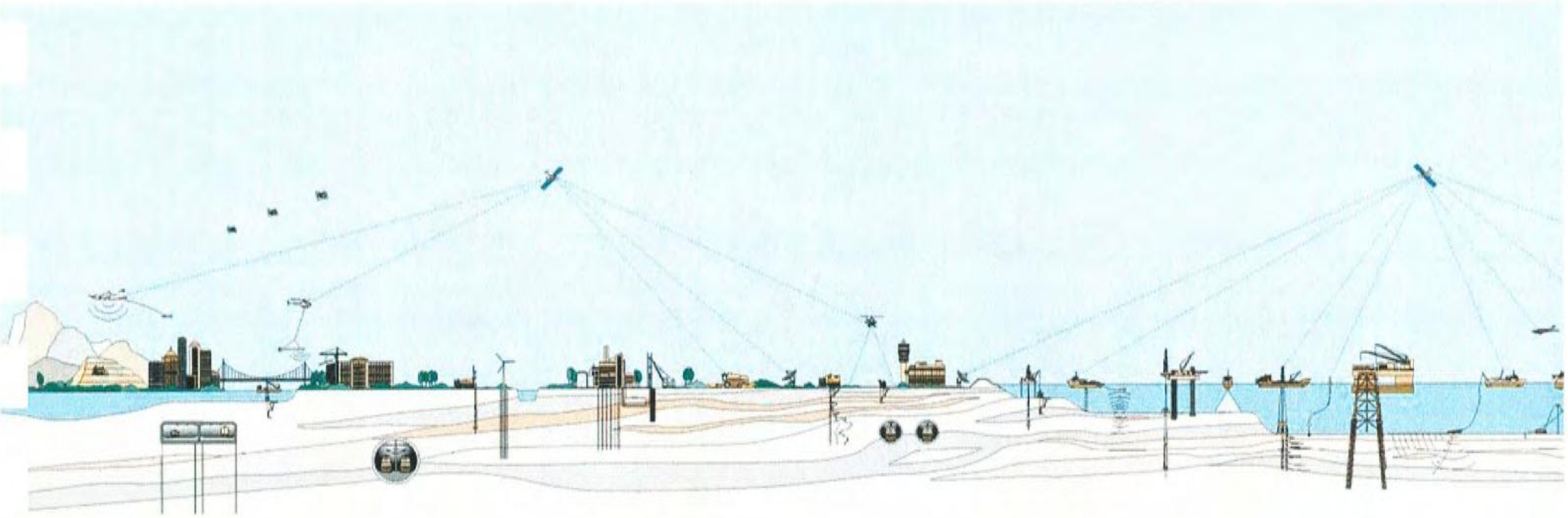

LOGISTICS AND PROCESSING REPORT
AIRBORNE MAGNETIC AND MEGATEM® SURVEY
OLD FORT BAY PROPERTY
FORT MCMURRAY, ALBERTA

JOB NO. 04430

Client : Tirex Minerals Corp.
1410-650 West Georgia St.
Vancouver, BC
V6B 4N8

Date of Report : January, 2005

TABLE OF CONTENTS

INTRODUCTION **5**

SURVEY OPERATIONS **6**

- Location of the Survey Area 6
- Aircraft and Geophysical On-Board Equipment 7
- Base Station Equipment 10
- Field Office Equipment 10
- Survey Specifications 10
- Field Crew 11
- Production Statistics 11

QUALITY CONTROL AND COMPILATION PROCEDURES **12**

DATA PROCESSING **13**

- Flight Path Recovery 13
- Altitude Data 13
- Base Station Diurnal Magnetics 13
- Airborne Magnetics 13
  - *Residual Magnetic Intensity* *14*
  - *Magnetic First Vertical Derivative* *14*
- Electromagnetics 14
  - *dB/dt data* *14*
  - *B-field data* *15*
  - *Coil Oscillation Correction* *16*
  - *Apparent Conductance* *17*
  - *Moments of the Impulse Response* *17*
  - *Decay Constant (TAU)* *18*
  - *Conductivity-Depth-Transforms (CDT)* *18*

FINAL PRODUCTS **19**

- Digital Archives 19
- Maps 19
- Profile Plots 19
- Report 19

APPENDICES

A GEOTEM® ELECTROMAGNETIC SYSTEM

B GEOTEM® INTERPRETATION

C MULTICOMPONENT GEOTEM® MODELLING

D THE USEFULNESS OF MULTICOMPONENT, TIME-DOMAIN AIRBORNE ELECTROMAGNETIC MEASUREMENTS

E DATA ARCHIVE DESCRIPTION

F MAP PRODUCT GRIDS

I

Introduction

Between October 20th and November 12th, 2004 Fugro Airborne Surveys conducted a MEGATEM® electromagnetic and magnetic survey of the Old Fort Bay Property on behalf of Triex Minerals Corp. and Roughrider Uranium Corp. Using Fort McMurray, Alberta as the base of operations, a total of 2924 line kilometres of data was collected using a Dash 7 modified aircraft (Figure 1).

The survey data were processed and compiled in the Fugro Airborne Surveys Ottawa office. The collected and processed data are presented on colour or black and white maps, and multi-parameter profiles. The following maps were produced: Flight Path, Residual Magnetic Intensity (RMI), First Vertical Derivative of RMI, Apparent Conductance, 3rd Order Moment of B Field X and Z Coils, and Decay Constant derived from B Field Z Coil Channels 12-20. In addition, digital archives of the raw and processed survey data in line format, and gridded EM data were delivered.

Figure 1: Specially modified Dash-7 aircraft used by Fugro Airborne Surveys.

II

Survey Operations

Location of the Survey Area

The Old Fort Property (Figure 2) was flown with Fort McMurray, Alberta as the base of operations. A total of 123 traverse lines were flown, with a spacing of 400 m between lines, and 12 tie lines were flown with a spacing of 2000 m between tie-lines totalling 2924 kms in the complete survey.

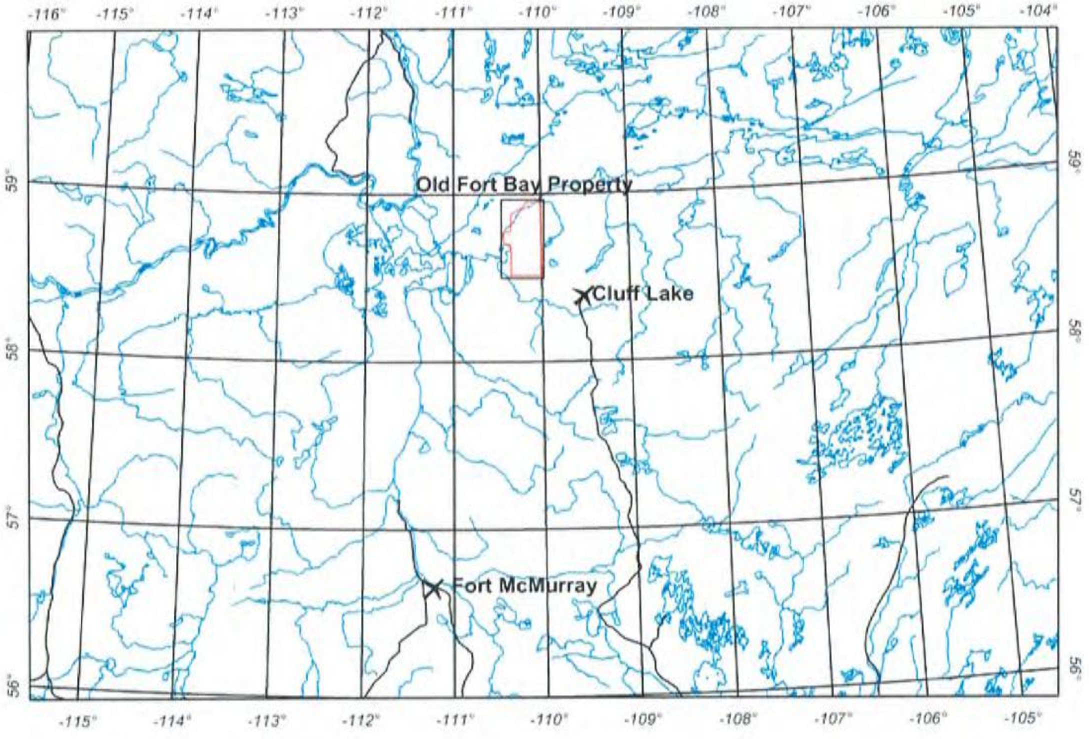

Figure 2: Survey area location.

Aircraft and Geophysical On-Board Equipment

Figure 3: EM receiver bird.

Aircraft: DeHavilland DHC-7-102 Dash-7

Operator: FUGRO AIRBORNE SURVEYS

Registration: C-GJPI

Survey Speed: 125 knots / 145 mph / 70 m/s

Magnetometer: Scintrex Cs-2 single cell cesium vapour, towed-bird installation, sensitivity = 0.01 nT[1], sampling rate = 0.1 s, ambient range 20,000 to 100,000 nT. The general noise envelope was kept below 0.5 nT. The nominal sensor height was ~73 m above ground.

Electromagnetic system: MEGATEM® 20 channel Multicoil System

Transmitter: Vertical axis loop mounted on aircraft of 406 m^2

Number of turns: 6

Nominal height above ground of 120 m

Receiver: Multicoil system (x, y and z) with a final recording rate of 4 samples/second, for the recording of 20 channels of x, y and z-coil data. The nominal height above ground is ~70 m, placed ~130 m behind the centre of the transmitter loop.

Base frequency: 90 Hz

Pulse width: 2287 µs

Pulse delay: 100 µs

Off-time: 3169 µs

Point value: 43.4 µs

Transmitter Current: 641 A

Dipole moment: 1.56x10^6Am^2

Figure 4: Modified Dash-7 in flight.

---

[1] One nanotesla (nT) is the S.I. equivalent of one gamma.

Table 1: Electromagnetic Data Windows.

Channel	Start (p)	End (p)	Width (p)	Start (ms)	End (ms)	Width (ms)	Mid (ms)
1	4	11	8	0.130	0.477	0.347	0.304
2	12	25	14	0.477	1.085	0.608	0.781
3	26	39	14	1.085	1.693	0.608	1.389
4	40	53	14	1.693	2.300	0.608	1.997
5	54	59	6	2.300	2.561	0.260	2.431
6	60	61	2	2.561	2.648	0.087	2.604
7	62	64	3	2.648	2.778	0.130	2.713
8	65	67	3	2.778	2.908	0.130	2.843
9	68	71	4	2.908	3.082	0.174	2.995
10	72	75	4	3.082	3.255	0.174	3.168
11	76	79	4	3.255	3.429	0.174	3.342
12	80	83	4	3.429	3.602	0.174	3.516
13	84	87	4	3.602	3.776	0.174	3.689
14	88	92	5	3.776	3.993	0.217	3.885
15	93	97	5	3.993	4.210	0.217	4.102
16	98	102	5	4.210	4.427	0.217	4.319
17	103	108	6	4.427	4.688	0.260	4.557
18	109	114	6	4.688	4.948	0.260	4.818
19	115	121	7	4.948	5.252	0.304	5.100
20	122	128	7	5.252	5.556	0.304	5.404

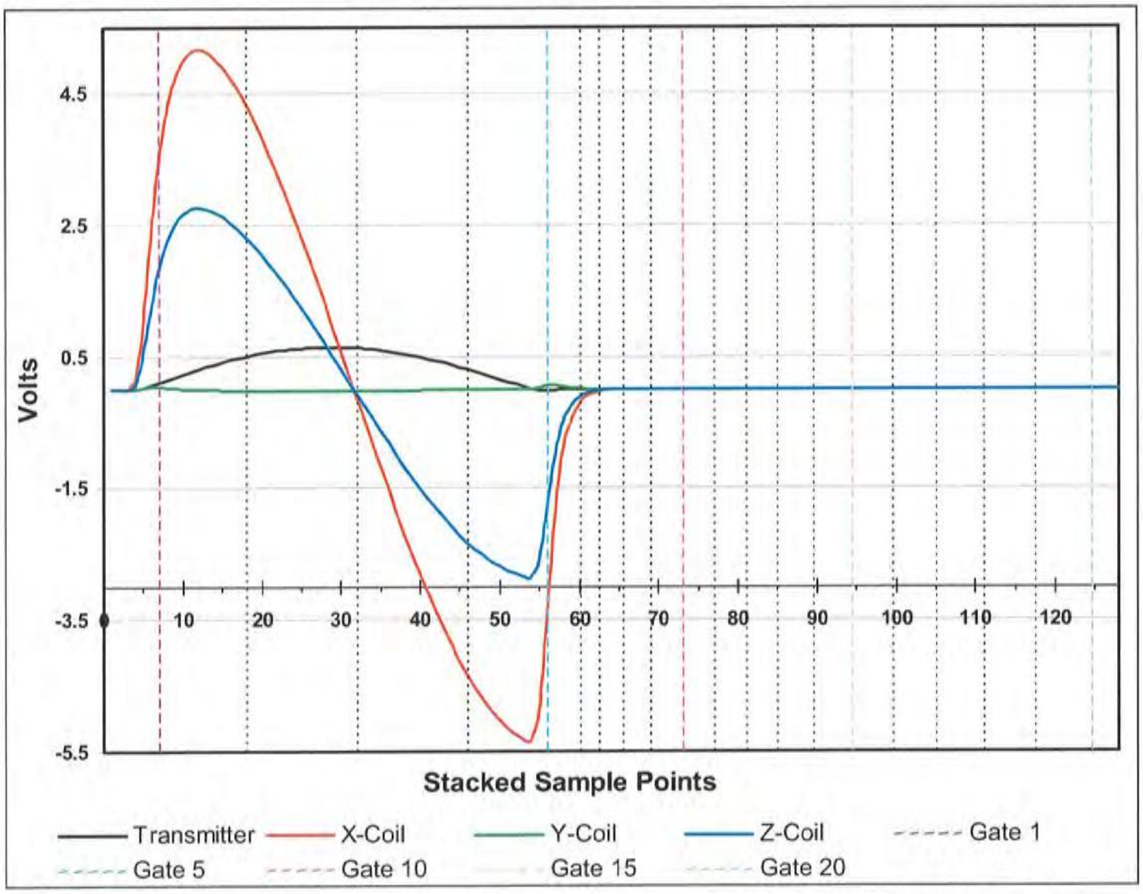

Figure 5: MEGATEM Waveform and response with gate centres showing positions in sample points.

Digital Acquisition:	FUGRO AIRBORNE SURVEYS GEODAS SYSTEM.
Analogue Recorder:	RMS GR-33, see below for analogue display and setup.
Barometric Altimeter:	Rosemount 1241M, sensitivity 1 ft, 1 sec recording interval.
Radar Altimeter:	Sperry RT 300, accuracy 2%, sensitivity 1 ft, range 0 to 2500 ft, 1 sec recording interval.
Camera:	Panasonic colour video, super VHS, model WV-CL302.
Electronic Navigation:	NovAtel Propak 4E-3151-R, 1 sec recording interval, with a resolution of 0.00001 degree and an accuracy of ±10m.

Analogue Recorder Display Setup:

Name	**Description**	**Scale**	**Unit**
ZF07	dB/dt Z coil Time Filtered Channel 07	10000	pV/cm
ZF13	dB/dt Z coil Time Filtered Channel 13	10000	pV/cm
ZF18	dB/dt Z coil Time Filtered Channel 18	10000	pV/cm
BZ07	B-Field Z coil Time Filtered Channel 07	10000	fT/cm
BZ13	B-Field Z coil Time Filtered Channel 13	10000	fT/cm
BZ18	B-Field Z coil Time Filtered Channel 18	10000	fT/cm
XF07	dB/dt X coil Time Filtered Channel 07	10000	pV/cm
XF13	dB/dt X coil Time Filtered Channel 13	10000	pV/cm
XF18	dB/dt X coil Time Filtered Channel 18	10000	pV/cm
BX07	B-Field X coil Time Filtered Channel 07	10000	fT/cm
BX13	B-Field X coil Time Filtered Channel 13	10000	fT/cm
BX18	B-Field X coil Time Filtered Channel 18	10000	fT/cm
BZ20	B-Field Z coil Raw channel 20	20000	fT/cm
BX20	B-Field X coil Raw channel 20	20000	fT/cm
X20	dB/dt X coil Raw channel 20	20000	pV/cm
Y20	dB/dt Y coil Raw channel 20	20000	pV/cm
Z20	dB/dt X coil Raw channel 20	20000	pV/cm
X01	dB/dt X coil Raw channel 01	50000	pV/cm
Z01	dB/dt Z coil Raw channel 01	50000	pV/cm
XPL	Powerline Monitor	0.2	V/cm
XEFM	Earth Field Monitor	1	V/cm
ZEFM	Earth Field Monitor	1	V/cm
XPRM	X Primary Field	0.4	V/cm
YPRM	Y Primary Field	13.3	V/cm
TPRM	Transmitter Primary Field	0.02	V/cm
CMAG	Coarse Total Field Magnetic Intensity	300	nT/cm
FMAG	Fine Total Field Magnetic Intensity	100	nT/cm
4DIF	Magnetic 4th Difference Filtered	1	nT/cm
RADR	Radar Altimeter	50	ft/cm
BARO	Barometric Altimeter	100	ft/cm

Base Station Equipment

Magnetometer:	Scintrex CS-2 single cell cesium vapour, mounted in a magnetically quiet area, measuring the total intensity of the earth's magnetic field in units of 0.01 nT at intervals of 0.5 sec, within a noise envelope of 0.20 nT.
GPS Receiver:	NovAtel, measuring all GPS channels, for up to 10 satellites
Computer:	Laptop, model Pentium II, 220 MHz
Converter:	Picodas, model MEP710 3/10901 GTS 780008

Field Office Equipment

Computers:	Dell Inspiron 8000 Pentium III laptop
Printer:	Canon bubblejet printer BJC-85
DVD writer Drive:	Ricoh 5.125 DVD+RW format
Hard Drive:	30 GB Removable hard drive

Survey Specifications

Traverse Line Direction:	090° - 270°
Traverse Line Spacing:	400 m
Tie Line direction:	000° - 180°
Tie Line spacing:	2000 m
Navigation:	Differential GPS. Traverse and tie line spacing was not to exceed the nominal by > 50% for more than 3 km.
Altitude:	The survey was flown at a mean terrain clearance of 120 m. Altitude was not to exceed 140 m over 3 km.
Magnetic Noise Levels:	The noise envelope on the magnetic data was not to exceed ± 0.25 nT over 3 km.
EM Noise Levels:	The noise envelope on the raw electromagnetic dB/dt X- and Z-coil channel 20 was not to exceed ± 3500 pT/s over a distance greater than 3 km as displayed on the raw analogue traces.

Field Crew

Data Processor:	D. Murray
Pilots:	A. Kirejew, M. Williston
Electronics Operator:	E. Aparicio
Engineer:	S. Dinel, C. Beattie

Production Statistics

Flying dates:	October 20th – November 12th, 2004
Total production:	2924 line kilometres
Number of production flights:	8
Days lost weather:	13

III

Quality Control and Compilation Procedures

In the field after each flight, all analogue records were examined as a preliminary assessment of the noise level of the recorded data. Altimeter deviations from the prescribed flying altitudes were also closely examined as well as the diurnal activity, as recorded on the base station.

All digital data were verified for validity and continuity. The data from the aircraft and base station was transferred to the PC's hard disk. Basic statistics were generated for each parameter recorded, these included: the minimum, maximum, and mean values; the standard deviation; and any null values located. All recorded parameters were edited for spikes or datum shifts, followed by final data verification via an interactive graphics screen with on-screen editing and interpolation routines.

The quality of the GPS navigation was controlled on a daily basis by recovering the flight path of the aircraft. The C3NavG2 correction procedure employs the raw ranges from the base station to create improved models of clock error, atmospheric error, satellite orbit, and selective availability. These models are used to improve the conversion of aircraft raw ranges to aircraft position.

Checking all data for adherence to specifications was carried out in the field by the FUGRO AIRBORNE SURVEYS field processor.

IV

Data Processing

Flight Path Recovery

GPS Recovery:	GPS positions recalculated from the recorded raw range data, and differentially corrected.
Projection:	Universal Transverse Mercator (UTM Zone 12N)
Datum:	NAD83
Central meridian:	111° West
False Easting:	500000 metres
False Northing:	0 metres
Scale factor:	0.9996

Altitude Data

Noise editing:	Alfatrim median filter used to eliminate the highest and lowest values from the statistical distribution of a 5 point sample window for the radar altimeter, GPS elevation, and barometric altimeter.

Base Station Diurnal Magnetics

Noise editing:	Alfatrim median filter used to eliminate the two highest and two lowest values from the statistical distribution of a 9 point sample window.
Culture editing:	Polynomial interpolation via a graphic screen editor.
Noise filtering:	Running average filter set to remove wavelengths less than 8 seconds.
Extraction of long wavelength component:	Running average filter to retain wavelengths greater than 62 seconds.

Airborne Magnetics

Lag correction:	3.3 s
Noise editing:	4th difference editing routine set to remove spikes greater than 0.5 nT.
Noise filtering:	Triangular filter set to remove noise events having a wavelength less than 0.9 seconds.
Diurnal subtraction:	The long wavelength component of the diurnal (greater than 62 seconds) was removed from the data with a base value of 59058 nT added back.
IGRF removal date:	2004.95

Gridding:	The data was gridded using an minimum curvature routine with a grid cell size of 100 m.

Residual Magnetic Intensity

The residual magnetic intensity (RMI) is calculated from the total magnetic intensity (TMI), the diurnal, and the regional magnetic field. The TMI is measured in the aircraft, the diurnal is measured from the ground station and the regional magnetic field is calculated from the International Geomagnetic Reference Field (IGRF). The low frequency component of the diurnal is extracted from the filtered ground station data and removed from the TMI. The average of the diurnal is then added back in to obtain the resultant TMI. The regional magnetic field, calculated for the specific survey location and the time of the survey, is removed from the resultant TMI to obtain the RMI. The final step is to Tie line level and micro-level the RMI data.

Magnetic First Vertical Derivative

As a map product the first vertical derivative was calculated in the frequency domain from the final grid values of the RMI to enhance subtleties related to geological structures.

A first vertical derivative has also been displayed in profile form. This was calculated from the line data combining the transfer functions of the 1st vertical derivative and a low-pass filter (cut-off value = 0.045, roll-off value = 0.03). The low-pass filter was designed to attenuate the high frequencies representing non-geological signal, which are normally enhanced by the derivative operator. This parameter is also stored in the final digital archive.

Electromagnetics

dB/dt data

Lag correction:	3.0 s
Data correction:	The x, y and z-coil data were processed from the 20 raw channels recorded at 4 samples per second.

The following processing steps were applied to the dB/dt data from all coil sets:

a) The data from channels 1 to 5 (on-time) and 6 to 20 (off-time) were corrected for drift in flight form (prior to cutting the recorded data back to the correct line limits) by passing a low order polynomial function through the baseline minima along each channel, via a graphic screen display;

b) The data were edited for residual spheric spikes by examining the decay pattern of each individual EM transient. Bad decays (i.e. not fitting a normal exponential function) were deleted and replaced by interpolation;

c) Corrections were made in the x- and z-coil data for low frequency, incoherent noise elements (that do not correlate from channel to channel) in the data, by analysing the decay patterns of channels 15 to 20 (OMEGA process).

d) Noise filtering was done using an adaptive filter technique based on time domain triangular operators. Using a 2nd difference value to identify changes in gradient along each channel, minimal filtering (3 point convolution) is applied over the peaks of the anomalies, ranging in set increments up to a maximum amount of filtering in the resistive background areas (29 points for both the x-coil and the z-coil data).

e) The filtered data from the x, y and z-coils were then re-sampled to a rate of 5 samples/s and combined into a common file for archiving.

B-field data

Processing steps: The processing of the B-Field data stream is very similar to the processing for the regular dB/dt data. The lag adjustment used was the same, followed by:

1) Drift adjustments;
2) Spike editing for spheric events;
3) Correction for low frequency, incoherent and non-decaying noise events, by analysing the decay patterns of channels 16 to 20 (OMEGA process);
4) Correction for coherent noise. By nature, the B-Field data will contain a higher degree of coherency of the noise that automatically gets eliminated (or considerably attenuated) in the regular dB/dt, since this is the time derivative of the signal.
5) Final noise filtering with an adaptive filter.

Note: The introduction of the B-Field data stream, as part of the MEGATEM system, provides the explorationist with a more effective tool for exploration in a broader range of geological environments and for a larger class of target priorities.

The advantage of the B-Field data compared with the normal voltage data (dB/dt) are as follows:

1. A broader range of target conductance that the system is sensitive to. (The B-Field is sensitive to bodies with conductance as great as 100,000 Siemens);
2. Enhancement of the slowly decaying response of good conductors;
3. Suppression of rapidly decaying response of less conductive overburden;
4. Reduction in the effect of spherics on the data;
5. An enhanced ability to interpret anomalies due to conductors below thick conductive overburden;
6. Reduced dynamic range of the measured response (easier data processing and display).

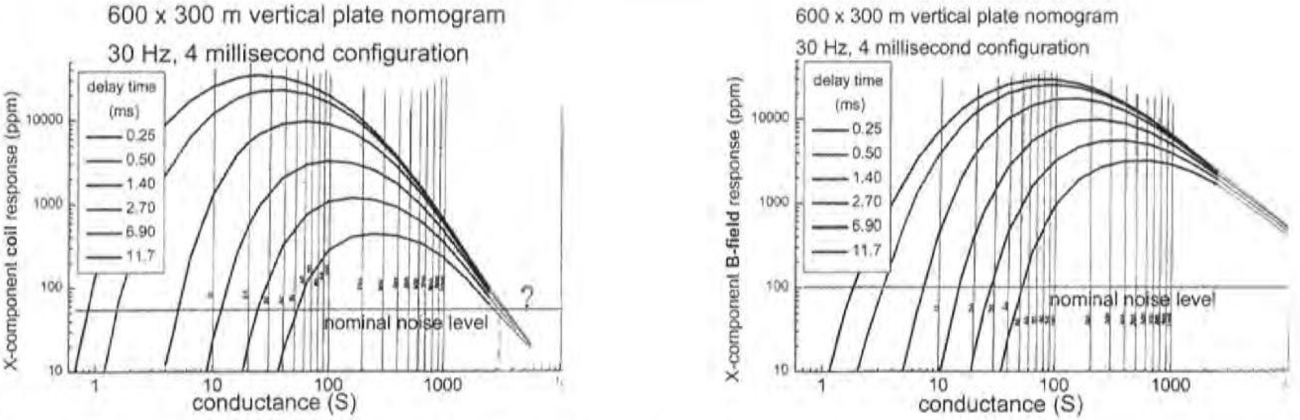

Figure 6: dB-dt vertical plate nomogram (left), B-field vertical plate nomogram (right).

Figure 6 displays the calculated vertical plate response for the MEGATEM® signal for the dB/dt and B-Field. For the dB/dt response, you will note that the amplitude of the early channel peaks at about 25 Siemens, and the late channels at about 250 Siemens. As the conductance exceeds 1000 Siemens the response curves quickly roll back into the noise level. For the B-Field response, the early channel amplitude peaks at about 80 Siemens and the late channel at about 550 Siemens. The projected extension of the graph in the direction of increasing conductance, where the response would roll back into the noise level, would be close to 100,000 Siemens. Thus, a strong conductor, having a conductance of several thousand Siemens, would be difficult to interpret on the dB/dt data, since the response would be mixed in with the background noise. However, this strong conductor would stand out clearly on the B-Field data, although it would have an unusual character, being a moderate to high amplitude response, exhibiting almost no decay.

In theory, the response from a super conductor (50,000 to 100,000 Siemens) would be seen on the B-Field data as a low amplitude, non-decaying anomaly, not visible in the off-time channels of the dB/dt stream. Caution must be exercised here, as this signature can also reflect a residual noise event in the B-Field data. In this situation, careful examination of the dB/dt on-time (in-pulse) data is required to resolve the ambiguity. If the feature were strictly a noise event, it would be not be present in the dB/dt off-time data stream. This would locate the response at the resistive limit, and the mid in-pulse channel (normally identified as channel 3) would reflect little but background noise, or at best a weak negative peak. If, on the other hand, the feature does indeed reflect a superconductor, then this would locate the response at the inductive limit. In this situation, channel 3 of the dB/dt stream will be a mirror image of the transmitted pulse, i.e. a large negative.

Coil Oscillation Correction

The electromagnetic receiver sensor is housed in a bird, which is towed behind the aircraft using a cable. Any changes in airspeed of the aircraft, variable crosswinds, or other turbulence will result in the bird swinging from side to side. This can result in the induction sensors inside the bird rotating about their mean orientation. The rotation is most marked when the air is particularly turbulent. The changes in orientation result in variable coupling of the induction coils to the primary and secondary fields. For example, if the sensor that is normally aligned to measure the x-axis response pitches upward, it will be measuring a response that will include a mixture of the X and Z component responses. The effect of coil oscillation on the data increases as the signal from the ground (conductivity) increases and may not be noticeable when flying over areas which are generally resistive. This becomes more of a concern when flying over highly conductive ground.

Using the changes in the coupling of the primary field, it is possible to estimate the pitch, roll and yaw of the receiver sensors. In the estimation process, it is assumed that a smoothed version of the primary field represents the primary field that would be measured when the sensors are in the mean orientation. The orientations are estimated using a non-linear inversion procedure, so erroneous orientations are sometimes obtained. These are reviewed and edited to insure smoothly varying values of orientations. These orientations can then be used to unmix the measured data to generate a response that would be measured if the sensors were in the correct orientation. (For more information on this procedure, see:
http://www.fugroairborne.com/TechnicalPapers/r_atem.shtml).

For the present dataset, the data from all 20 channels of dB/dt and B-Field parameters have been corrected for coil oscillation.

Apparent Conductance

The apparent conductance was calculated by fitting all 20 channels of the combined X and Z-coil response of the dB/dt component to the thin sheet model. Prior to the fitting, the data is deconvolved to the step response in order to provide a linear relationship as the conductivity of the ground increases from the resistive limit to the inductive limit.

The apparent conductance provides the maximum information on the near-surface conductivity of the ground which, when combined with the magnetic signature, provides good geological mapping.

Moments of the Impulse Response

For this dataset, the moments of the impulse response are a good way of highlighting a number of features in the dataset. The n^{th} moment is defined as

$$M^n = \int_0^\infty t^n I(t)\, dt \,,$$

where $I(t)$ is the impulse response.

One advantage of the moments is that they place different emphasis on different parts of the transient. The low-order moments (n=1) place emphasis on the early-time data and this reflects the near-surface information. The higher order moments (n=2,3...) place emphasis on the late-time data (or deeper information). For a more detailed description of moments see:
http://www.fugroairborne.com/TechnicalPapers/moment.shtml.

Another advantage of the moments is that these quantities can be easily converted to conductivity or conductance. For more details on this transformation, see:
http://www.fugroairborne.com/TechnicalPapers/conductance-conductivity.shtml. The moments can also be used to characterize discrete conductors by using a small sphere model to determine the depth, dip, conductivity etc. For more details on this model see:
http://www.fugroairborne.com/TechnicalPapers/smallsphere.shtml.

For the present dataset, the 3rd order moment of the combined B Field X and Z responses was calculated as a map product. Also the 1st through 6th order moments for each of B Field X, Y and Z were calculated and included in the database.

Decay Constant (TAU)

The decay constant values are obtained by fitting the channel data from either the complete off-time signal of the decay transient or only a selected portion of it (as defined by specific channels) to a single exponential of the form

$$Y = A\,e^{-t/\tau}$$

where **A** is amplitude at time zero, **t** is time in microseconds and τ is the decay constant, expressed in microseconds. A semi-log plot of this exponential function will be displayed as a straight line, the slope of which will reflect the rate of decay and therefore the strength of the conductivity. A slow rate of decay, reflecting a high conductivity, will be represented by a high decay constant.

As a single parameter, the decay constant provides more useful information than the amplitude data of any given single channel, as it indicates not only the peak position of the response but also the relative strength of the conductor. It also allows better discrimination of conductive axes within a broad formational group of conductors.

For the present dataset, the decay constant was calculated by fitting the Z coil response from channels 12 to 20 (mean delay times of 1129 to 3017 µsec after turn-off) of the B-Field component to the exponential function.

Conductivity-Depth-Transforms (CDT)

The CDT sections were calculated using the entire waveform data of the Z coil channels. The B Field data was converted to conductivity as a function of depth, where the structure is assumed to be layers of infinite lateral extent. The features represented in the CDT sections are valid only when these assumptions are met. The electromagnetic method is most sensitive to conductive features so resistive features will be poorly resolved. The process of converting the data to conductivity as a function of depth tends to create smoother depth variations than in reality.

The CDT sections, derived from each survey line, are created as individual grids. These grids are not plan grids (i.e. with x, y coordinates in a true geographic space), but elevation grids, with an unmatched x and y grid spacing. The x spacing is calculated from the starting point of the line and a heading, while the y spacing is a fixed number of rows divided into the maximum depth of investigation. The CDT grids have been corrected for altitude variations such that the top of each section reflects the true terrain topography and displayed on the profiles.

For more information refer to "Wolfgram P. and Karlik G., 1995: Conductivity-Depth Transform from MEGATEM data; Exploration Geophysics

V

Final Products

Digital Archives

Line and grid data in the form of a Geosoft database, an ASCII text file (*.xyz) and Geosoft grids have been written to CD-ROM. The formats and layouts of these archives are further described in Appendix E (Data Archive Description). Hardcopies of all maps have been created as outlined below.

Maps

Black & White

Scale: 1:50,000
Parameter: Flight Path
Media/Copies: 1 Paper

Colour

Scale: 1:50,000
Parameters: Residual Magnetic Intensity
First Vertical Derivative of the Residual Magnetic Intensity
Apparent Conductance derived from dB/dt X and Z Coils
3rd Order Moment derived from B Field X and Z Coils
Decay Constant (Tau) derived from B Field Z Coil Channels 12-20
Basic EM Interpretation Map
Media/Copies: 1 Paper

Profile Plots

Scale: 1:50,000
Parameters: Multi-channel presentation with 12 channels of both dB/dt and B-field X and Z-coil, Residual Magnetic Intensity, First Vertical Derivative of RMI, Radar Altimeter, Terrain, EM Primary Field, Hz Monitor, and Terrain adjusted Conductivity Depth Section.
Media/Copies: 1 Paper of Each Line

Report

Media/Copies: 2 Paper & 1 digital (PDF format)

Appendix A

GEOTEM® ELECTROMAGNETIC SYSTEM

GEOTEM® ELECTROMAGNETIC SYSTEM

General

The operation of a towed-bird time-domain electromagnetic system (EM) involves the measurement of decaying secondary electromagnetic fields induced in the ground by a series of short current pulses generated from an aircraft-mounted transmitter. Variations in the decay characteristics of the secondary field (sampled and displayed as windows) are analyzed and interpreted to provide information about the subsurface geology. The response of such a system utilizing a vertical-axis transmitter dipole and a multicomponent receiver coil has been documented by various authors including Smith and Keating (1991, Geophysics v.61, p. 74-81).

The principle of sampling the induced secondary field in the absence of the primary field (during the "off-time") and the large separation of the receiver coils from the transmitter combine with the large dipole moment and power available from the fixed wing platform to provide excellent signal-to-noise ratio and depth of penetration. Such a system is also relatively free of noise due to air turbulence. However, also sampling in the "on-time" (Annan et al., 1991, Geophysics v.61, p. 93-99) can result in excellent sensitivity for mapping very resistive features and very conductive features, and thus mapping geology.

Through free-air model studies using the University of Toronto's Plate and Layered Earth programs it may be shown that the "depth of investigation" depends upon the geometry of the target. Typical depth limits would be 400 m below surface for a homogeneous half-space, 550 m for a flat-lying inductively thin sheet or 350 m for a large vertical plate conductor. These depth estimates are based on the assumptions that the overlying or surrounding material is resistive.

The method also offers very good discrimination of conductor geometry. This ability to distinguish between flat-lying and vertical conductors combined with excellent depth penetration results in good differentiation of bedrock conductors from surficial conductors.

Methodology

GEOTEM® (GEOterrex Transient ElectroMagnetic system) is a time-domain towed-bird electromagnetic system incorporating a high-speed digital EM receiver. The primary electromagnetic pulses are created by a series of discontinuous sinusoidal current pulses fed into a three- or six-turn transmitting loop surrounding the aircraft and fixed to the nose, tail and wing tips. The base frequency rate is selectable: 25, 30, 75, 90, 125, 150, 225 and 270 Hz. The length of the pulse can be tailored to suit the targets. Standard pulse widths available are 0.6, 1.0, 2.0 and 4.0 ms. The available off-time can be selected to be as great as 16 ms. The current depends on the pulse width but the dipole moment can be as great as 6.7×10^5 Am ^{2}.

The receiver is a three-axis (x,y,z) induction coil which is towed by the aircraft on a 135-metre or 125-metre cable. The tow cable is non-magnetic, to reduce noise levels. The usual mean terrain clearance for the aircraft is 120 m with the EM bird being situated nominally 50 m below and 125 m behind the aircraft (see figure 1).

For each primary pulse a secondary magnetic field is produced by decaying eddy currents in the ground. These in turn induce a voltage in the receiver coils, which is the electromagnetic response.

The measured signals pass through anti-aliasing filters and are then digitized with an A/D converter at sampling rates of up to 80 kHz. The digital data flows from the A/D converter into an industrial-grade computer where the data are processed to reduce the noise.

Operations, which are carried out in the receiver, are:

1. *Primary-field removal:*
   In addition to measuring the secondary response from the ground, the receiver sensor coils also measure the primary response from the transmitter. During flight, the bird position and orientation changes slightly, and this has a very strong effect on the magnitude of the total response (primary plus secondary) measured at the receiver coils. The variable primary field response is distracting because it is unrelated to the ground response. The primary field can be measured by flying at an altitude such that no ground response is measurable. These calibration signals are used to define the shape of the primary waveform. By definition this primary field includes the response of the current in the transmitter loop plus the response of any slowly decaying eddy currents induced in the aircraft. We assume that the shape of the primary will be unchanged as the bird position changes, but that the amplitude will vary. The primary field removal procedure involves solving for the amplitude of the primary field in the measured response and removing this from the total response to leave a secondary response. Note that this procedure removes any ("in-phase") response from the ground which has the same shape as the primary field. For more details on the primary-field removal procedure, see http://www.fugroairborne.com/TechnicalPapers/inphasequad.shtml

1. *Transient Analysis:* Transient analysis permits the separation of specific types of noise from the signal in real time.

2. *Digital Stacking:* Stacking is carried out to reduce the effect of broadband noise on the data.

3. *Windowing of data*: The GEOTEM® digital receiver samples the secondary and primary electromagnetic field at 64, 128 or 384 points per EM pulse and windows the signal in up to 20 time gates whose centres and widths are software selectable and which may be placed anywhere within or outside the transmitter pulse. This flexibility offers the advantage of arranging the gates to suit the goals of a particular survey, ensuring that the signal is appropriately sampled through its entire dynamic range.

4. *Power Line Filtering:* Digital comb filters are applied to the data during real-time processing to remove power line interference while leaving the EM signal undisturbed. The RMS power line voltage (at all harmonics in the receiver passband) are computed, displayed and recorded for each data stack.

5. *Primary Field:* The primary field at the towed sensor is measured for each stack and recorded as a separate data channel to assess the variation in coupling between the aircraft and the towed sensor induced by changes in system geometry.

6. *Earth Field Monitor:* A monitor of sensor coil motion noise induced by coil motion in the Earth's magnetic field is also extracted in the course of the real-time digital processing. This information is also displayed on the real-time chart as well as being recorded for post-survey diagnostic processes.

7. *Noise/Performance:* A monitor computes the RMS signal level on an early off-time channel over a running 10-second window. This monitor provides a measure of noise levels in areas of low ground response. This information is printed at regular intervals on the side of the flight record and is recorded for every data stack.

One of the major roles of the GEOTEM® digital receiver is to provide diagnostic information on system functions and to allow for identification of noise events, such as sferics, which may be selectively removed from the EM signal.

GEOTEM®'s high digital sampling rate yields maximum resolution of the secondary field. The absence of an analog system time-constant filter results in minimal signal distortion and, therefore, superior representation of the anomaly amplitudes and shapes.

System Hardware

The GEOTEM® system is an integrated whole, consisting of the CASA 212 aircraft, the on-board hardware, and the software packages controlling the hardware.
The software packages in the GEODAS data acquisition system and in the GEOTEM® receiver were developed in-house. Likewise, certain elements of the hardware (GEOTEM® transmitter, system timing clock, towed-bird receiver system) were developed in-house.

Transmitter System

The transmitter system drives high-current pulses of an appropriate shape and duration through the coils mounted on the CASA aircraft.

System Timing Clock

This subsystem provides appropriate timing signals to the transmitter, and also to the analog-to-digital converter, in order to produce output pulses and capture the ground response.

Towed-Bird Receiver System

A three-axis induction coil is mounted inside a towed bird, which is typically 50 metres below and 125 metres behind the aircraft. (A second bird, housing the magnetometer sensor, is typically 45 metres below and 80 metres behind the aircraft.)

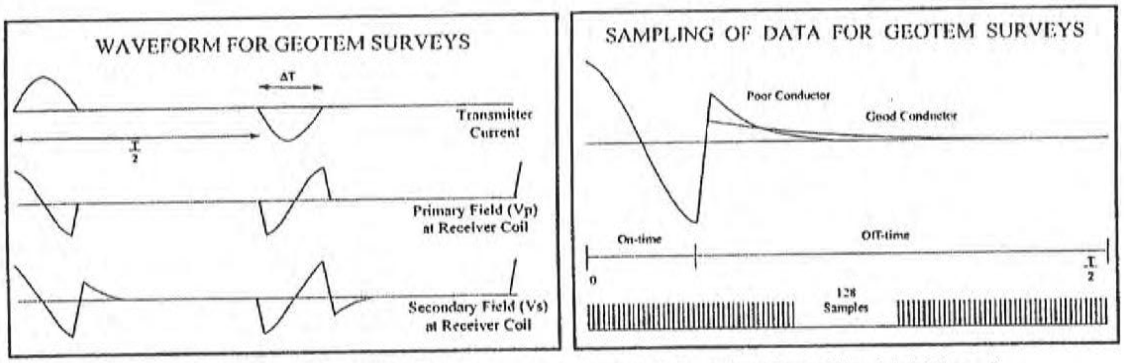

The GEOTEM system waveform (left frame) and sampling (right frame)

Timing of GEOTEM™ data acquisition for typical configurations

Base Frequency [Hz]	**150**	**90**	**30**	**125**	**75**	**25**
Pulse Width [ms]	**1.02**	**2.04**	**4.14**	**1.02**	**2.04**	**4.14**
Total Halfcycle [ms]	3.33	5.56	16.67	4.00	6.67	20.00
Off-Time [ms]	2.31	3.52	12.53	2.98	4.63	15.86
TX pulses / second	240	144	48	200	120	40
Eff.Digitising Rate [samples/sec]	38,400	23,040	7,680	32,000	19,200	6,400
Pulses per Reading	60	36	12	50	30	10
Stored readings / second	4	4	4	4	4	4
Samples per transient	128	128	128	128	128	128
Number of Channels	20	20	20	20	20	20
- off-time	16	15	15	16	15	16
- in-pulse	4	5	5	4	5	4

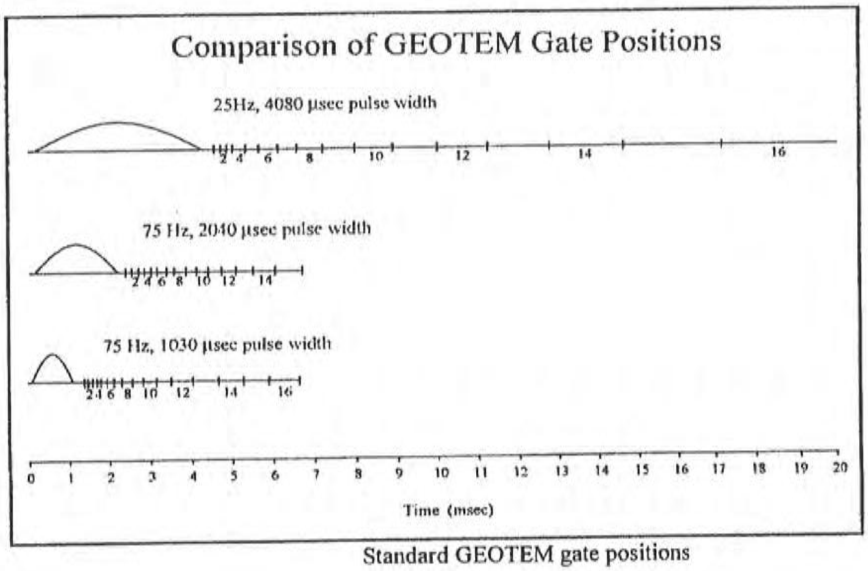

Standard GEOTEM gate positions

Appendix B

GEOTEM® Interpretation

GEOTEM® Interpretation

Introduction

The basis of the transient electromagnetic (EM) geophysical surveying technique relies on the premise that changes in the primary EM field produced in the transmitting loop will result in eddy currents being generated in any conductors in the ground. The eddy currents then decay to produce a secondary EM field which may be sensed as a voltage in the receiver coil.

GEOTEM1 (GEOterrex Transient ElectroMagnetic system) is an airborne transient (or time-domain) towed-bird EM system incorporating a high-speed digital receiver which records the secondary field response with a high degree of accuracy. Most often the total magnetic field is recorded concurrently.

Although the approach to GEOTEM interpretation varies from one survey to another depending on the type of data presentation, objectives and local conditions, the following generalizations may provide the reader with some helpful background information.

The main purpose of the interpretation is to determine the probable origin of the conductors detected during the survey and to suggest recommendations for further exploration. This is possible through an objective analysis of all characteristics of the different types of conductors and associated magnetic anomalies, if any. If possible the airborne results are compared to other available data. A certitude is seldom reached, but a high probability is achieved in identifying the conductive causes in most cases. One of the most difficult problems is usually the differentiation between surface conductors and bedrock conductors.

Types Of Conductors

Bedrock Conductors

The different types of bedrock conductors normally encountered are the following:

1. *Graphites*. Graphitic horizons (including a large variety of carbonaceous rocks) occur in sedimentary formations of the Precambrian as well as in volcanic tuffs, often concentrated in shear zones. They correspond generally to long, multiple conductors lying in parallel bands. They have no magnetic expression unless associated with pyrrhotite or magnetite. Their conductivity is variable but generally high.

2. *Massive sulphides*. Massive sulphide deposits usually manifest themselves as short conductors of high conductivity, often with a coincident magnetic anomaly. Some massive sulphides, however, are not magnetic, others are not very conductive (discontinuous mineralization), and some may be located among formational conductors so that one must not be too rigid in applying the selection criteria.

   In addition, there are syngenetic sulphides whose conductive pattern may be similar to that of graphitic horizons but these are generally not as prevalent as graphites.

---

[1] GEOTEM®: Registered Trade Mark of Fugro Airborne Surveys Corporation.

3. *Magnetite and some* serpentinized ultrabasics. These rocks are conductive and very magnetic.

4. *Manganese oxides*. This mineralization may give rise to a weak EM response.

Surficial Conductors

1. Beds of clay and alluvium, some swamps, and brackish ground water are usually poorly conductive to moderately conductive.

2. Lateritic formations, residual soils and the weathered layer of the bedrock may cause surface anomalous zones, the conductivity of which is generally low to medium but can occasionally be high. Their presence is often related to the underlying bedrock.

Cultural Conductors (Man-Made)

3. *Power lines*. These frequently, but not always, produce a conductive type of response on the GEOTEM record. In the case of direct radiation of its field, a power line is easily recognized by a GEOTEM anomaly which exhibits phase changes between different channels. In the case of a grounded wire, or steel pylon, the anomaly may look very much like a bedrock conductor.

4. *Grounded fences or pipelines*. These will invariably produce responses much like a bedrock conductor. Whenever they cannot be identified positively, a ground check is recommended.

5. *General culture*. Other localized sources such as certain buildings, bridges, irrigation systems, tailings ponds etc., may produce GEOTEM anomalies. Their instances, however, are rare and often they can be identified on the visual path recovery system.

Analysis Of The Conductors

The apparent conductivity alone is not generally a decisive criterion in the analysis of a conductor. In particular, one should note:

its shape and size,
all local variations of characteristics within a conductive zone,
any associated geophysical parameter (e.g. magnetics),
the geological environment,
the structural context, and
the pattern of surrounding conductors.

The first objective of the interpretation is to classify each conductive zone according to one of the three categories which best defines its probable origin. The categories are cultural, surficial and bedrock. A second objective is to assign to each zone a priority rating as to its potential as an economic prospect.

Bedrock Conductors

This category comprises those anomalies which cannot be classified according to the criteria established for cultural and surficial responses. It is difficult to assign a universal set of values which typify bedrock conductivity because any individual zone or anomaly might exhibit some, but not all, of these values and still be a bedrock conductor. The following criteria are considered indicative of a bedrock conductor:

An intermediate to high conductivity identified by a response with slow decay, with deflections most often present in the later channels.

The anomaly should be narrow, relatively symmetrical, with a well-defined peak.

There should be no serious displacement of anomaly position or change in anomaly shape (other than mirror image) with respect to flight direction, except in the case of non-vertical dipping bodies. The alternating character of the response as a result of line direction can be diagnostic of conductor geometry. Figures 2 to 6 illustrate anomalies associated with different target models.

A small to intermediate amplitude. Large amplitudes are normally associated with surficial conductors. The amplitude varies according to the depth of the source.

A degree of continuity of the EM characteristics across several lines.

An associated magnetic response of similar dimensions. One should note, however, that those rocks which weather to produce a conductive upper layer will possess this magnetic association. In the absence of one or more of the characteristics defined in 1, 2, 3 and 4, the related magnetic response cannot be considered significant.

Most obvious bedrock conductors occur in long, relatively monotonous, sometimes multiple zones following formational strike. Graphitic material is usually the most probable source. Massive syngenetic sulphides extending for many kilometres are known in nature but, in general, they are not common. Long formational structures associated with a strong magnetic expression may be indicative of banded iron formations.

A bedrock conductor reflecting the presence of a massive sulphide would normally exhibit the following characteristics:

a high conductivity,
a good anomaly shape (narrow and well-defined peak),
a small to intermediate amplitude,
an isolated setting,
a short strike length (in general, not exceeding one kilometre), and
preferably, with a localized magnetic anomaly of matching dimensions.

Surficial Conductors

This term is used for geological conductors in the overburden, either glacial or residual in origin, and in the weathered layer of the bedrock. Most surficial conductors are probably caused by clay minerals. In some environments the presence of salts will contribute to the conductivity. Other possible electrolytic conductors are residual soils, swamps, brackish ground water and alluvium such as lake or river-bottom deposits, flood plains and estuaries.

Normally, most surficial materials have low to intermediate conductivity so they are not easily mistaken for highly conductive bedrock features. Also, many of them are wide and their anomaly shapes are typical of broad horizontal sheets.

When surficial conductivity is high it is usually still possible to distinguish between a horizontal plate (more likely to be surficial material) and a vertical body (more likely to be a bedrock source) thanks to the asymmetry of the GEOTEM responses observed at the edges of a broad conductor when flying adjacent lines in opposite directions. The configuration of the system is such that the response recorded at the leading edge is more pronounced than that registered at the trailing edge. Figure 1 illustrates the "edge effect" and the resulting conductive pattern in plan view. In practice there are many variations on this very diagnostic phenomenon.

One of the more ambiguous situations as to the true source of the response is when surface conductivity is related to bedrock lithology as for example, surface alteration of an underlying bedrock unit. At times, it is also difficult to distinguish between a weak conductor within the bedrock (e.g. near-massive sulphides) and a surficial source.

In the search for massive sulphides or other bedrock targets, surficial conductivity is generally considered as interference but there are situations where the interpretation of surficial-type conductors is the primary goal. When soils, weathered or altered products are conductive, and in-situ, the GEOTEM responses are a very useful aid to geologic mapping. Shears and faults are often identified by weak, usually narrow, anomalies.

Analysis of surficial conductivity can be used in the exploration for such features as lignite deposits, kimberlites, paleochannels and ground water. In coastal or arid areas, surficial responses may serve to define the limits of fresh, brackish and salty water.

Cultural Conductors

The majority of cultural anomalies occur along roads and are accompanied by a response on the power line monitor. (This monitor is set to 50 or 60 Hz, depending on the local power grid.) Power lines are the most common source of the anomalies and many are recognized immediately by virtue of phase reversals or an abnormal rate of decay. A certain number yield normal GEOTEM anomalies which could be mistaken for bedrock responses. There are also some power lines which have no GEOTEM response whatsoever.

The power line monitor, of course, is of great assistance in identifying cultural anomalies of this type. It is important to note, however, that geological conductors in the vicinity of power lines may exhibit a weak response on the monitor because of current induction via the earth.

Fences, pipelines, communication lines, railways and other man-made conductors can give rise to GEOTEM responses, the strength of which will depend on the grounding of these objects.

Another facet of this analysis is the line-to-line comparison of anomaly character along suspected man-made conductors. In general, the amplitude, the rate of decay, and the anomaly width should not vary a great deal along any one conductor, except for the change in amplitude related to terrain clearance variation. A marked departure from the average response character along any given feature gives rise to the possibility of a second conductor.

In most cases a visual examination of the site will suffice to verify the presence of a man-made conductor. If a second conductor is suspected the ground check is more difficult to accomplish. The object would be to determine if there is (i) a change in the man-made construction, (ii) a difference in the grounding conditions, (iii) a second cultural source, or (iv) if there is, indeed, a geological conductor in addition to the known man-made source.

The selection of targets from within extensive (formational) belts is much more difficult than in the case of isolated conductors. Local variations in the EM characteristics, such as in the amplitude, decay, shape etc., can be used as evidence for a relatively localized occurrence. Changes in the character of the EM responses, however, may be simply reflecting differences in the conductive formations themselves rather than indicating the presence of massive sulphides and, for this reason, the degree of confidence is reduced.

Another useful guide for identifying localized variations within formational conductors is to examine the magnetic data compiled as isomagnetic contours. Further study of the magnetic data can reveal the presence of faults, contacts, and other features which, in turn, help define areas of potential economic interest.

Finally, once ground investigations begin, it must be remembered that the continual comparison of ground knowledge to the airborne information is an essential step in maximizing the usefulness of the GEOTEM data.

EDGE EFFECT

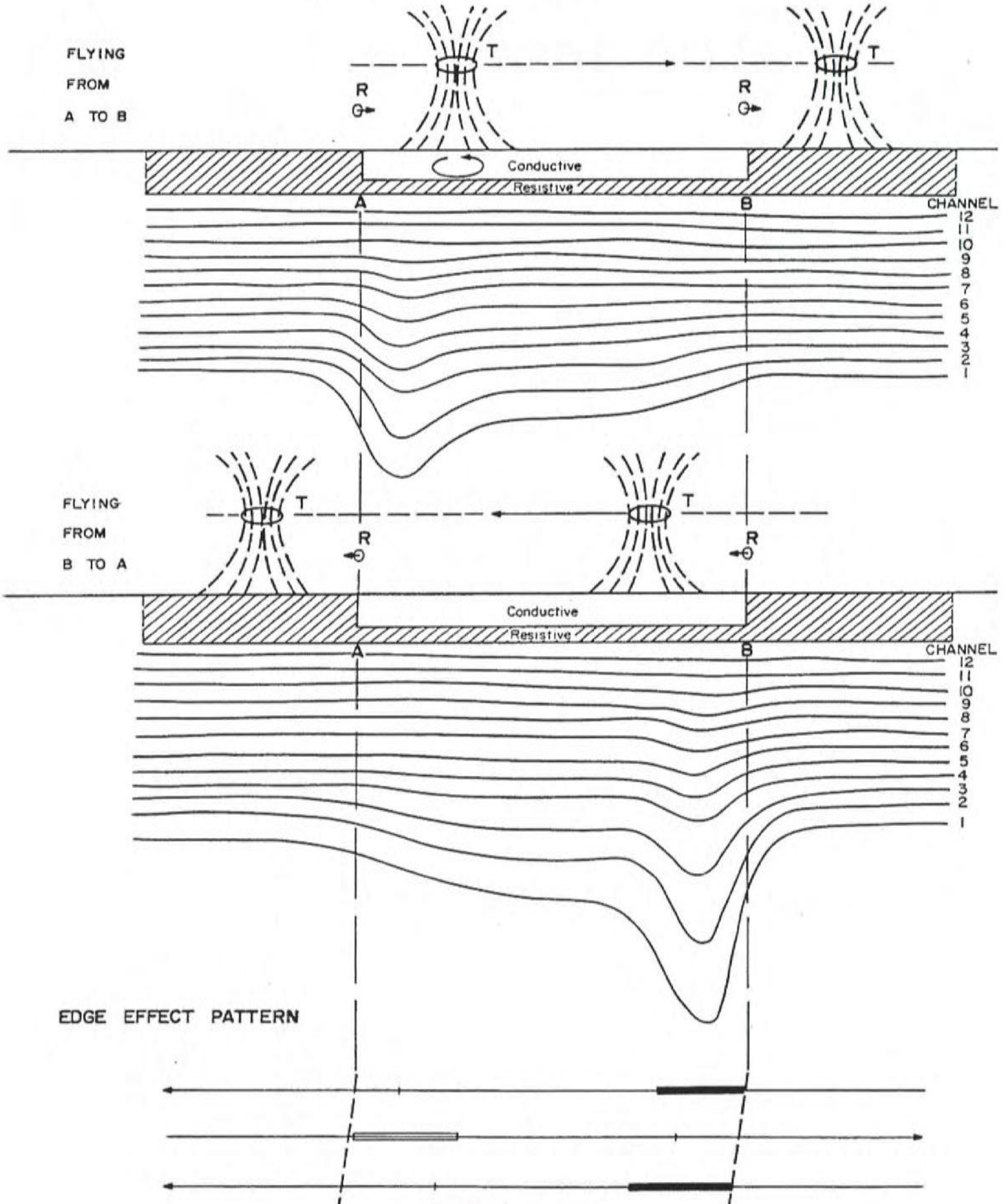

FIGURE 1

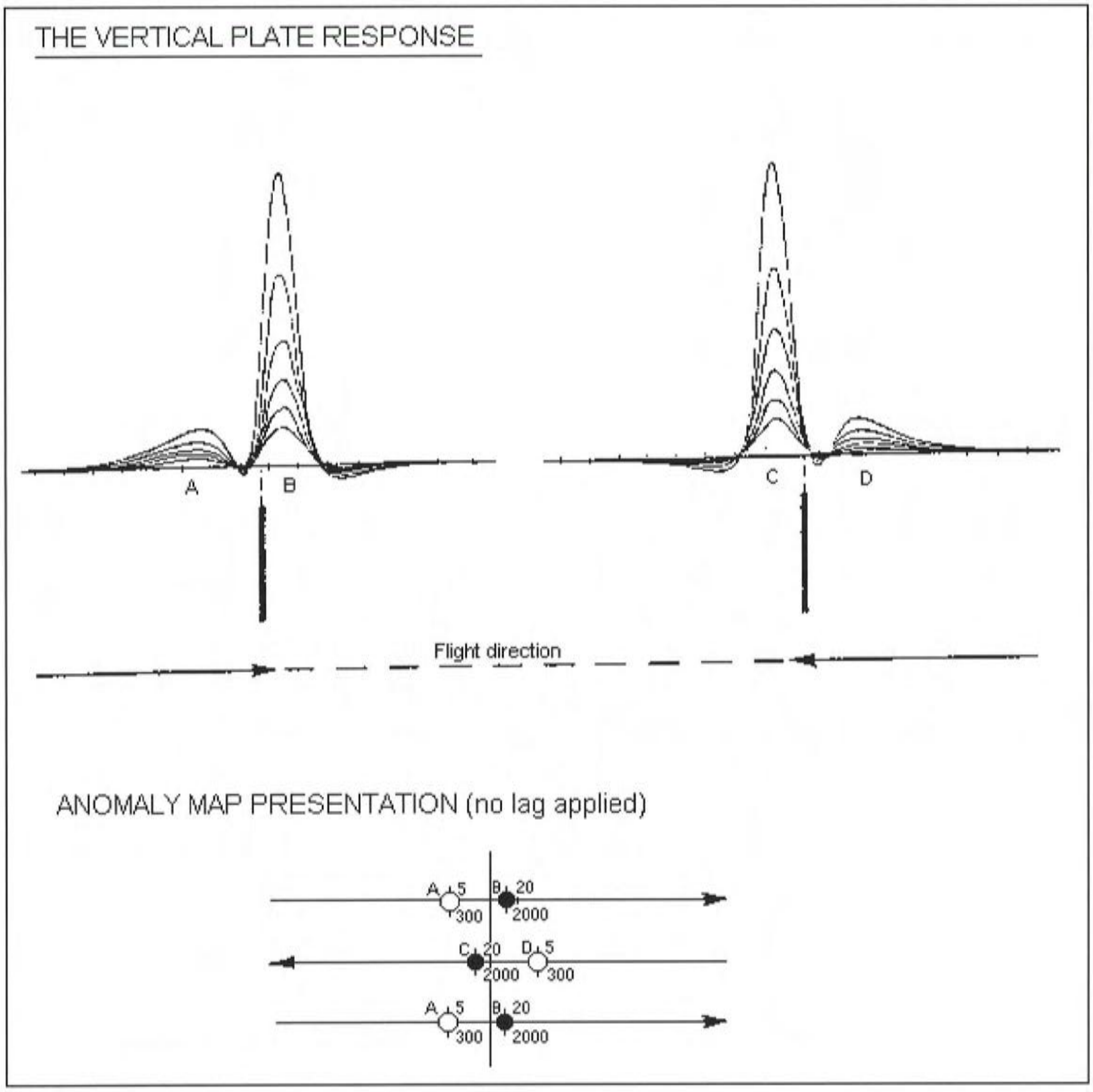
THE VERTICAL PLATE RESPONSE
A
B
C
D
Flight direction
ANOMALY MAP PRESENTATION (no lag applied)
A 5 300
B 20 2000
C 20 2000
D 5 300
A 5 300
B 20 2000

Figure 2

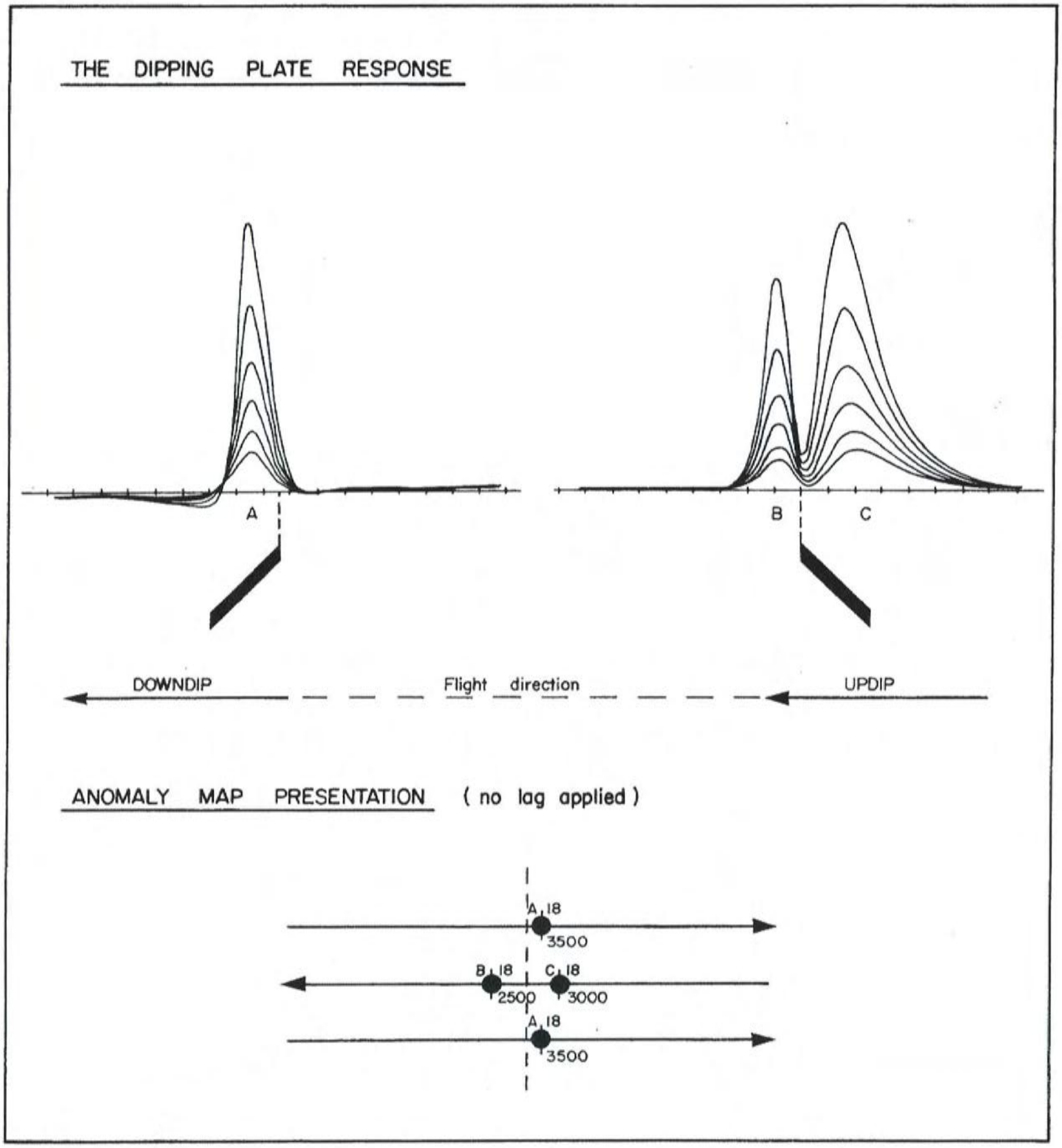
THE DIPPING PLATE RESPONSE
A
B
C
DOWNDIP
Flight direction
UPDIP
ANOMALY MAP PRESENTATION (no lag applied)
A 18
3500
B 18
2500
C 18
3000
A 18
3500

Figure 3

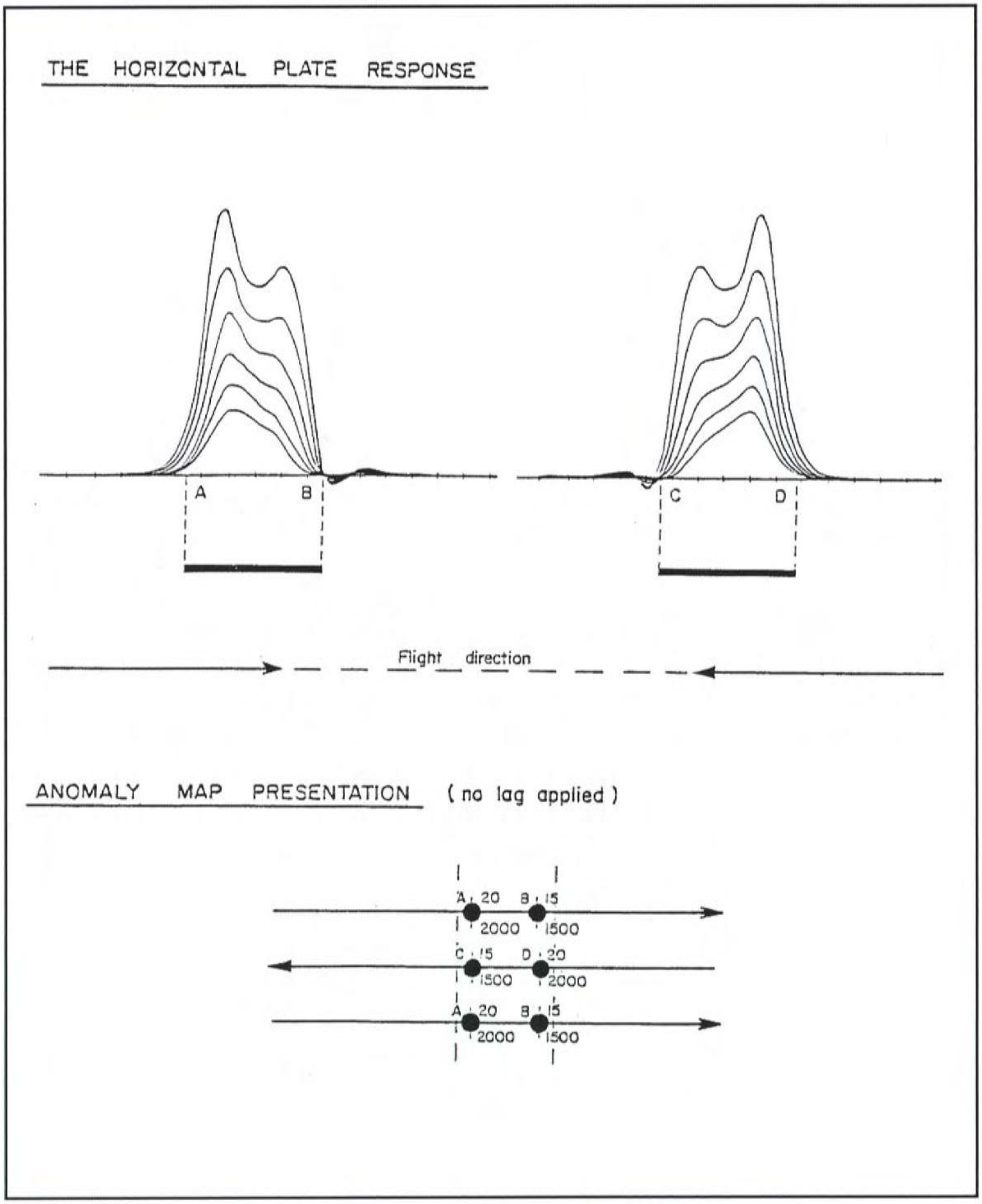
THE HORIZONTAL PLATE RESPONSE
A
B
C
D
Flight direction
ANOMALY MAP PRESENTATION (no lag applied)
A 20
B 15
2000
1500
C 15
D 20
1500
2000
A 20
B 15
2000
1500

Figure 4

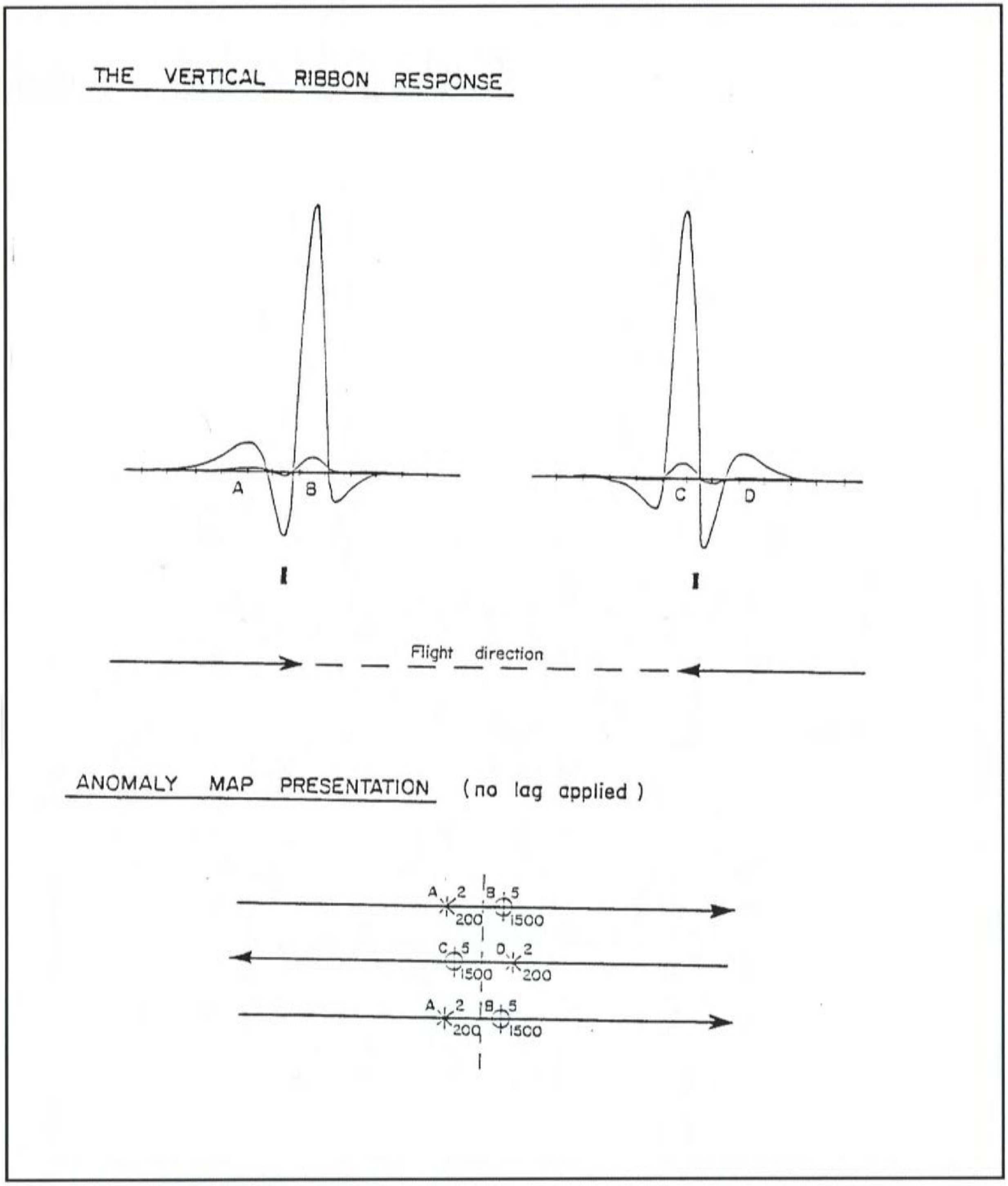
THE VERTICAL RIBBON RESPONSE
A
B
C
D
Flight direction
ANOMALY MAP PRESENTATION (no lag applied)
A 2 200
B 5 1500
C 5 1500
D 2 200
A 2 200
B 5 1500

Figure 5

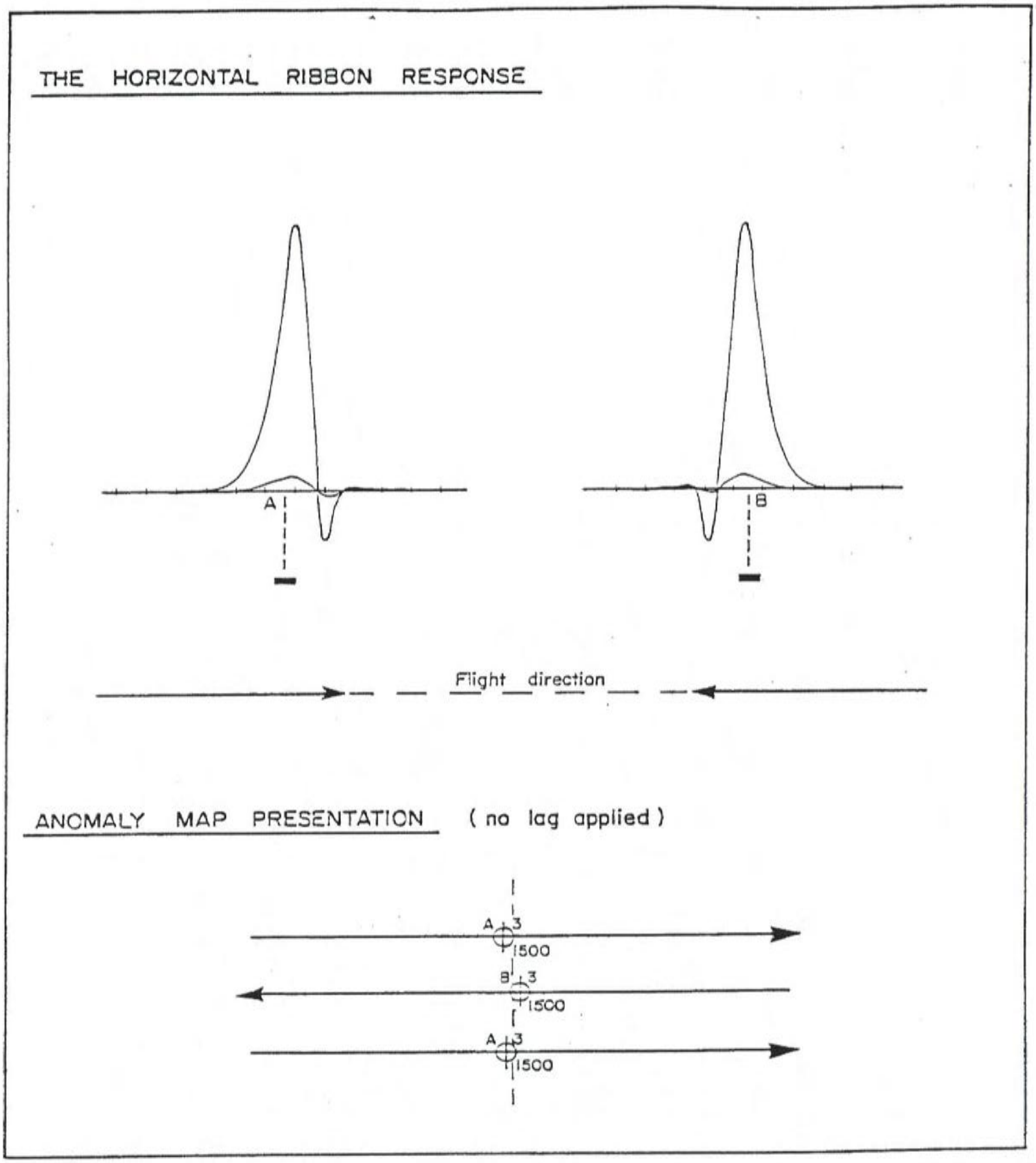
THE HORIZONTAL RIBBON RESPONSE
A
B
Flight direction
ANOMALY MAP PRESENTATION
(no lag applied)
A
3
1500
B
3
1500
A
3
1500

Figure 6

Appendix C

Multicomponent GEOTEM® modelling

Multicomponent GEOTEM® modelling

Introduction

The PLATE program has been used to generate synthetic responses over a number of plate models with varying depth of burial (0, 150 and 300m) and dips (0, 45, 90 and 135 degrees). The geometry assumed for the GEOTEM system is shown on the following page, and the transmitter waveform on the subsequent page. For simplicity, only six receiver gates have been calculated and plotted.

In all cases the plate has a strike length of 600 m with a strike direction into the page. The width of the plate is 300 m. As the flight path traverses the centre of the plate, the y component is zero and has not been plotted.

The conductance of the plate is 20 S. In cases when the conductance is different, an indication of how the amplitudes may vary can be obtained from the nomogram included.

In the following plots all components are normalized to the total primary field.

Nominal GEOTEM geometry

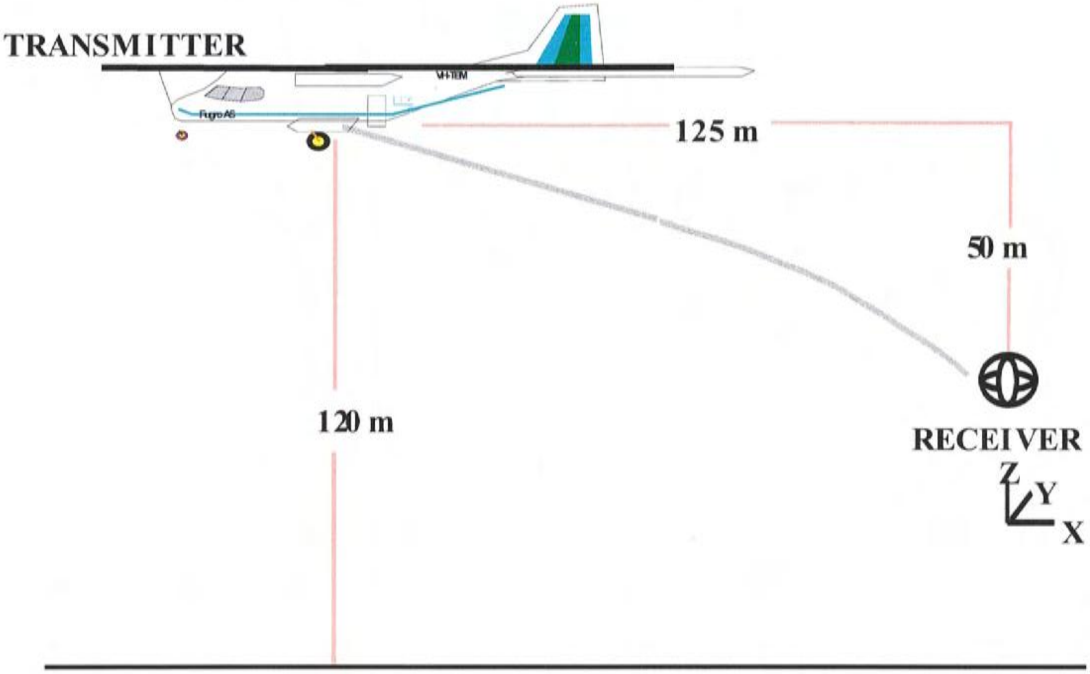

Transmitter waveform and receiver sampling (90 Hz)

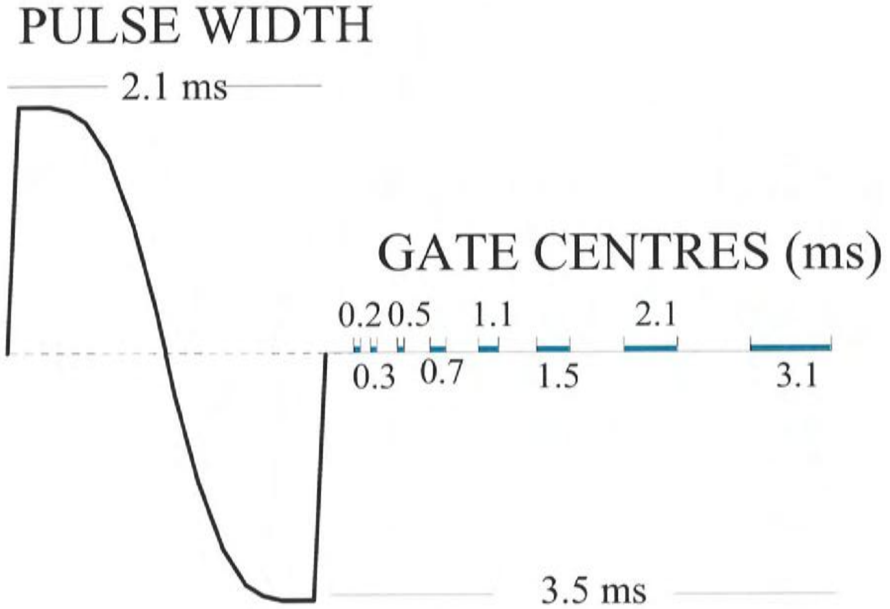

Nomogram

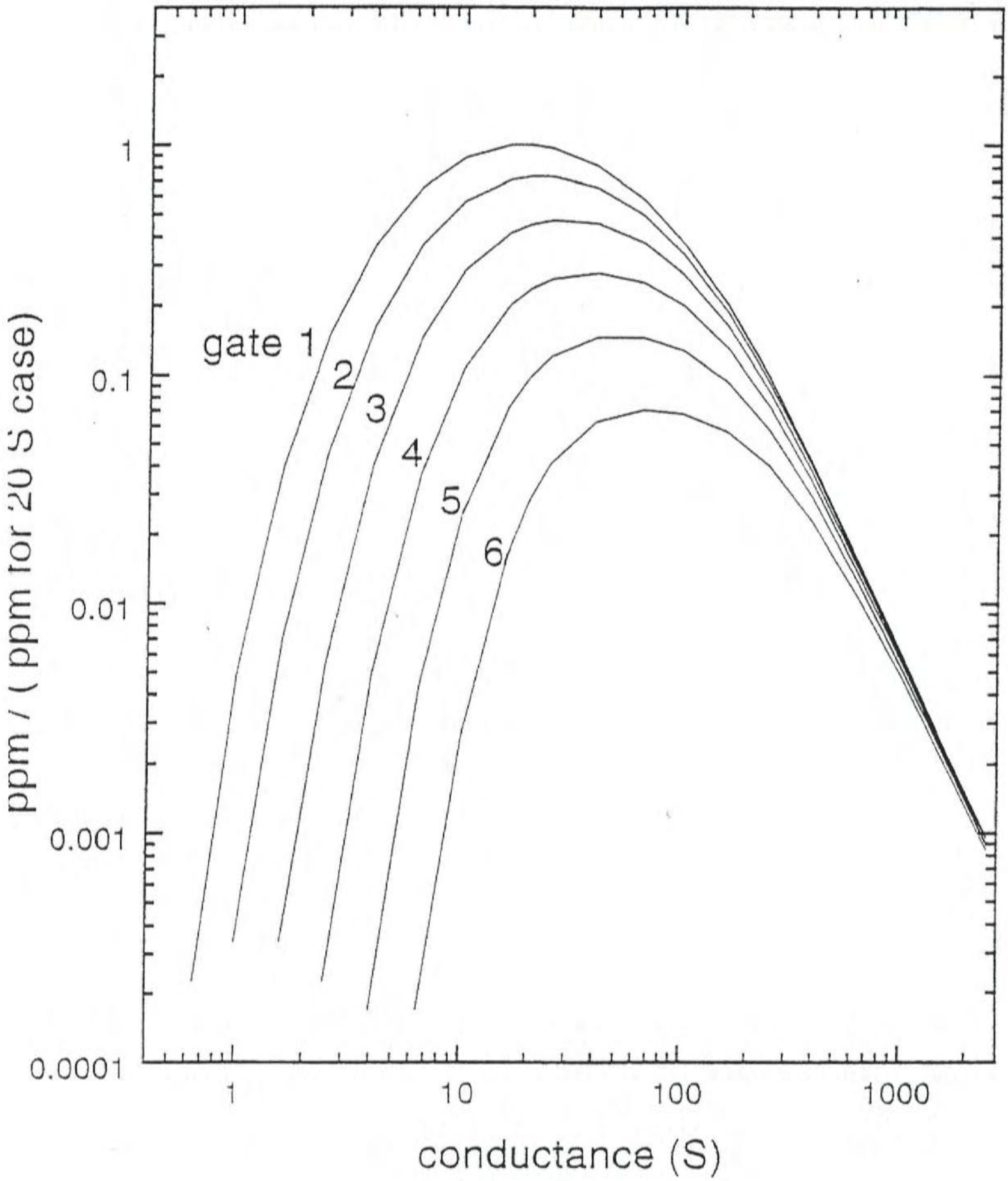
ppm / (ppm for 20 S case)
1
0.1
0.01
0.001
0.0001
1
10
100
1000
conductance (S)
gate 1
2
3
4
5
6

Plate: depth =0; dip =0

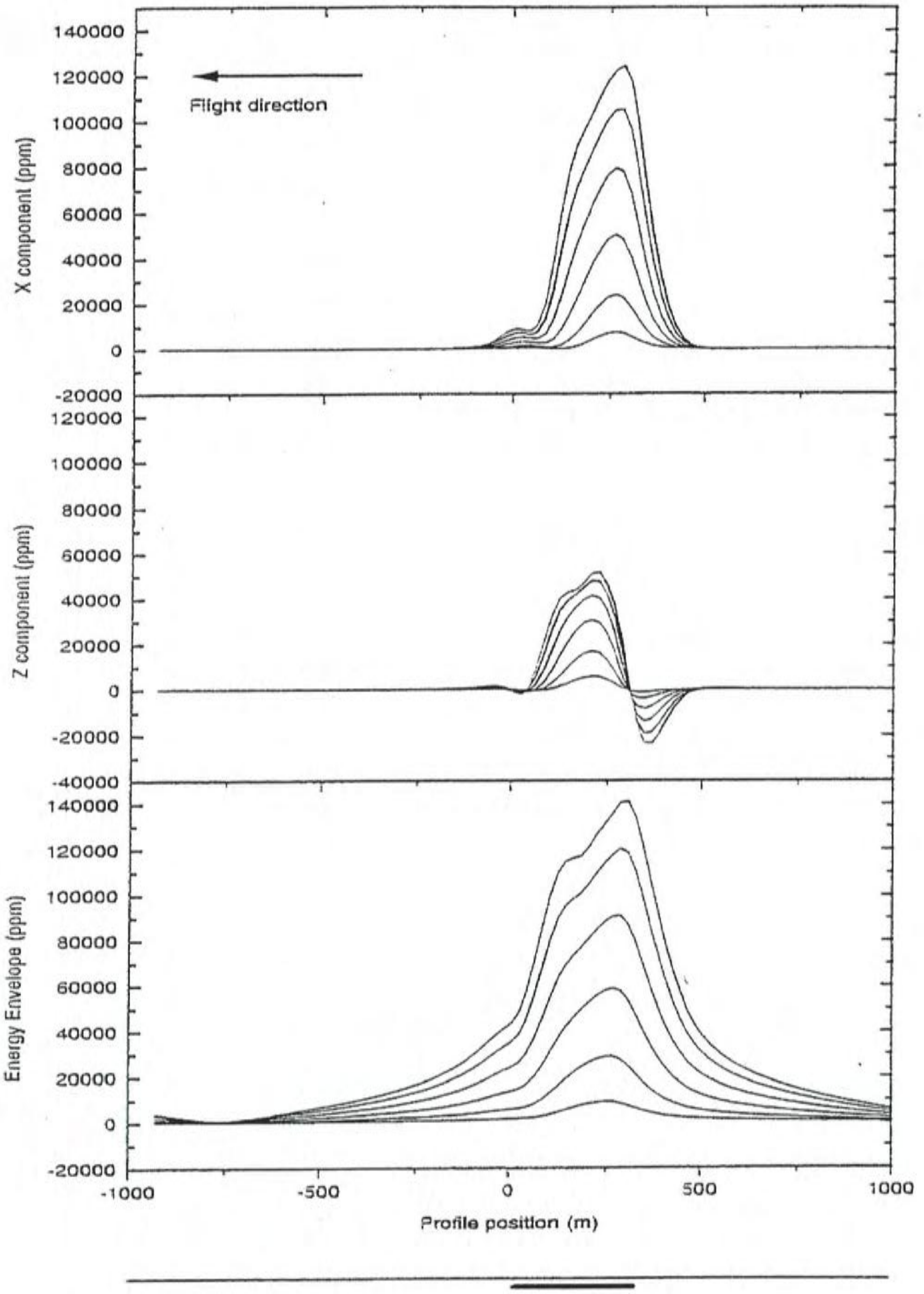

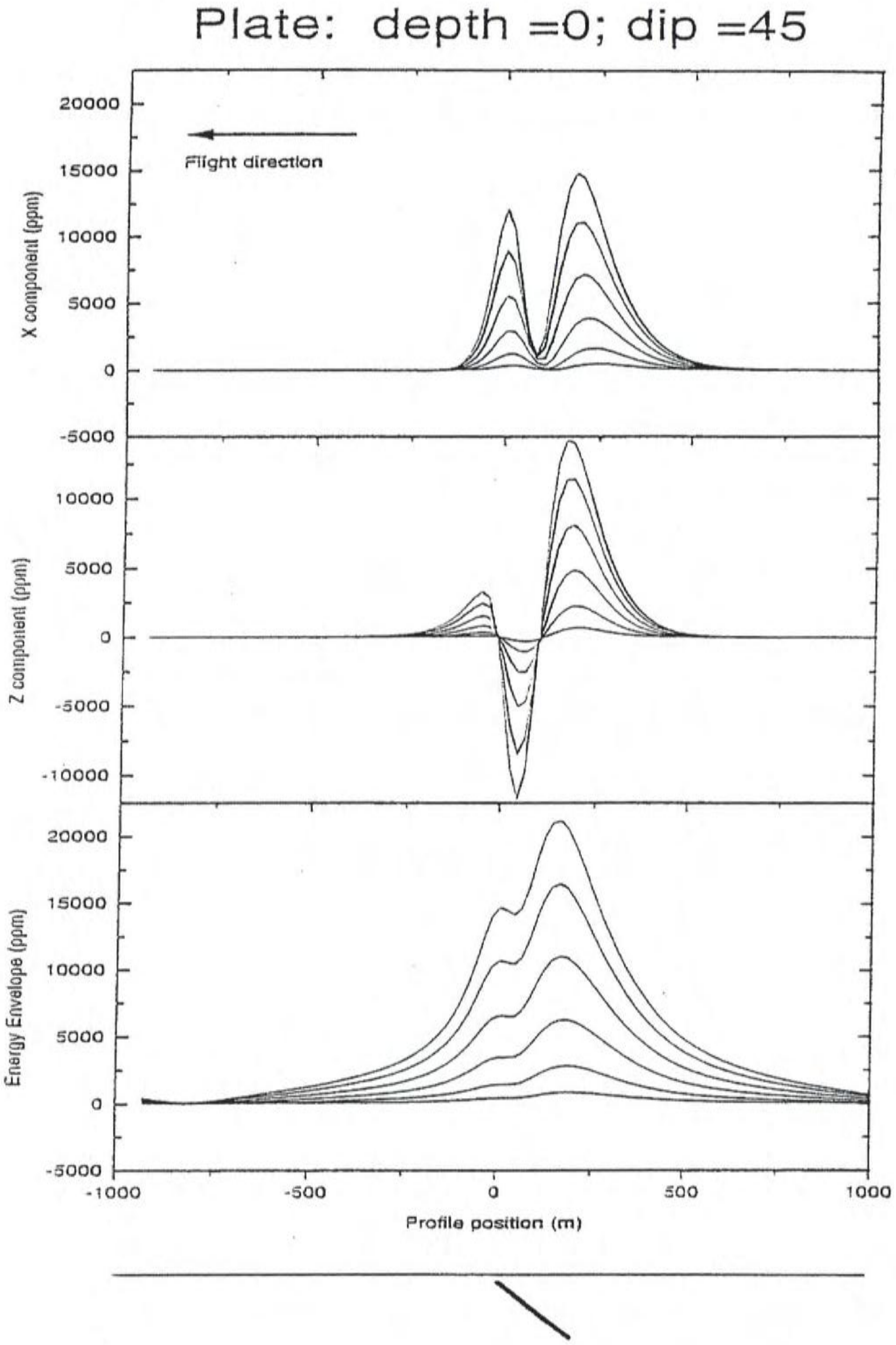
Plate: depth =0; dip =45
Flight direction
20000
15000
10000
5000
0
-5000
X component (ppm)
10000
5000
0
-5000
-10000
Z component (ppm)
20000
15000
10000
5000
0
-5000
Energy Envelope (ppm)
-1000
-500
0
500
1000
Profile position (m)

Plate: depth =0; dip =90

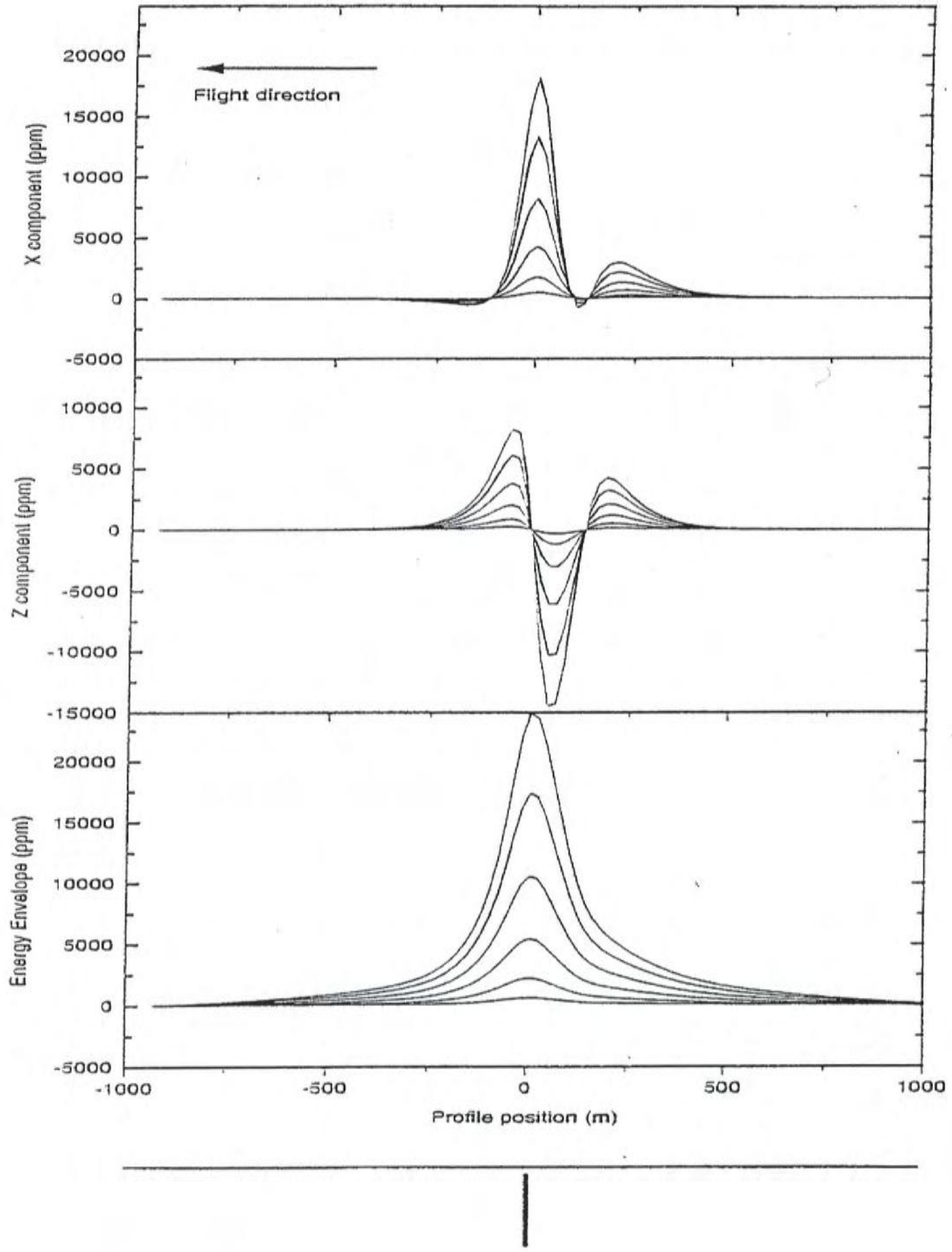

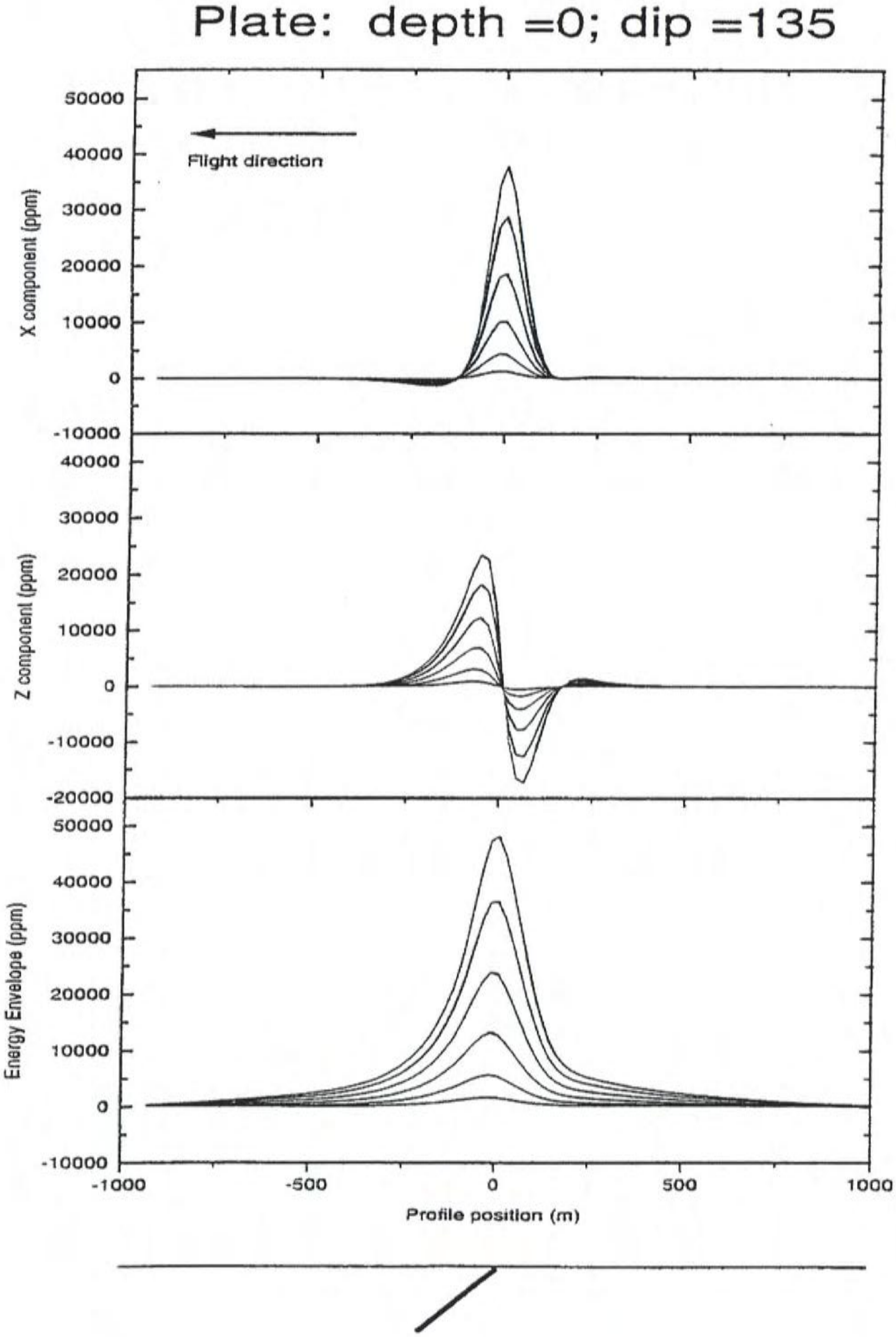

Plate: depth =0; dip =135

Plate: depth =150; dip =0

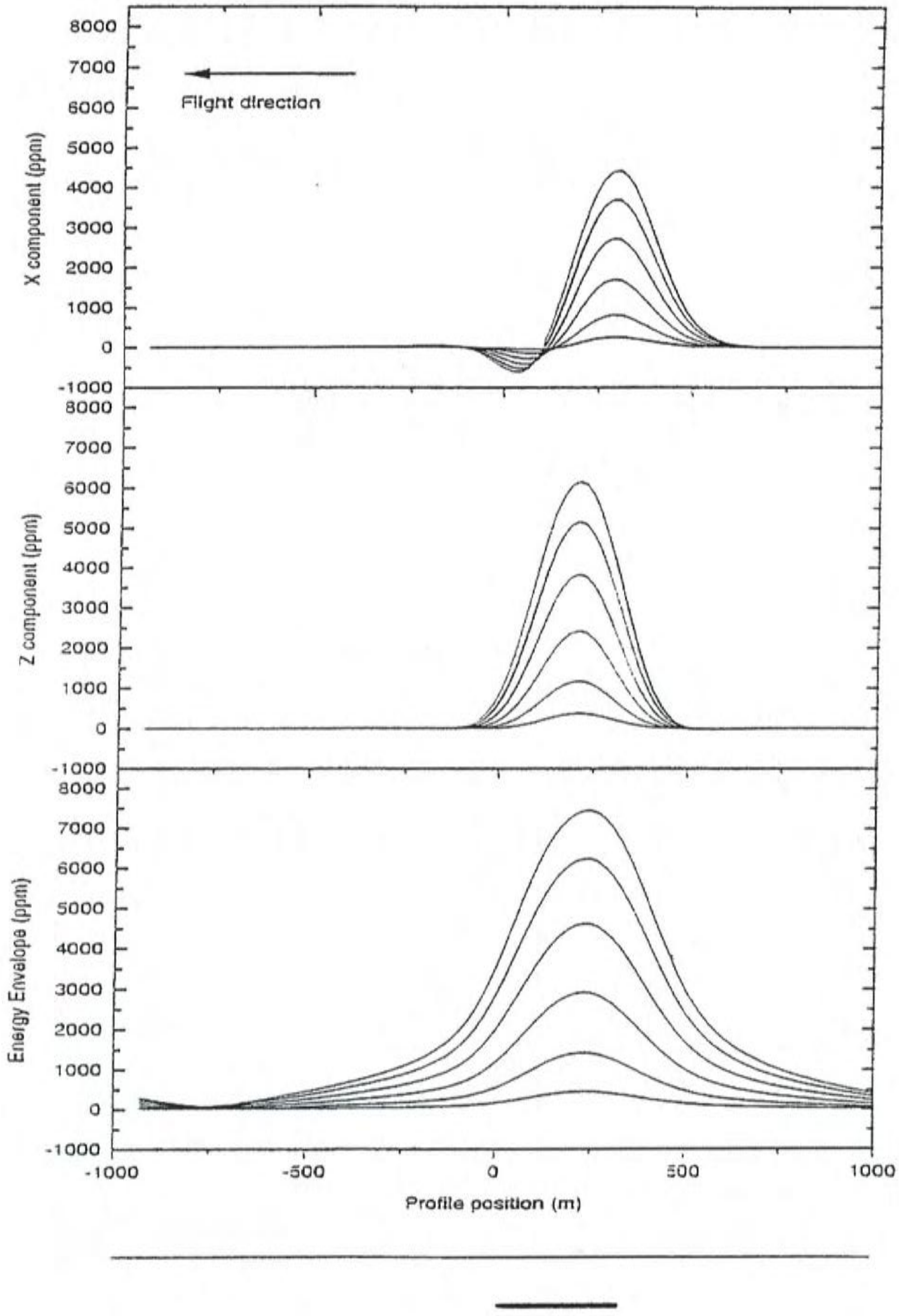

Plate: depth =150; dip =45

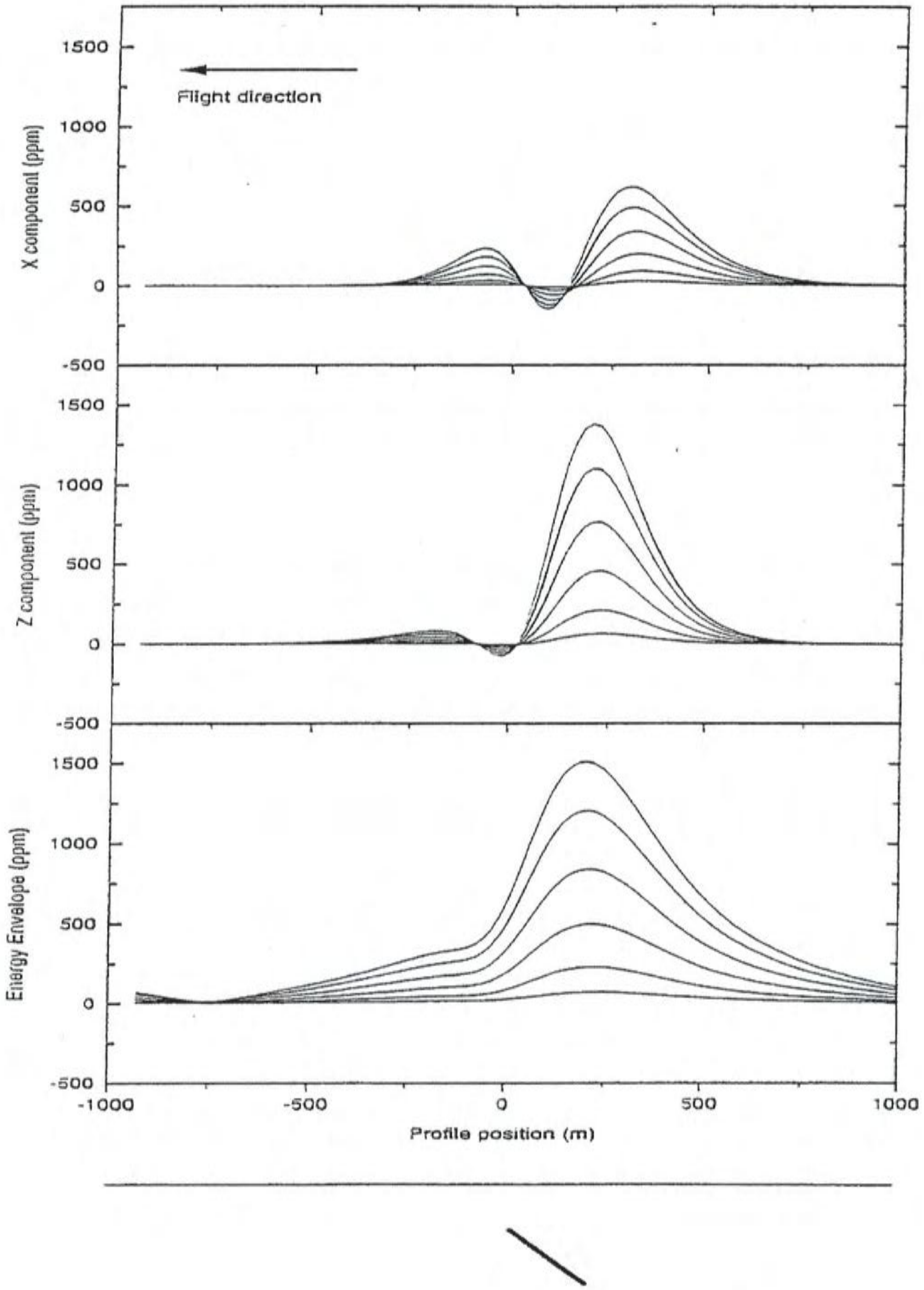

Plate: depth =150; dip =90

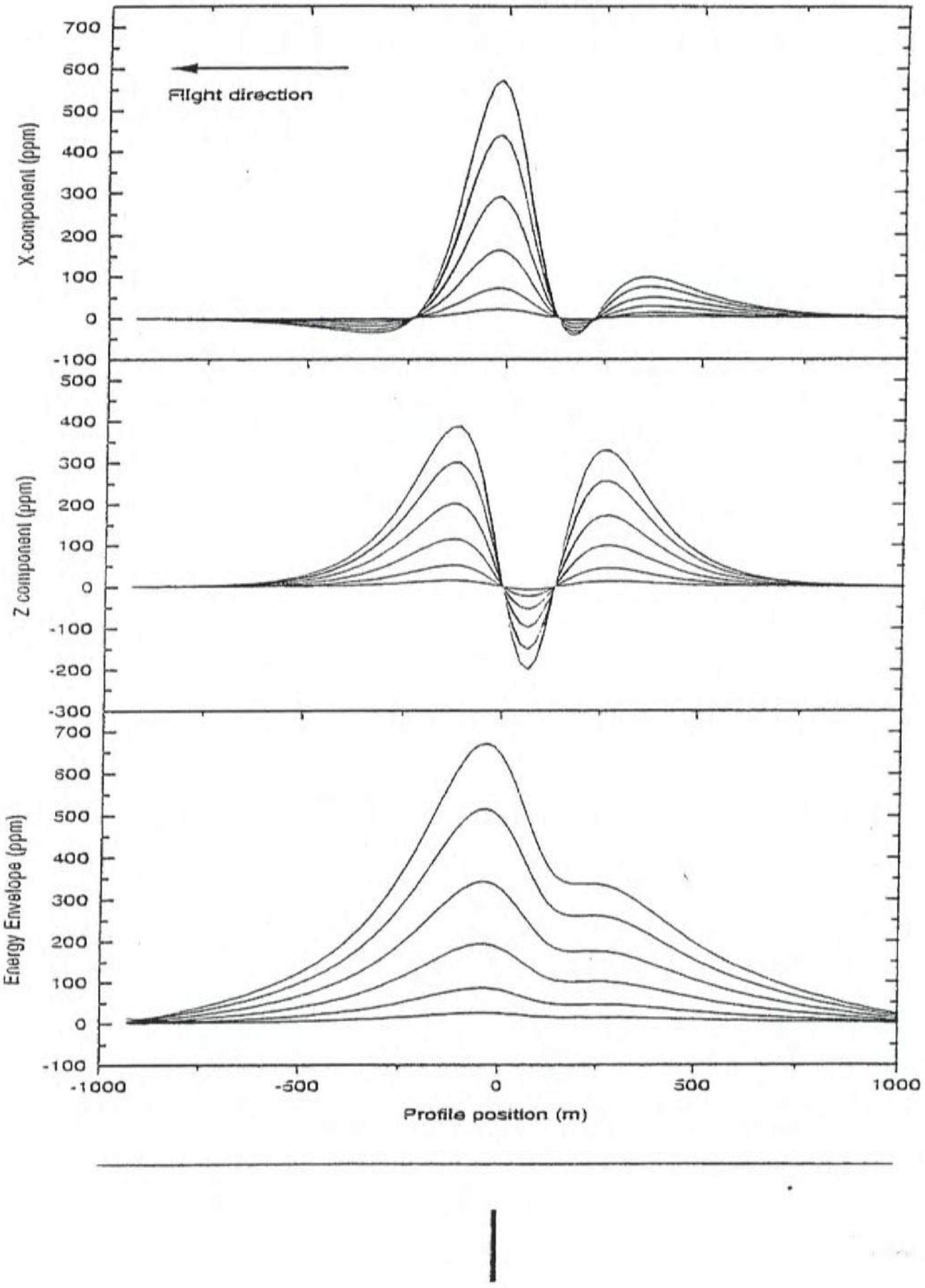

Plate: depth =150; dip =135

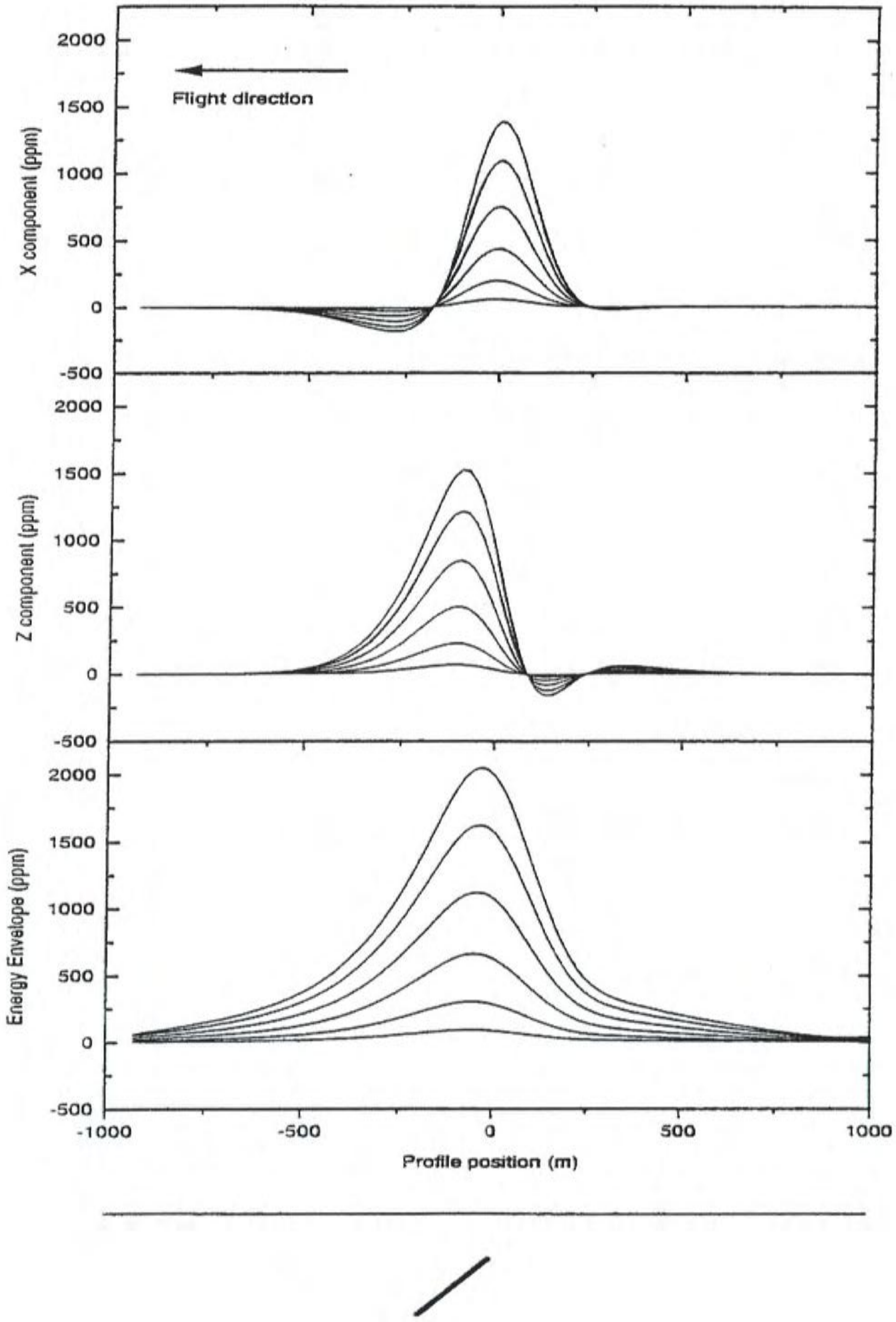

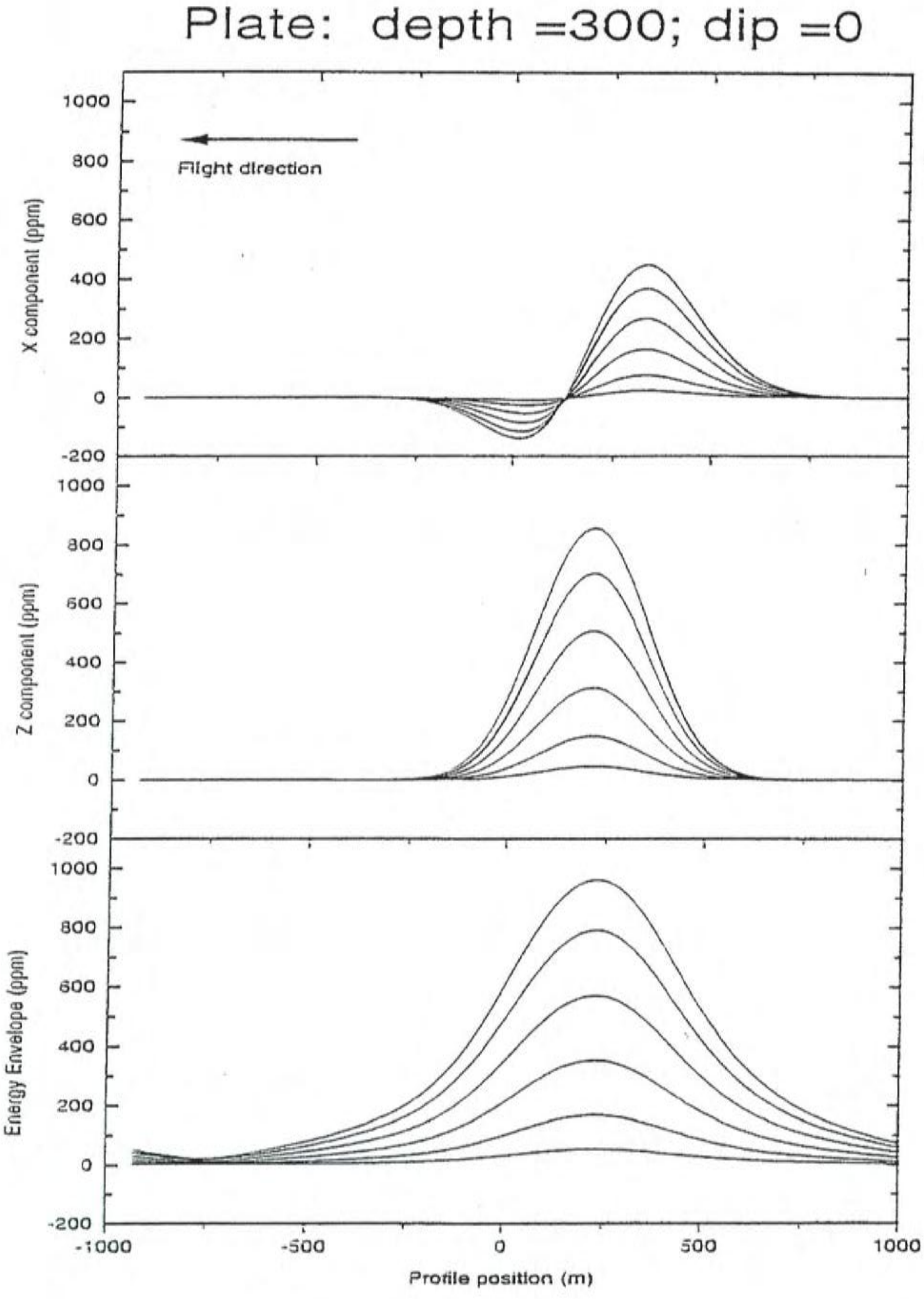

Plate: depth =300; dip =0
Flight direction
X component (ppm)
Z component (ppm)
Energy Envelope (ppm)
1000
800
600
400
200
0
-200
-1000
-500
0
500
1000
Profile position (m)

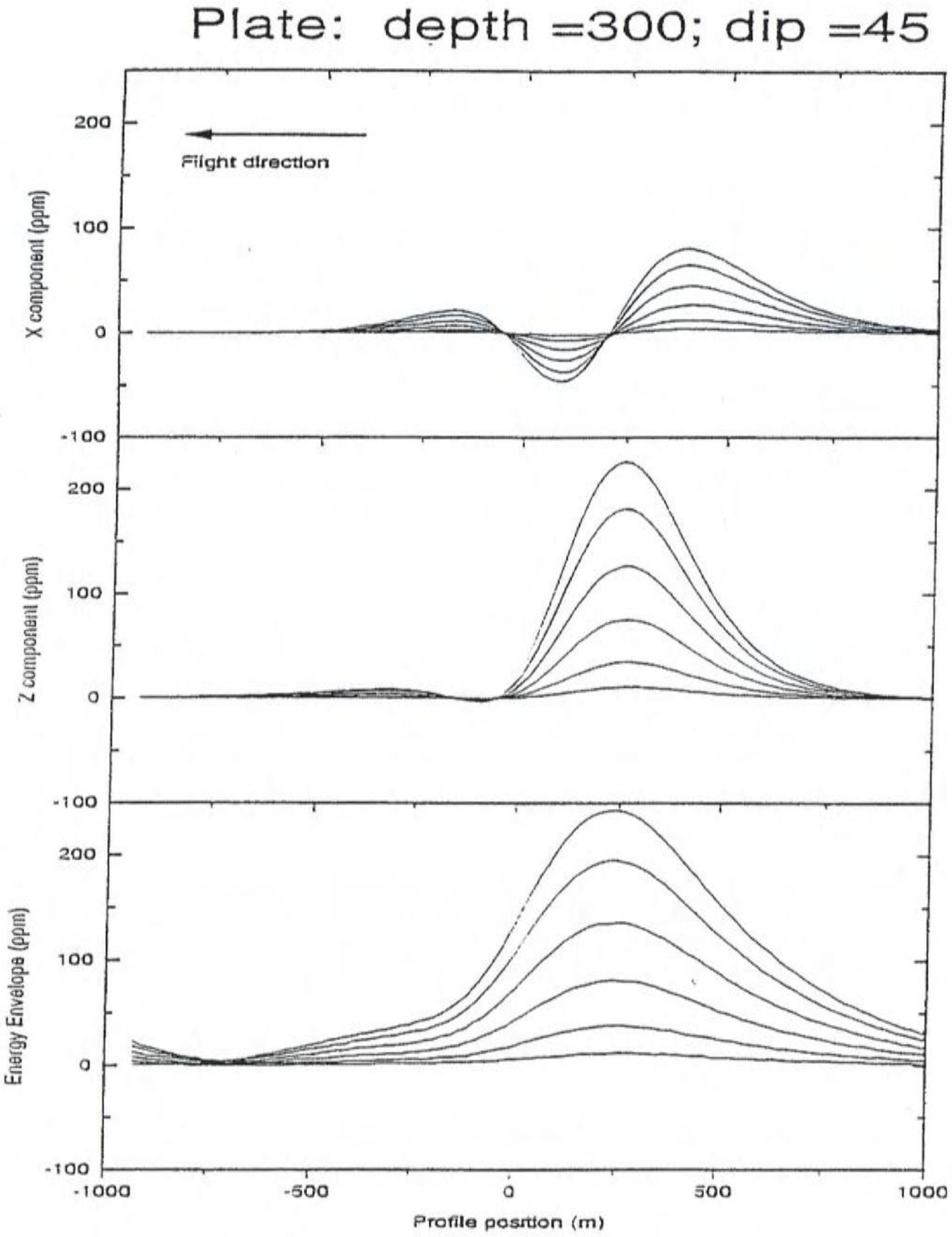
Plate: depth =300; dip =45
Flight direction
X component (ppm)
Z component (ppm)
Energy Envelope (ppm)
200
100
0
-100
-1000
-500
0
500
1000
Profile position (m)

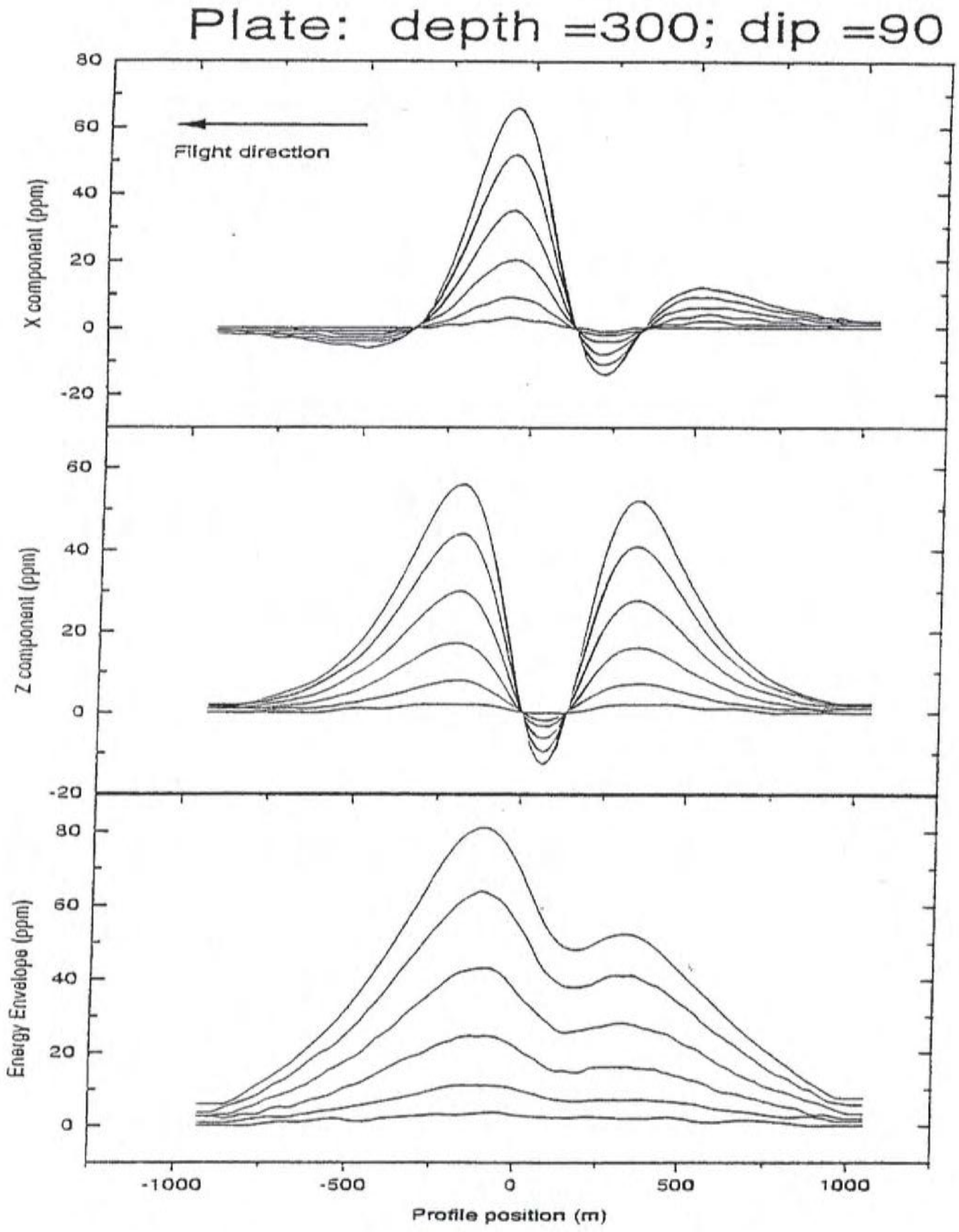
Plate: depth =300; dip =90
Flight direction
X component (ppm)
80
60
40
20
0
-20
Z component (ppm)
60
40
20
0
-20
Energy Envelope (ppm)
80
60
40
20
0
-1000
-500
0
500
1000
Profile position (m)

Plate: depth =300; dip =135

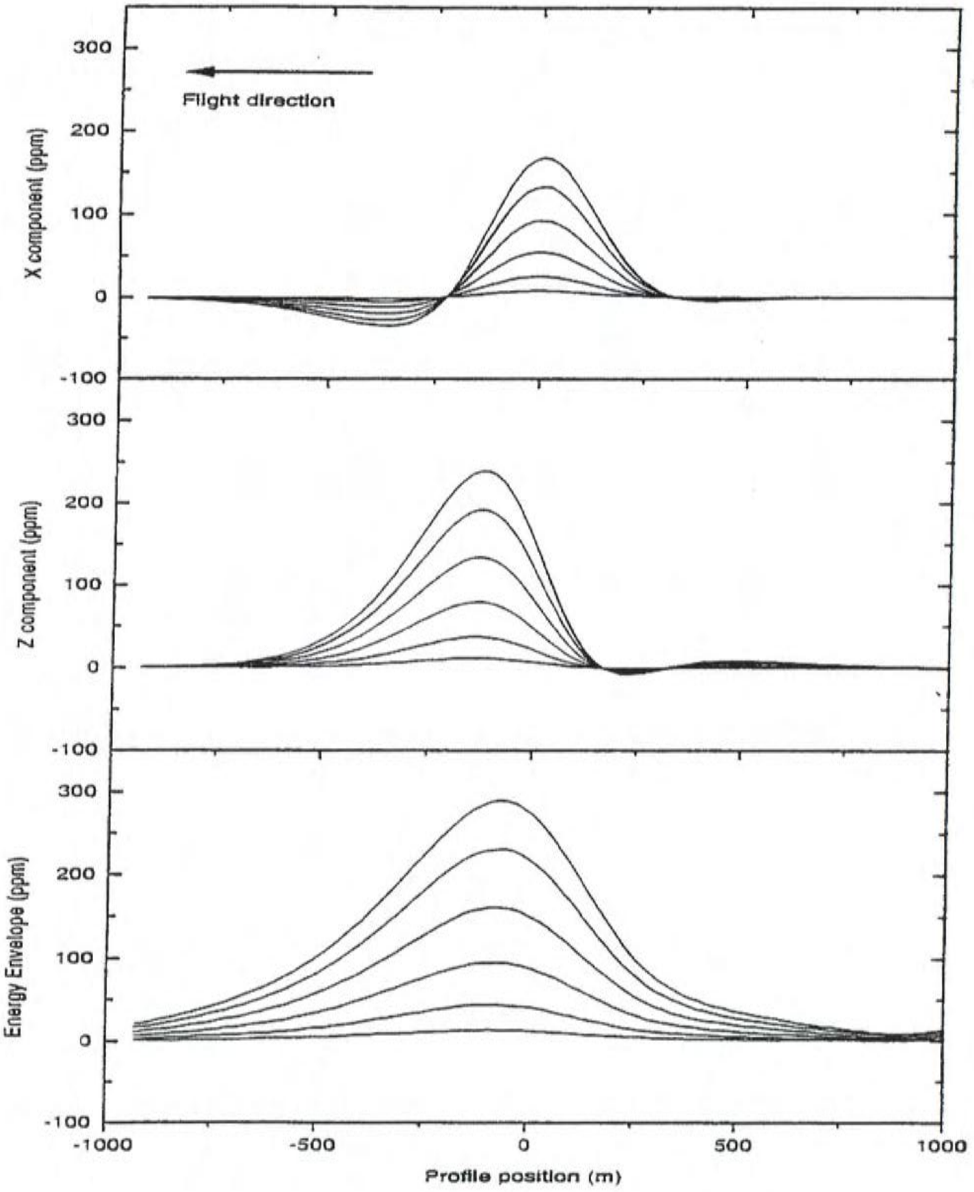

Appendix D

The Usefulness Of Multicomponent, Time-Domain Airborne Electromagnetic Measurements

GEOPHYSICS, VOL 61, NO. 1 (JANUARY-FEBRUARY 1996); P. 74-81, 17 FIGS.

The Usefulness Of Multicomponent, Time-Domain Airborne Electromagnetic Measurements

Richard S. Smith* and Pierre B. Keating ‡

ABSTRACT

Time-domain airborne electromagnetic (AEM) systems historically measure the inline horizontal (*x*) component. New versions of the electromagnetic systems are designed to collect two additional components [the vertical (*z*) and the lateral horizontal (*y*) component] to provide greater diagnostic information.

In areas where the geology is near horizontal, the *z*-component response provides greater signal to noise, particularly at late delay times. This allows the conductivity to be determined to greater depth. In a layered environment, the symmetry implies that the *y* component will be zero; hence a non-zero *y* component will indicate a lateral inhomogeneity.

Three components can be combined to give the "energy envelope" of the response. Over a vertical plate, the response profile of this envelope has a single positive peak and no side lobes. The shape of the energy envelope is dependent on the flight direction, but less so than the *x* component.

In the interpretation of discrete conductors, the *z* component data can be used to ascertain the dip and depth to the conductor using simple rules of thumb. When the profile line is perpendicular to the strike direction and over the center of the conductor, the *y* component will be zero; otherwise it appears to be a combination of the *x* and *z* components. The extent of contamination by the *x* and *z* components can be used to ascertain the strike direction and the lateral offset of the target respectively.

Having the *z* and *y* component data increases the total response when the profile line has not traversed the target. This increases the possibility of detecting a target located between adjacent flight lines or beyond a survey boundary.

Presented at the Airborne Electromagnetics Workshop, Tucson, AZ, September 13-16, 1993. Manuscript received by the Editor February 28, 1994; revised manuscript received September 16, 1994.

*Geoterrex, 2060 Walkley Rd., Ottawa, Ontario, K1G 3P5, Canada.

‡Geological Survey of Canada, 1 Observatory Crescent, Ottawa, Ontario K1A 0Y3, Canada.

INTRODUCTION

The acquisition of multiple-component electromagnetic (EM) data is becoming more commonplace. In some techniques, such as those which use the plane-wave assumption (MT, CSAMT and VLF) more than one component has been acquired as a matter of routine for some time (see reviews by Vozoff, 1990, 1991; Zonge and Hughes, 1991; McNeill and Labson, 1991). Historically, commercially available controlled-waveform finite-source systems generally measure only one component. The only systems designed to acquire multiple component data are generally experimental [e.g., those described in the appendixes of Spies and Frischknecht (1991) or proprietary (the EMP system of Newmont Exploration).

Slingram EM systems, comprising a moving dipolar transmitter and a moving receiver, generally only measure one component of the response. Although the MaxMin system was designed with a capability to measure a second (minimum coupled) component, this capability is not used extensively in practice. The only systems that use two receiver coils in practice are those that measure the wavetilt or polarization ellipse (Frischknecht et al., 1991).

Historically, time-domain EM systems have been capable of collecting multicomponent data in a sequential manner by reorienting the sensor for each component direction. The usefulness of additional components is discussed by Macnae (1984) for the case of the UTEM system. Macnae concluded that, as extra time was required to acquire the additional components, this time was better spent collecting more densely spaced vertical-component data. The vertical-component, which is less subject to sferic noise, could subsequently be converted to the horizontal components using the Hilbert transform operators.

Recent instrument developments have been towards multicomponent systems. For example, commercially available ground-EM systems such as the Geonics PROTEM, the Zonge GDP-32 and the SIROTEM have been expanded to include multiple input channels that allow three (or more) components to be acquired simultaneously. There is also a version of the UTEM system currently being developed at Lamontagne Geophysics Ltd. These multichannel receivers require complimentary multicomponent sensors -- for ground-based systems these have been developed by Geonics Ltd and Zonge Engineering and Research Organization. The interpretation of fixed-source, multi-component ground-EM data is described in Barnett (1984) and Macnae (1984).

In the past, multi-component borehole measurements have been hindered by the lack of availability of multi-component sensor probes. Following the development of two prototype probes (Lee, 1986; Hodges et al., 1991), multi-component sensors are now available from Crone Geophysics and Exploration Ltd and Geonics. Three component UTEM and SIROTEM borehole sensors are also in development at Lamontagne and Monash University (Cull, 1993), respectively. Hodges et al. (1991) present an excellent discussion of techniques that can be used to interpret three-component borehole data.

Airborne systems such as frequency-domain helicopter electromagnetic methods acquire data using multiple sensors. However, each receiver has a corresponding transmitter that either operates at a different frequency or has a different coil orientation (Palacky and West, 1991). Hence, these systems are essentially multiple single-component systems. The exception to this rule is the now superseded Dighem III system (Fraser, 1972) which used one transmitter and three receivers.

The only multicomponent airborne EM (AEM) system currently in operation is the SPECTREM system (Macnae, et al., 1991). This is a proprietary (owned and operated by Anglo-

American Corporation of South Africa Ltd.), based on the PROSPECT system (Annan, 1986). The Prospect system was originally designed to acquire the x, y and z components, but SPECTREM is apparently only collecting two components (x and z) at the time of writing. Other multi-component systems currently in development are:

i) the SALTMAP system,
ii) a helicopter time-domain system (Hogg, 1986), and
a new version of the GEOTEM® system (GEOTEM is a registered trademark of Geoterrex).

Apart from a few type curves in Hogg (1986), there is little literature available which describes how to interpret data from these systems.

This paper is intended to give an insight into the types of responses expected with the new multi-component AEM systems, and the information that can be extracted from the data. The insight could be of some assistance in interpreting data from multicomponent moving-source ground EM systems (should this type of data be acquired).

The use of multi-component data will be discussed for a number of different applications. For illustration purposes, this paper will use the transmitter-receiver geometry of the GEOTEM system (Figure 1), which is comparable to the other fixed-wing geometries (SPECTREM and SALTMAP). The GEOTEM system is a digital transient EM system utilizing a bipolar half-sinusoidal current waveform [more details are in Annan and Lockwood (1991)]. The sign convention used in this paper is shown in Figure 1, with the *y* component being into the page. In a practical EM system, the receiver coils will rotate in flight. We will assume that the three components of the measured primary field and an assumed bird position have been used to correct for any rotation of the coil.

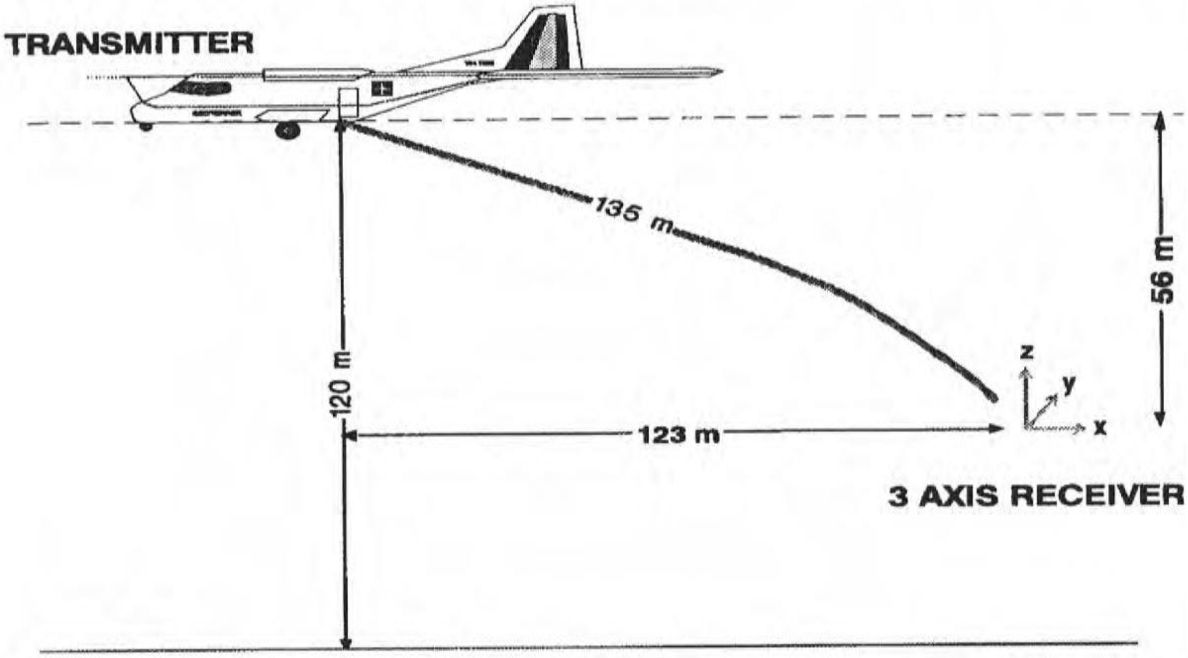

Figure 1: The geometric configuration of the GEOTEM system. The system comprises a transmitter on the aircraft and a receiver sensor in a "bird" towed behind the aircraft. The z direction is positive up, x is positive behind the aircraft, and y is into the page (forming a right-hand coordinate system).

SOUNDING IN LAYERED ENVIRONMENTS

In a layered environment, the induced current flow is horizontal (Morrison et al., 1969) so the *z* component of the secondary response (V_z) is much larger than the *x* component (V_x), particularly in resistive ground and/or at late delay times. At the same time, the sferic noise in the *z* direction is 5 to 10 times less than in the horizontal directions(Macnae, 1984; McCracken et al., 1986), so V_z has a greater signal-to-noise ratio. Figure 2 shows theoretical curves over two different, but similar, layered earth models. One model is a half-space of 500 Ω·m and the other is a 350 m thick layer of 500 Ω·m overlying a highly resistive basement. In this plot the data have been normalized by the total primary field. The *z* component (V_z) is 6 to 10 times larger than V_x, and both curves are above the noise level, at least for part of the measured transient. On this plot, a noise level of 30 ppm has been assumed, which would be a typical noise level for both components when the sferic activity is low. To distinguish between the response of the half-space and thick layer, the difference between the response of one model and the response of the other model must be greater than the noise level. Figure 3 shows this difference for both components. Only the V_z difference is above the noise level. Hence for the case shown, V_z is more useful than V_x for determining whether there is a resistive layer at 350 m depth. Because V_z is generally larger in a layered environment, the vertical component will generally be better at resolving the conductivity at depth.

In the above discussion, we have assumed that corrections have been made for the coil rotation. An alternative approach is to calculate and model the magnitude of the total field, as this quantity is independent of the receiver orientation. Macnae et al. (1991) used this strategy when calculating the conductivity depth sections for SPECTREM data.

The symmetry of the secondary field of a layered environment is such that the *y* component response (V_y) will always be zero. In fact, the V_y component will be zero whenever the conductivity structure on both sides of the aircraft is the same. A non-zero V_y is therefore useful in identifying off-line lateral inhomogeneities in the ground.

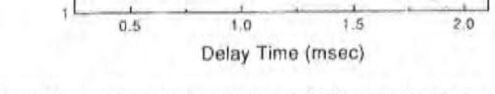

Figure 2: The response for a 500 Ω·m half-space (solid line) and a 500 Ω·m layer of thickness 350 m overlying a resistive half-space (dashed line). The *z*-component responses are the two curves with the larger amplitudes and the two *x*-component response curves are 6 to 10 times smaller than the corresponding *z* component. A noise level of 30 ppm is considered to be typical of both components in the absence of strong sferics.

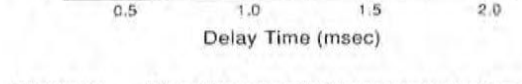

Figure 3: The difference in the response of each component for the half-space and thick layer models of Figure 2. Only the *z* component difference is above the noise level for a significant portion of the transient. Therefore, this is the only component capable of distinguishing between the responses of the two models.

DISCRETE CONDUCTORS

In our discrete conductor study, models have been calculated using a simple plate in free-space model (Dyck and West, 1984) to provide some insight into the geometry of the induced field. The extension to more complex models, such as those incorporating current gathering, will not be considered in this paper.

Historically, airborne transient electromagnetic (TEM) data have been used for conductor detection. The old INPUT system was designed to measure V_x because this component gave a large response when the receiver passed over the top of a vertical conductor. The bottom part of Figure 4 shows the response over a vertical conductor, which has been plotted at the receiver position. The V_x profile (smaller of the two solid lines) has a large peak corresponding with the conductor position. Note that there is also a peak at 200 m, just before the transmitter passes over the conductor, and a trailing edge negative to the left of the conductor. The z component (dashed line) has two peaks and a large negative trough just before the conductor. Because of the symmetry, the V_y response (dotted line) is zero.

All the peaks, troughs and negatives make the response of a single conductor complicated to display and hence interpret. The display can be simplified by plotting the "energy envelope" (EE) of the response. This quantity is defined as follows:

$$EE = \sqrt{V_x^2 + \overline{V}_x^2 + V_y^2 + \overline{V}_y^2 + V_z^2 + \overline{V}_z^2},$$

where $\overline{}$ denotes the Hilbert transform of the quantity. The energy envelope plotted on Figure 4 (the larger of the two solid curves) is almost symmetric, and would be a good quantity to present in plan form (as contours or as an image). For flat-lying conductors, the energy envelope has a maximum at the leading edge (just after the aircraft flies onto the conductor).

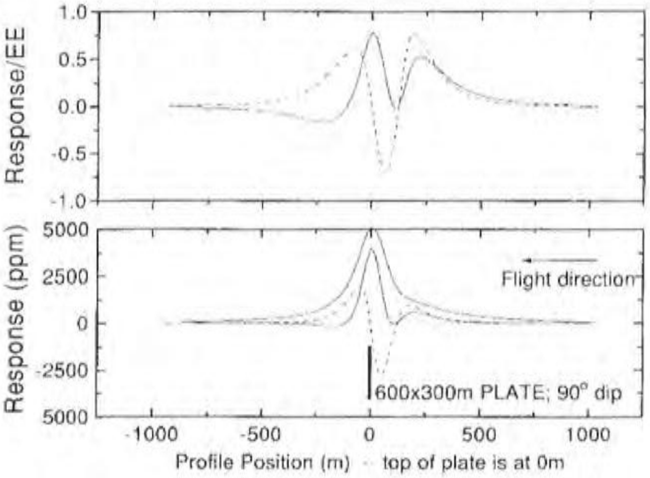

Figure 4: (Bottom) The response of a 600 by 300 m plate 120 m below an aircraft flying from right to left. The plotting point for the response is below the receiver. The x-component response is the smaller amplitude solid line, the z-component is the dashed line, and the y-component response is the dotted line. The larger amplitude solid line is the "energy envelope" of all three components. (Top) The z- and x-components normalized by the energy envelope. These and all subsequent curves are for a delay time of 0.4 ms after the transmitter current is turned off.

What little asymmetry remains in the energy envelope is a good indication of the coupling of the AEM system to the conductor. If the response profile for each component is normalized by the energy envelope, then the effect of system coupling will be removed (at least partially) and the profiles will appear more symmetric. For example, the top part of Figure 4 shows the Vx and Vz normalized by the energy envelope at each point. The size of the two x peaks and the two z peaks are now roughly comparable.

Dip determination

The response of a plate with a dip of 120° is shown on Figure 5. For the V_x/EE and V_z/EE profiles, the peak on the down dip side is larger. For shallow dips, it becomes difficult to identify both V_x/EE peaks, but the two positive V_z/EE peaks remain discernable. Plotting the ratio of the magnitudes of these two V_z/EE peaks, as has been done with solid squares on Figure 6, shows that the ratio is very close to the tangent of the dip divided by 2. Hence, calculating the ratio of the peak amplitudes (R) will yield the dip angle θ using the following formula:

$$\theta = 2 \tan^{-1}(R).$$

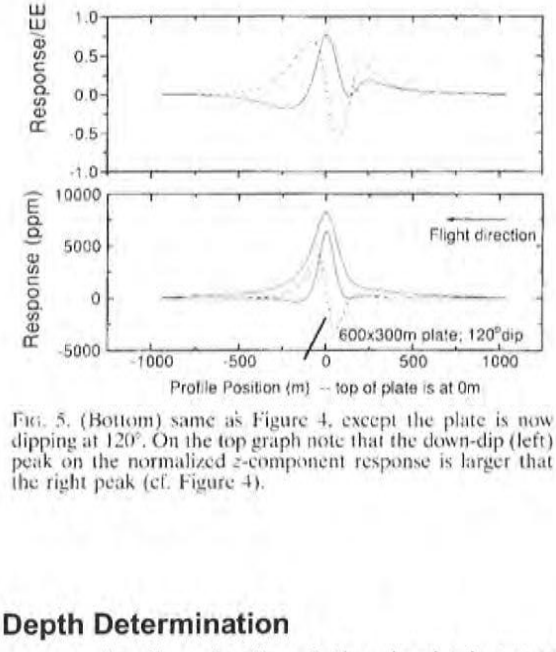

FIG. 5. (Bottom) same as Figure 4, except the plate is now dipping at 120°. On the top graph note that the down-dip (left) peak on the normalized z-component response is larger that the right peak (cf. Figure 4).

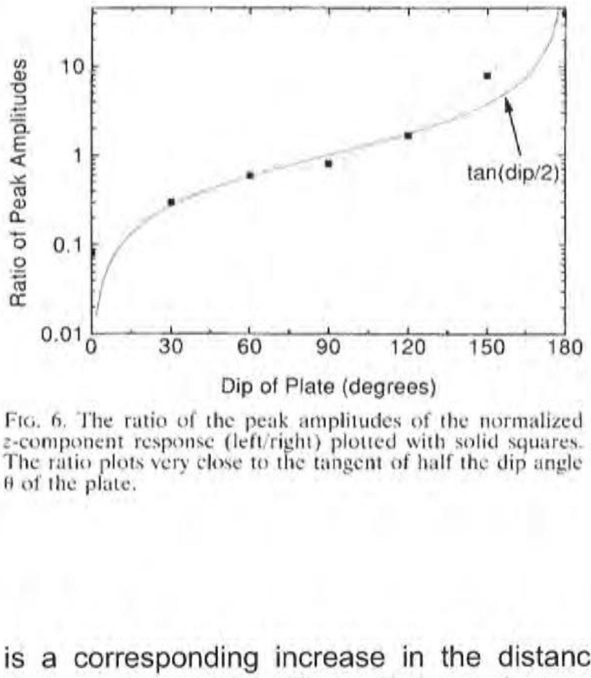

FIG. 6. The ratio of the peak amplitudes of the normalized z-component response (left/right) plotted with solid squares. The ratio plots very close to the tangent of half the dip angle θ of the plate.

Depth Determination

As the depth of the body increases, there is a corresponding increase in the distance between the two positive peaks in the V_z/EE profile. As an example of this, Figure 7 shows the case of a plate 150 m deeper than the plate of Figure 4. The peaks are now 450 m apart, as compared with 275 m on Figure 4. A plot of the peak-to-peak distances for a range of depths is shown on Figure 8 for plates with 60, 90 and 120° dips. Because the points follow a straight line, it can be concluded that for near vertical bodies (60° to 120° dips), the depth to the top of the body d can be determined from the measured peak-to-peak distances using the linear relationship depicted in Figure 8. The expected error would be about 25 m. Such an error is tolerable in airborne EM interpretation. More traditional methods for determining d analyze the rate of decay of the measured response (Palacky and West, 1973). Our method requires only the V_z/EE response profile at a single delay time. Analyzing this response profile for each delay time allows d to be determined as a function of delay time, and hence any migration of the current system in the conductor could be tracked.

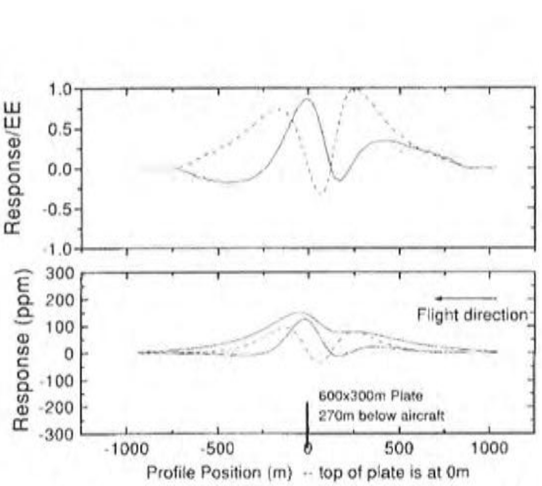

FIG. 7. The same as Figure 4, except the plate is now 270 m below the aircraft. Note that the distance between the z-component peaks is now much greater.

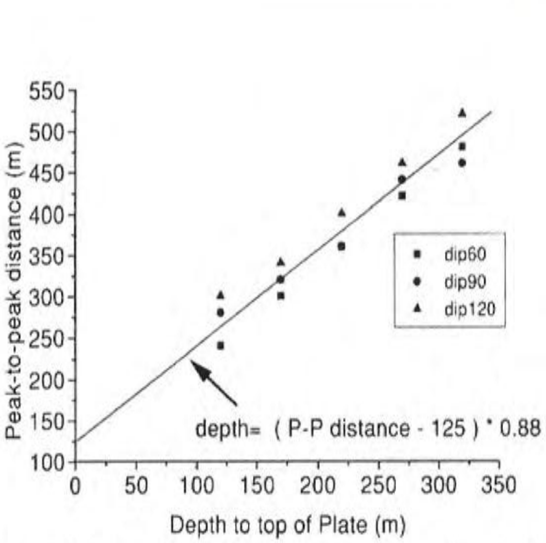

FIG. 8. The peak-to-peak distance as a function of plate depth for three different dip angles θ. A variation in dip of ±30° does not result in a large change in the peak-to-peak distance.

Strike and offset determination

The response shown in Figure 4 varies in cases when the plate has a strike different from 90° or the flight path is offset from the center of the plate.

Figure 9 shows the response for a plate with zero offset and Figure 10 shows the plate when it is offset by 150 m from the profile line. The calculated voltages V_z and V_x are little changed from the no offset case, but the V_y response, is no longer zero. In fact, the shape of the V_y curve appears to be the mirror image of the V_z curve.

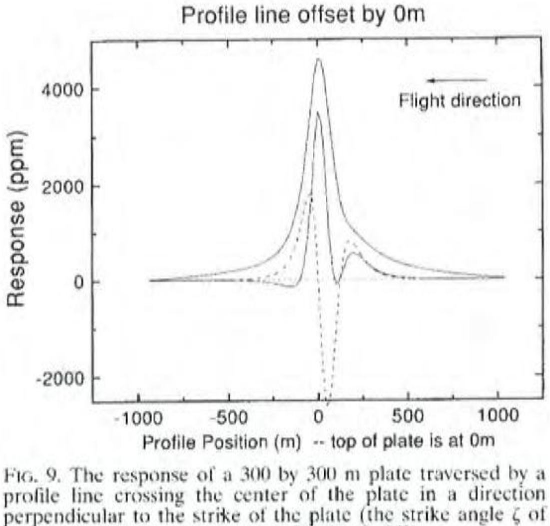

FIG. 9. The response of a 300 by 300 m plate traversed by a profile line crossing the center of the plate in a direction perpendicular to the strike of the plate (the strike angle ζ of the plate with respect to the profile line is 90°).

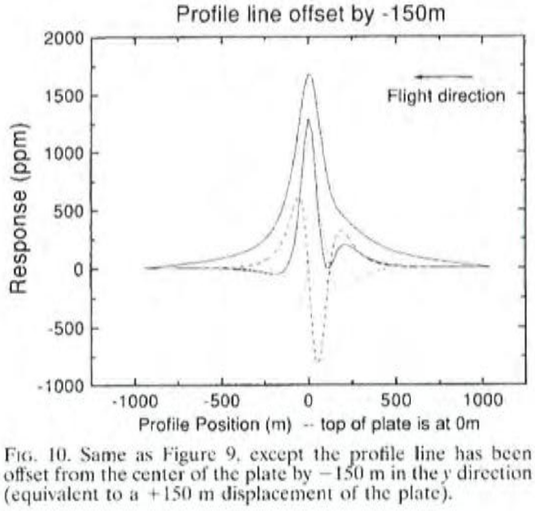

FIG. 10. Same as Figure 9, except the profile line has been offset from the center of the plate by −150 m in the y direction (equivalent to a +150 m displacement of the plate).

In the case when the plate strikes at 45°, the *y* component is similar in shape but opposite in sign to the *x*-component response (Figure 11).

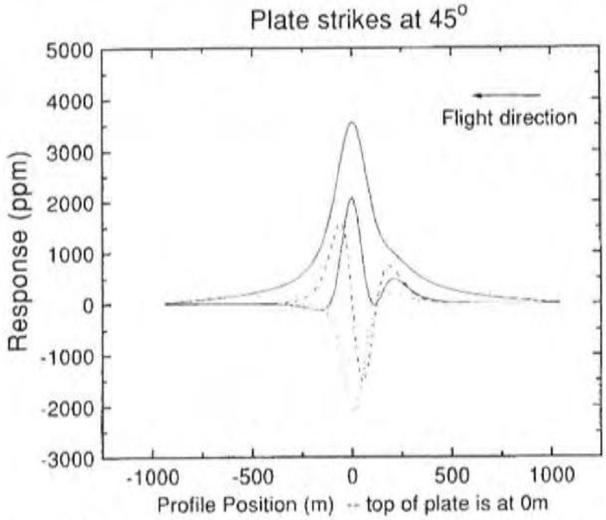

FIG. 11. Same as Figure 9, except the profile line traverses the plate such that the strike angle ζ of the plate, with respect to the profile line, is 45°.

These similarities can be better understood by looking at schematic diagrams of the secondary field from the plate. Figure 12 shows a plate and the field in section. For zero offset, the field is vertical (*z* only). As the offset increases, the aircraft and receiver moves to the right and the measured field rotates into the *y*-component.

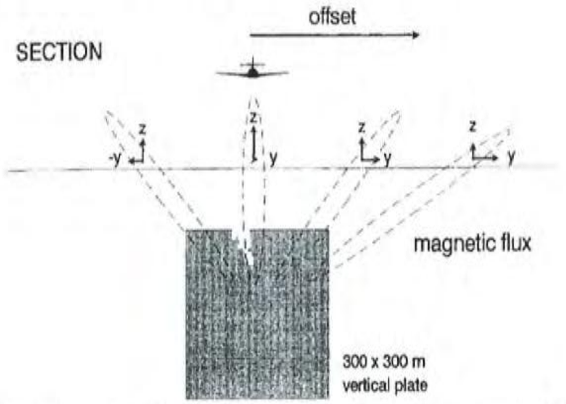

FIG. 12. A schematic diagram of the plate and the magnetic flux of the secondary field (section view). For increasing offset of the aircraft and receiver from the center of the plate, the magnetic field at the receiver rotates from the *z* to the *y* component.

The secondary field is depicted in plan view in Figure 13. Variable strike is simulated by leaving the plate stationary and changing the flight direction. When the strike of the plate is different from 90°, the effective rotation of the EM system means that the secondary field, which was previously measured purely in the *x* direction, is now also measured in the *y* direction.

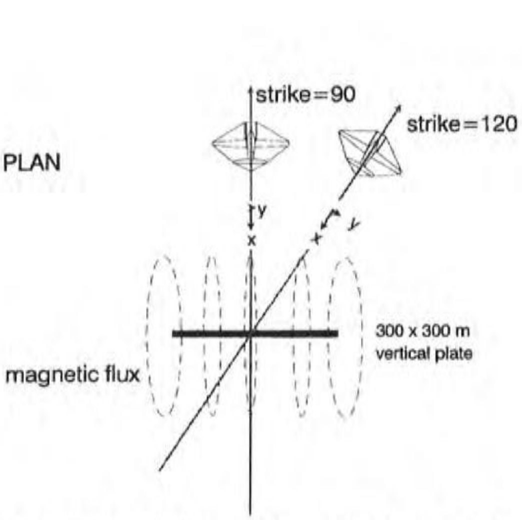

FIG. 13. A schematic diagram of the plate and the magnetic flux of the secondary field (plan view). Here varying strike is depicted by an equivalent variation of the flight direction. As the flight direction rotates from a strike angle of 90°, the receiver rotates so as to measure a greater response in the y direction.

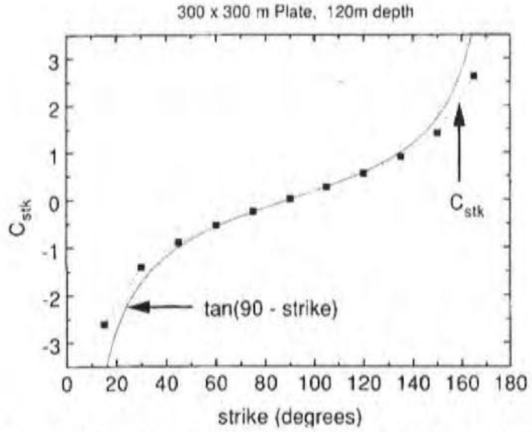

FIG. 14. The ratio $C_{stk} = V_y/V_x$ plotted as a function of varying strike angle (solid squares). The data agree very closely with the cotangent of the ζ.

The *y* component (V_y) can thus be considered to a be a mixture of V_x and V_z components,

$$V_y = C_{stk} V_x + C_{off} V_z ,$$

an equation that is only approximate. The response for a variety of strike angles and offset distances has been calculated and in each case the *y*-component response has been decomposed into the *x* and *z* components by solving for the constants of proportionality C_{stk} and C_{off}.

A plot of C_{stk} for the case of zero offset and varying strike direction ξ is seen on Figure 14. The values of C_{stk} determined from the data are plotted with solid squares and compared with the tan(90°- ξ). Because the agreement is so good, the formula

$$\xi = 90 - \tan^{-1} (C_{stk})$$

can be used to determine the strike. This relation was first obtained by Fraser (1972).

When the strike is fixed at 90°, and the offset varies, the corresponding values obtained for C_{off} have been plotted with solid squares on Figure 15. Again, there is good agreement with the arctangent of C_{off} and the angle φ between a vertical line and the line that joins the center of the top edge of the plate with the position where the aircraft traverse crosses the plate containing the plate. If an estimate of the distance to the top of the conductor *D* is already obtained using the method described above, or by the method described in Palacky and West (1973), then

$$D = \sqrt{(O2 + d2)} ,$$

(where *d* is the depth below surface). Hence, the offset distance *O* can be written as follows

$$O = d \tan (\varphi)$$
$$= d\, C_{off}$$
$$= C_{off} \sqrt{(D^2 - O^2)}$$

which can be rearranged to give

$$O = C_{off}\, D / \sqrt{(1 + C_{off}^2)} .$$

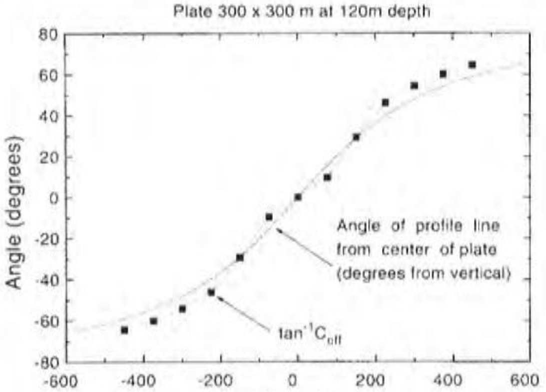

FIG. 15. The arctangent of $C_{eff} = V_y/V_z$, plotted as a function of varying offset (solid squares). There is good agreement between this quantity and the angle ϕ between a vertical line and the line from the center of the top edge of the plate to the profile line.

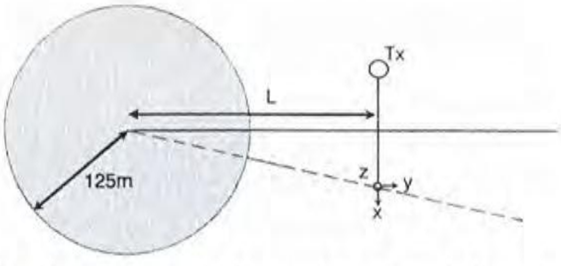

FIG. 16. Plan view of a flat-lying conductor (a circular loop with a radius of 125 m). The AEM system is offset a distance L from the center of the conductor in a direction perpendicular to the traverse direction. The traverse direction of the system is from the bottom to the top of the figure.

Lateral detectability

Figure 12 illustrates that V_y becomes relatively strong as the lateral displacement from the conductor is increased. Thus, if V_y is measured, then the total signal will remain above the noise level at larger lateral displacements of the traverse line from the conductor. This has been illustrated by assuming a flat-lying conductor, here approximated by a wire-loop circuit of radius 125 m (Figure 16). The *x*, *y* and *z* components of the response have been computed using the formula for the large-loop magnetic fields in Wait (1982). The results are plotted on Figure 17 as a function of increasing lateral displacement *L* of the transmitter/receiver from the center of the conductor. The transmitter and receiver are separated in a direction perpendicular *L* to simulate the case when the system is maximal coupled to the conductor, but the flight line misses the target by an increasing amount. The effect of varying the conductance or measurement time has been removed by normalizing the response to the total response measured when the system is at zero displacement. At displacements greater than 80 m, the *y* component is clearly larger than any other component. Assuming the same sensitivity and noise level for each component (which is a realistic assumption if the data are corrected for coil rotation and the sferic activity is low), it is clearly an advantage to measure V_y, as this will increase the chances of detecting the target when the flight line has not passed directly over the conductor.

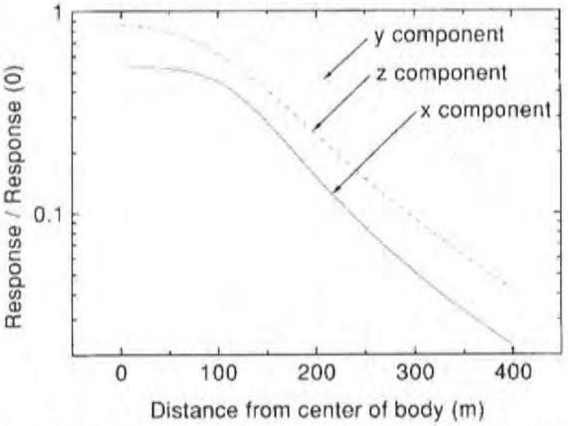

FIG. 17. The normalized response of the EM system plotted as a function of increasing offset distance L. The x component falls off most rapidly and the y component most slowly with increasing offset distance.

CONCLUSIONS

AEM systems measuring three components of the response can be used to infer more and/or better information than those systems that measure with only one component, i.e., V_x.

The z-component data enhances the ability of the AEM system to resolve layered structures as the z-component has a larger signal and a smaller proportion of sferic noise than any other component. If all the components are employed to correct for coil rotation, then the data quality and resolving power is increased further, as individual components are not contaminated by another component. Having better signal-to-noise and greater fidelity in the data will allow deeper layers to be interpreted with confidence.

A non-zero *y* component is helpful in identifying when the conductivity structure has a lateral inhomogeneity that is not symmetric about the flight line.

All components can be used to calculate the energy envelope, which is a valuable quantity to image. The energy envelope has a single peak over a vertical conductor and two peaks over a dipping conductor (one at either end). The asymmetry in the response profile of each individual component can be reduced by normalizing each profile by the energy envelope.

All three components are of great use in determining the characteristics of discrete conductors. For example, the distance between the two positive peaks in the V_z/EE profile can be employed to determine the depth. Also, the ratio of the magnitude of the two V_z/EE peaks helps to ascertain the dip of the conductor. The *x* component has been used in the past for these purposes, but is not as versatile, as it requires the data at all delay times, or an ability to identify a very small peak.

The *y* component can be utilized to extract information about the conductor that cannot be obtained from single component AEM data. The degree of mixing between the *y* and *z* components can give the lateral offset of the conductor (provided the depth is known), while the mixing between the *y* and *x* component gives the strike of a vertical conductor.

Finally, because the *y* component decreases most slowly with increasing lateral offset, this component gives an enhanced ability to detect a conductor positioned at relatively large lateral distances from the profile line, either between lines or beyond the edge of a survey boundary.

ACKNOWLEDGMENTS

The authors wish to thank Geoterrex for the permission to publish the results of this model study. This paper has been allocated Geological Survey of Canada Contribution No. 36894.

REFERENCES

Annan, A. P., 1986, Development of the PROSPECT I airborne electromagnetic system, in Palacky. G. J., Ed., Airborne resistivity mapping : Geol. Surv. Can. Paper 86-22, 63-70.

Annan, A. P., and Lockwood, R., 1991, An application of airborne GEOTEM in Australian conditions: Expl., Geophys., 22, 5-12.

Barnett, C. T., 1984, Simple inversion of time-domain electromagnetic data: Geophysics, 49, 925-933.

Cull, J. P., 1993, Downhole three component TEM probes: Expl. Geophys., 24, 437-442.

Dyck, A. V., and West G. F., 1984, The role of simple computer models in interpretations of wide-band, drill-hole electromagnetic surveys in mineral exploration: Geophysics, 49, 957-980.

Fraser, D. C., 1972, A new multicoil aerial electromagnetic prospecting system: Geophysics, 37, 518-537.

Frischknecht, F. C., Labson, V. F., Spies, B. R., and Anderson, W. L., 1991, Profiling methods using small sources, in Nabighian M. N., Ed., Electromagnetic methods in applied geophysics, Vol. 2, Applications: Soc. Expl. Geophys. Investigations in geophysics, no. 3, 105-270.

Hodges, D. G., Crone, J. D., and Pemberton, R., 1991, A new multiple component downhole pulse EM probe for directional interpretation: Proc. 4th Int. MGLS/KEGS Sym. on Borehole Geophys. For Min. Geotech. And Groundwater Appl.

Hogg, R. L. S., 1986, The Aerodat multigeometery, broadband transient helicopter electromagnetic system, in Palacky. G. J., Ed., Airborne resistivity mapping: Geol. Surv. Can. Paper 86-22, 79-89.

Lee, J., 1986, A three component drill-hole EM receiver probe: M.Sc. thesis, Univ. of Toronto.

Macnae, J. C., 1984, Survey design for multicomponent electromagnetic systems: Geophysics, 49, 265-273.

Macnae, J. C., Smith, R. S., Polzer, B. D., Lamontagne, Y., and Klinkert, P. S., 1991, Conductivity-depth imaging of airborne electromagnetic step-response data: Geophysics, 56, 102-114.

McCracken, K. G., Oristaglio, M. L., and Hohmann, G. W., 1986, Minimization of noise in electromagnetic exploration systems: Geophysics, 51, 819-132.

McNeill, J.D., and Labson, V., 1991, Geological mapping using VLF radio fields, in Nabighian M. N., Ed., Electromagnetic methods in applied geophysics, Vol. 2, Applications: Soc. Expl. Geophys. Investigations in geophysics, no. 3, 521-640.

Morrison, H.F., Phillips, R.J., and O'Brien, D.P., 1969, Quantitative interpretation of transient electromagnetic fields over a layered earth: Geophys. Prosp. 17, 82-101.

Palacky, G. J., and West, G. F., 1973, Quantitative measurements of Input AEM measurements: Geophysics, 38, 1145-1158.

Palacky, G. J., and West, G. F., 1991, Airborne electromagnetic methods, in Nabighian M. N., Ed., Electromagnetic methods in applied geophysics, Vol. 2, Applications: Soc. Expl. Geophys. Investigations in geophysics, no. 3, 811-879.

Spies, B. R., and Frischknecht, F. C., 1991, Electromagnetic sounding, in Nabighian M. N., Ed., Electromagnetic methods in applied geophysics, Vol. 2, Applications: Soc. Expl. Geophys. Investigations in geophysics, no. 3, 285-425.

Vozoff, K., 1990, Magnetotellurics: Principles and practices: Proc. Indian Acad. Sci., 99, 441-471.

Vozoff, K., 1991, The magnetotelluric method, in Nabighian M. N., Ed., Electromagnetic methods in applied geophysics, Vol. 2, Applications: Soc. Expl. Geophys. Investigations in geophysics, no. 3, 641-711.

Wait, J. R., 1982, Geo-electromagnetism: Academic Press Inc.

Zonge K. L., and Hughes, L. J., 1991, Controlled-source audio-magnetotellurics, in Nabighian M. N., Ed., Electromagnetic methods in applied geophysics, Vol. 2, Application: Soc. Expl. Geophys. Investigations in geophysics, no. 3, 713-809

Appendix E

Data Archive Description

Data Archive Description:

Survey Details

Survey Area Name	Old Fort Bay Property
Job number	04430
Client	Triex Minerals Corp.
Survey Company Name	Fugro Airborne Surveys
Flown and compiled dates	October 20th – November 12th, 2004
Archive Creation Date	January, 2005

Survey Specifications

Traverse Line Azimuth	090°-270°
Traverse Line Spacing	400 m
Tie Line Azimuth	000°-180°
Tie Line Spacing	2000 m
Flying Elevation	120 m Mean Terrain Clearance
Average Aircraft Speed	70 m/s

Geodetic Information for map products

Projection:	Universal Transverse Mercator
Datum:	NAD83
Central meridian:	111° West
False Easting:	500000 metres
False Northing:	0 metres
Scale factor:	0.9996
UTM Zone	12 North
I.G.R.F. Model	2003
I.G.R.F. Correction Date	2004.95

Equipment Specifications:

Navigation

Differential GPS Receiver	NovAtel Propak 4E-3151-R 12 Channel
Aircraft	DeHavilland DHC-7-102 Dash-7
Video Camera	Panasonic WV-CL302

Magnetics

Type	Scintrex CS-2 Cesium Vapour
Installation	Towed bird
Sensitivity	0.01 nT
Sampling	0.10s

Electromagnetics

Type	MEGATEM®, 20 channel multicoil system
Installation	Vertical axis loop (406m^2 area with 6 turns) mounted on the aircraft. Receiver coils in a towed bird.
Coil Orientation	X, Y and Z
Frequency	90 Hz
Pulse width	2287 µs
Off-time	3169 µs
Geometry	Tx-Rx horizontal separation of ~130 m Tx-Rx vertical separation of ~50 m
Sampling	0.25 s

Data Windows:

CHANNEL	START (P)	END (P)	WIDTH (P)	START (MS)	END (MS)	WIDTH (MS)	MID (MS)
1	4	11	8	0.130	0.477	0.347	0.304
2	12	25	14	0.477	1.085	0.608	0.781
3	26	39	14	1.085	1.693	0.608	1.389
4	40	53	14	1.693	2.300	0.608	1.997
5	54	59	6	2.300	2.561	0.26	2.431
6	60	61	2	2.561	2.648	0.087	2.604
7	62	64	3	2.648	2.778	0.130	2.713
8	65	67	3	2.778	2.908	0.130	2.843
9	68	71	4	2.908	3.082	0.174	2.995
10	72	75	4	3.082	3.255	0.174	3.168
11	76	79	4	3.255	3.429	0.174	3.342
12	80	83	4	3.429	3.602	0.174	3.516
13	84	87	4	3.602	3.776	0.174	3.689
14	88	92	5	3.776	3.993	0.217	3.885
15	93	97	5	3.993	4.210	0.217	4.102
16	98	102	5	4.210	4.427	0.217	4.319
17	103	108	6	4.427	4.688	0.260	4.557
18	109	114	6	4.688	4.948	0.260	4.818
19	115	121	7	4.948	5.252	0.304	5.100
20	122	128	7	5.252	5.556	0.304	5.404

Line Archive File Layout (04430_archive.xyz, and 04430_archive.gdb):

Field	Variable	Description	Units
1	Line	Line Number	
2	Fiducial	Seconds after midnight	sec
3	Flight	Flight number	-
4	Date	Date of the survey flight	ddmmyy
5	Lat_NAD83	Latitude in NAD83	degrees
6	Long_NAD83	Longitude in NAD83	degrees
7	X_NAD83	Easting (X) in NAD83 UTM Zone 12 North	m
8	Y_NAD83	Northing (Y) in NAD83 UTM Zone 12 North	m
9	GPS_Z	GPS elevation (above WGS84 datum)	m
10	Radar	Radar altimeter	m
11	DTM	Terrain (above WGS84 datum)	m
12	Diurnal	Ground Magnetic Intensity	nT
13	TMI_raw	Raw Airborne Total Magnetic Intensity	nT
14	IGRF	International Geomagnetic Reference Field	nT
15	RMI	Final Airborne Residual Magnetic Intensity	nT
16	Primary_field	Electromagnetic Primary Field	µV
17	Hz_monitor	Powerline Monitor (60 Hz)	µV
18-37	x01-x20	Final dB/dt X-Coil Channels 1-20	pT/s
38-57	y01-y20	Final dB/dt Y-Coil Channels 1-20	pT/s
58-77	z01-z20	Final dB/dt Z-Coil Channels 1-20	pT/s
78-97	Bx01-Bx20	Final B-Field X-coil Channels 1-20	fT
98-117	By01-By20	Final B-Field Y-coil Channels 1-20	fT
118-137	Bz01-Bz20	Final B-Field Z-coil Channels 1-20	fT
138-157	raw_x01-x20	Raw dB/dt X-coil Channels 1-20	pT/s
158-177	raw_y01-y20	Raw dB/dt Y-coil Channels 1-20	pT/s
178-197	raw_z01-z20	Raw dB/dt Z-coil Channels 1-20	pT/s
198-217	raw_Bx01-Bx20	Raw B-Field X-coil Channels 1-20	fT
218-237	raw_By01-By20	Raw B-Field Y-coil Channels 1-20	fT
238-257	raw_Bz01-Bz20	Raw B-Field Z-coil Channels 1-20	fT
258-258	RMI_1VD	First Vertical Derivative of RMI	nT/m
259-259	Cond_TS	Apparent Conductance Derived from dB/dt X and Z	mS
260-260	Momxz3	3rd Order Moment derived from B Field X and Z	ppm
261-261	Taubz12_20	Decay Constant (Tau) derived from B Field Z Channels 12-20	µsec
262-267	Momx1-6	1st – 6th Order Moment derived from B Field X	ppm
268-273	Momy1-6	1st – 6th Order Moment derived from B Field Y	ppm
274-279	Momz1-6	1st – 6th Order Moment derived from B Field Z	ppm

CDT Archive File Layout (04430_cdt_archive.xyz, and 04430_cdt_archive.gdb):

Field	Variable	Description	Units
1	Line	Line Number	
2	Fiducial	Seconds after midnight	sec
3	X_NAD83	Easting (X) in NAD83 UTM Zone 12 North	m
4	Y_NAD83	Northing (Y) in NAD83 UTM Zone 12 North	m
5	GPS_Z	GPS elevation (above WGS84 datum)	m
6	Radar	Radar altimeter	m
7	DTM	Terrain (above WGS84 datum)	m
8-87	Cond_array	Conductivity-Depth Channels 1-80	S/m
88-167	Depth_array	Depth Channels 10 m - 800 m in 10m increments	m

First 3 samples of ASCII File 04430_archive.xyz

```
   109801     80238.0        8     121104   58.513248  -110.354836    537587    6486034     372.16     113.08
259.08     59091.00    59785.84   59716.01     65.94     1036393     18174     238192    -112648    -132139
-74514     332213      26063      39768      12414      6882       4350       3705       3037       2621       2008
1918       1675        1546       1210       830        529      -2165233   3292802    2049395    -931793      -
6155607   -1776652    -548423    -121242    -20795     -8267      -7732      -4790      -9773      -7942       -
2333      -3229      -4277      -3651      -2925      -2409      579477    -272359    -418052    -180567     798956
473315     211828      95001      49383      29894      21127      15355      12166       9718       6718
5443       4466        3656       3027       2483      -57444     -53160      29961      93793      71252      16289
10540      8295        7214       6382       5745       5226       4692       4330       3708       3376       2963
2677       2364        2080      584664    -249589   -2000130   -2283317   -1010958    -137090     -53078       -
24407     -17990      -16270     -14854     -13827     -12528     -10841      -9985      -9175      -8126      -7167
-6170      -5406     -125578    -141961     101499     291601     230760      84443      55806      39628
30385      24251       20099      17139      14818      12707      10928       9645       8559       7583       6667
5852       241019    -122002    -135031     -69577     333472     133535      43441      13916       8438
4768       6163        3233       3362       3636       2357       1648       2600        405        788       1599   -
2830355    4302860     2675628   -1222358   -8061521   -2407200    -746220    -166321     -26180     -12397
-10207     -8679      -14553     -10297      -2910      -5724      -6107      -7065      -4366      -3187     577693
-274166   -417154     -178799     792190     475389     212097      95377      48913      29954      21395
14857      12240       10351       6291       4849       4810       3397       3375       2454     -58403     -50554
36221      99486       76141      18830      12437       9853       8329       7317       6332       5769       5120
4577       3835        3556       3097       2629       2471       2197     761363    -331166   -2626312   -2996739
-1332132   -187273     -73257     -33946     -25479     -23082     -21256     -19622     -17566     -15305       -
14210     -12797      -11413      -9649      -8082      -7041    -129107    -144849     106747     300239
236486     85378       55957      39719      30313      24291      19995      17126      14720      12507
10686      9387        8192       7331       6406       5562    0.136314    34.4304   79.05637   1100.586
286.58814    49.39352    24.12979   13.36274   7.96546   4.97730  -3959.77294  -345.25796  -88.12399     -
34.47140   -17.96601   -10.78914  936.19031  166.14152  75.22825  39.83727  23.17656  14.29410
```

```
   109801     80238.2        8     121104   58.513252  -110.354591    537602    6486035     372.61     112.64
259.97     59091.03    59787.20   59716.04     67.28     1029291     18068     236360    -111913    -131177
-73222     329053      24077      39152      12466      7164       4500       3718       3033       2638       2050
1947       1623        1451       1160       806        519      -2464631   3742276    2329153   -1060659      -
7007705   -2006452    -620119    -137661    -23877     -9674      -8831      -5527     -11214      -9001       -
2633      -3643      -4818      -4202      -3389      -2794      577936    -270895    -416178    -180493     797210
468202     209304      93817      49048      29346      20773      15203      12046       9530       6586
5368       4423        3657       2971       2414      -56846     -52588      29998      93195      70580      16067
10451      8200        7066       6230       5592       5054       4558       4177       3567       3271       2807
2585       2263        1949      664160    -284426   -2277785   -2600305   -1151945    -155279     -60326       -
27834     -20511      -18513     -16889     -15709     -14211     -12277     -11288     -10365      -9210       -
8103      -6956       -6064     -125171    -141638     100528     290028     229454      83453      55272
39116      29985       23909      19856      16918      14619      12539      10832       9570       8504       7538
6629       5826       243339    -125681    -137399     -65894     326782     135417      44512      15681
8461       4272        4948       3827       2726       2304       1773       1370        332       1555        669   -
321     -2758962     4199545    2607142   -1191795   -7863413   -2349062    -725194    -161012     -29493
-12766    -10146       -7331     -14383     -11199      -2751      -4252      -5487      -4951      -5315      -2664
```

```
579452      -278354     -416220     -175978     791180      477758      212548      94552       47843       28716
21660       14543       11878       10725       5754        4658        3553        3788        3021        2415        -60581
-52108      37005       99616       76111       19356       12800       9993        8505        7471        6698        6140
5485        5157        4649        4369        4212        3973        3590        3805        742498      -324528     -2562174
-2922327    -1299560    -182389     -71255      -33319      -24609      -22003      -19993      -18540      -16644
-14226      -13053      -12016      -10726      -9370       -7799       -6695       -127265     -141352     104517
292939      231747      84651       55756       39501       30481       24503       20393       17542       15235
13115       11448       10341       9434        8501        7496        6766        0.134849    34.3176     78.14447
1103.422    282.00843   47.68194    23.15489    12.77470    7.59526     4.73679     -4508.48306 -392.58984  -
99.91731    -38.96116   -20.26238   -12.15303   929.33826   164.59744   74.59632    39.53685    23.01761
14.20330
```

```
    109801      80238.4     8           121104      58.513260   -110.354347 537616      6486036     373.06      112.17
260.89      59091.06    59788.55    59716.08    68.62       1019558     17916       235931      -111640     -131036
-72355      327808      22672       38573       12538       7351        4647        3650        3121        2623        2090
1966        1584        1345        1069        745         484         -2729762    4140295     2576819     -1174669    -
7762272     -2189971    -677348     -150796     -26414      -10796      -9749       -6058       -12387      -9888       -
2920        -3941       -5256       -4632       -3794       -3118       574382      -268541     -413091     -180018     792909
462652      206355      92627       48663       28886       20488       15082       11913       9316        6491
5286        4371        3635        2924        2360        -56534      -52375      30121       93091       70247       15863
10205       7998        6803        5950        5308        4773        4310        3920        3329        3039        2582
2416        2117        1784        734557      -315289     -2523632    -2880986    -1276792    -169816     -66126      -
30591       -22534      -20315      -18517      -17216      -15566      -13433      -12334      -11326      -10089      -
8865        -7597       -6596       -124323     -140836     99292       287665      227604      82507       54747
38678       29664       23636       19665       16735       14464       12390       10750       9504        8480        7539
6625        5829        247080      -121560     -138377     -69002      327143      130440      42170       14604
8396        5691        4046        3632        2547        1973        1862        1322        596         1567        1291
-30         -2608518    3967433     2463817     -1123747    -7428457    -2208479    -681899     -151757     -27280
-11449      -9965       -5793       -12308      -9995       -3076       -3554       -5438       -3956       -4001       -3267
563710      -267496     -404854     -172595     767940      462529      206080      92191       48364       28420
20597       14833       11827       9583        6075        5340        3646        3547        2986        2290        -60560
-54530      33698       97784       74807       18751       12548       9874        8464        7234        6597        5950
5449        5118        4598        4374        4087        3848        3453        3467        702877      -304481     -2417144
-2757942    -1224449    -170936     -66465      -30764      -22584      -20240      -18373      -17113      -15464
-13345      -12184      -11273      -9999       -8869       -7669       -6602       -122294     -137398     99237
282293      223766      82430       54589       38795       29810       23826       19841       16941       14765
12746       11166       9972        9003        8063        7088        6439        0.133290    34.1289     77.32315
1097.846    276.28925   44.95309    21.63557    11.87947    7.04371     4.38528     -4991.56170 -433.31491  -
109.78316   -42.62345   -22.11168   -13.24654   921.83234   163.48185   74.21928    39.39243    22.95773
14.17724
```

First 3 samples of ASCII File 04430_cdt_archive.xyz (nulls are represented as *)

```
    109801      80238.0     537587      6486034     113.08      372.16      259.08      0.01995     0.01171     0.00710
0.00410     0.00222     0.00112     0.00064     0.00054     0.00053     0.00057     0.00060     0.00060     0.00069
0.00077     0.00077     0.00077     0.00077     0.00077     0.00096     0.00202     0.00202     0.00202     0.00267
0.00358     0.00361     0.00813     0.01111     0.01111     0.01287     0.01655     0.01632     0.01217     0.01561
0.01036     *       *       *       *       *       *       *       *       *       *       *       *
*       *       *       *       *       *       *       *       *       *       *       *       *       *
*       *       *       *       *       *       *       *       *       *       *       *       *       *
*       *       *       *       *       *       10      20      30      40      50      60      70
80      90      100     110     120     130     140     150     160     170     180     190
200     210     220     230     240     250     260     270     280     290     300     310
320     330     340     350     360     370     380     390     400     410     420     430
440     450     460     470     480     490     500     510     520     530     540     550
560     570     580     590     600     610     620     630     640     650     660     670
680     690     700     710     720     730     740     750     760     770     780     790
800
```

```
    109801      80238.2     537602      6486035     112.64      372.61      259.97      0.01995     0.01171     0.00710
0.00410     0.00222     0.00112     0.00064     0.00054     0.00053     0.00057     0.00060     0.00060     0.00069
0.00077     0.00077     0.00077     0.00077     0.00077     0.00096     0.00202     0.00202     0.00202     0.00267
0.00358     0.00361     0.00813     0.01111     0.01111     0.01287     0.01655     0.01632     0.01217     0.01561
0.01036     *       *       *       *       *       *       *       *       *       *       *       *
*       *       *       *       *       *       *       *       *       *       *       *       *       *
*       *       *       *       *       *       *       *       *       *       *       *       *       *
```

```
*        *        *        *        *        *       10       20       30       40       50       60       70
80       90      100      110      120      130      140      150      160      170      180      190
200      210      220      230      240      250      260      270      280      290      300      310
320      330      340      350      360      370      380      390      400      410      420      430
440      450      460      470      480      490      500      510      520      530      540      550
560      570      580      590      600      610      620      630      640      650      660      670
680      690      700      710      720      730      740      750      760      770      780      790
800
------------------------------------------------------------------------------------------------------------
     109801    80238.4     537616    6486036     112.17     373.06     260.89    0.01995    0.01171    0.00710
0.00410    0.00222    0.00112    0.00064    0.00054    0.00053    0.00057    0.00060    0.00060    0.00069
0.00077    0.00077    0.00077    0.00077    0.00077    0.00096    0.00202    0.00202    0.00202    0.00267
0.00358    0.00361    0.00813    0.01111    0.01111    0.01287    0.01655    0.01632    0.01217    0.01561
0.01036       *       *       *       *       *       *       *       *       *       *       *       *
*       *       *       *       *       *       *       *       *       *       *       *       *       *
*       *       *       *       *       *       *       *       *       *       *       *       *       *
*        *        *        *        *        *       10       20       30       40       50       60       70
80       90      100      110      120      130      140      150      160      170      180      190
200      210      220      230      240      250      260      270      280      290      300      310
320      330      340      350      360      370      380      390      400      410      420      430
440      450      460      470      480      490      500      510      520      530      540      550
560      570      580      590      600      610      620      630      640      650      660      670
680      690      700      710      720      730      740      750      760      770      780      790
800
```

Grid Archive File Description:

The grids are in Geosoft format. A grid cell size of 100 m was used for all area grids.

FILE	DESCRIPTION	UNITS
04430_rmi.grd	Residual Magnetic Intensity	nT
04430_1vd.grd	First Vertical Derivative of RMI	nT/m
04430_cond_ts.grd	Conductance derived from dB/dt X and Z Coils	mS
04430_taubz12_20.grd	Decay Constant (Tau) derived from B Field Z Coil Channels 12-20	μsec
04430_momxz3.grd	Third Order Moment of B Field X and Z Coils	ppm

Conductivity Depth Section grid archive Description:

The conductivity depth section grids are named according to the following convention:

*cdt_**LINE**_**PART***.grd

where ***LINE*** is the line number of the section grid and ***PART*** is the part number. Grids are in Geosoft format with units in Siemens/metre.

Line List for Old Fort Bay Property:

FLIGHT	LINE	PART	START FIDUCIAL	END FIDUCIAL
8	1098	1	80238	80536
8	1099	1	79822	80117
3	1100	1	62458	62769
8	1101	1	79418	79719
8	1102	1	79002	79297
7	1103	1	69677	69979
7	1104	1	69246	69546
7	1105	1	68820	69119
7	1106	1	68387	68692
7	1107	1	67957	68254
7	1108	1	67526	67834
7	1109	1	67097	67392
7	1110	1	66664	66972
7	1111	1	66232	66527
7	1112	1	65787	66095
7	1113	1	65347	65641
7	1114	1	64901	65208
7	1115	1	64475	64767
7	1116	1	64048	64356
7	1117	1	63632	63924
7	1118	1	63211	63516
7	1119	1	62791	63082
7	1120	1	62364	62670
7	1121	1	61712	62002
7	1122	1	61283	61590
7	1123	1	60844	61142
7	1124	1	60399	60711
7	1125	1	59967	60259
7	1126	1	59529	59836
7	1127	1	59095	59389
7	1128	1	58654	58965
7	1129	1	58227	58519
7	1130	1	57760	58073
6	1131	1	64941	65233
6	1132	1	64495	64815
6	1133	1	64065	64351
6	1134	1	63616	63934
6	1135	1	63173	63464
6	1136	1	62722	63045
6	1137	1	62285	62571

6	1138	1	61860	62181
6	1139	1	61450	61732
6	1140	1	61019	61340
6	1141	1	60601	60884
5	1142	1	67481	67772
5	1143	1	67068	67368
5	1144	1	66668	66962
5	1145	1	66246	66543
5	1146	1	65792	66116
5	1147	1	65347	65674
5	1148	1	64910	65241
5	1149	1	64448	64777
5	1150	1	63899	64278
5	1151	1	63359	63729
5	1152	1	62810	63186
5	1153	1	62280	62652
5	1154	1	61759	62128
5	1155	1	61260	61631
5	1156	1	60767	61140
5	1157	1	60274	60637
4	1158	1	85119	85511
4	1159	1	84651	84991
4	1160	1	84132	84524
4	1161	1	83643	83984
4	1162	1	83122	83522
4	1163	1	82629	82972
4	1164	1	82096	82496
4	1165	1	81599	81941
4	1166	1	81078	81476
4	1167	1	80613	80951
4	1168	1	80111	80510
4	1169	1	79637	79978
4	1170	1	79131	79524
4	1171	1	78653	78998
4	1172	1	77595	77919
4	1173	1	77157	77438
4	1174	1	76701	77017
4	1175	1	76283	76564
3	1176	1	71648	71947
3	1177	1	71200	71513
3	1178	1	70773	71075
3	1179	1	70348	70656
3	1180	1	69924	70226

3	1181	1	69493	69801
3	1182	1	69081	69381
3	1183	1	68655	68962
3	1184	1	68226	68531
3	1185	1	67803	68107
3	1186	1	67366	67672
3	1187	1	66918	67223
3	1188	1	66474	66785
3	1189	1	66036	66340
3	1190	1	65597	65907
3	1191	1	65146	65449
3	1192	1	64724	65034
2	1193	1	66976	67281
2	1194	1	66561	66859
2	1195	1	66116	66428
2	1196	1	65691	65987
2	1197	1	65237	65553
2	1198	1	64785	65087
2	1199	1	64338	64649
2	1200	1	63903	64204
2	1201	1	61268	61560
2	1202	1	63141	63423
2	1203	1	60475	60749
2	1204	1	62399	62664
2	1205	1	59584	59840
2	1206	1	61696	61936
2	1207	1	63540	63781
2	1208	1	60867	61090
2	1209	1	62792	63012
2	1210	1	59979	60178
2	1211	1	62075	62273
2	1212	1	59228	59410
2	1213	1	57744	57921
2	1214	1	58654	58822
2	1215	1	57178	57350
2	1216	1	58038	58206
2	1217	1	58945	59118
2	1218	1	57499	57666
2	1219	1	58369	58538
2	1220	1	56912	57079
4	1822	1	78366	78495
4	1823	1	78083	78240
5	1824	1	59715	60035

5	1824	2	68190	68587
5	1825	1	59045	59576
4	1826	1	75815	76050
4	1826	2	85755	86163
4	1827	1	75059	75691
3	1828	1	72354	73070
3	1829	1	62150	62190
3	1829	2	63700	64367
2	1830	1	67547	68298
2	1831	1	56028	56698
1	1832	1	79340	80095
1	1833	1	78533	79209

Appendix F

Map Product Grids

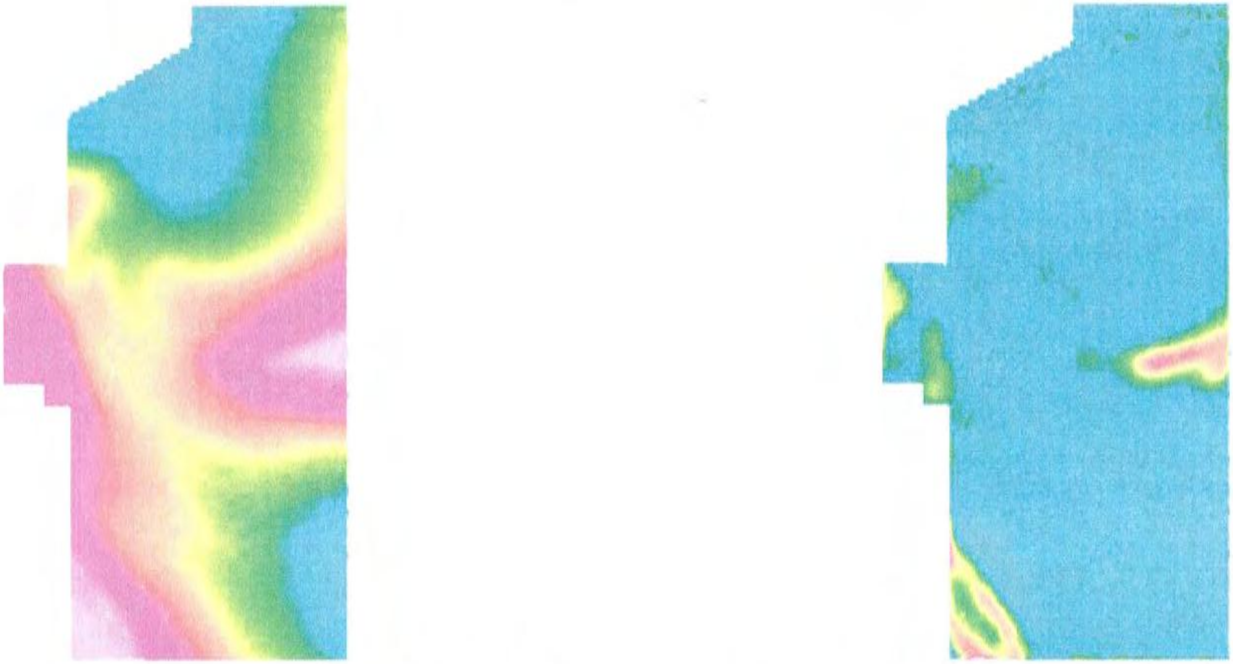

Figure F1. Residual Magnetic Intensity (left), First Vertical Derivative of the RMI (right).

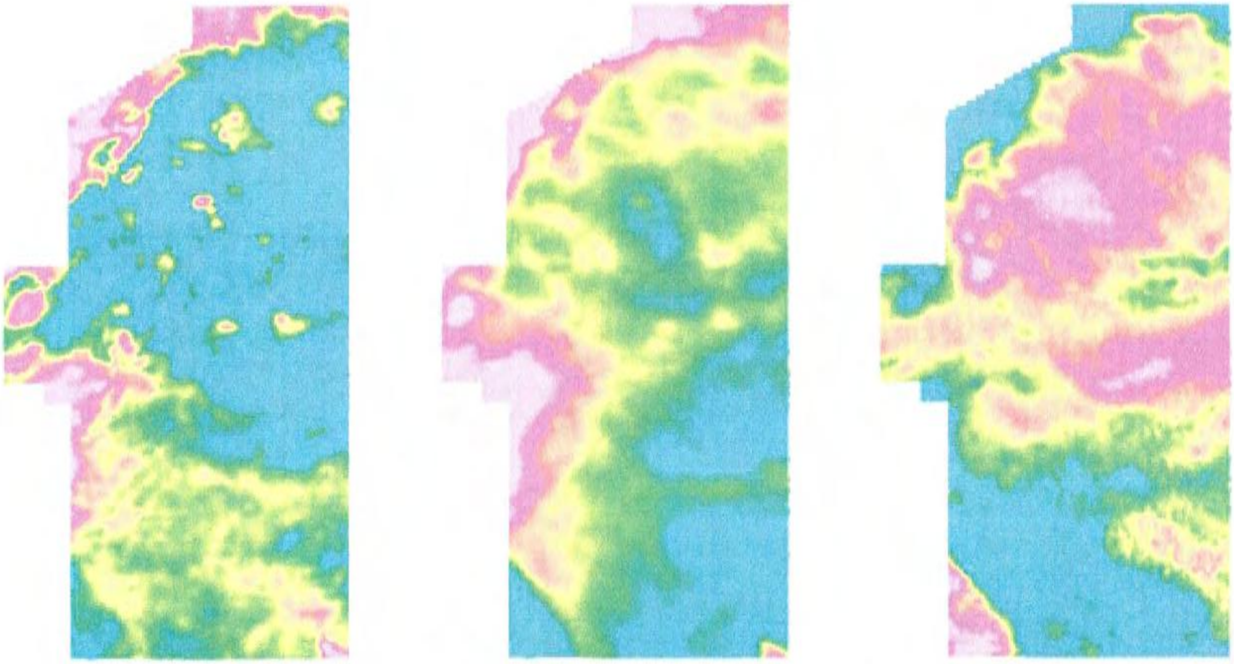

Figure F2. Apparent Conductance (left), 3rd Order Moment of B Field X and Z Coil (centre), and Tau from BZ channels 12-20

OLD FORT BAY PROPERTY

RESIDUAL MAGNETIC INTENSITY

INPUT GRID FILE NAME	**04430_RMI.GRD**
NUMBER OF ROWS & COLUMNS	512 320
PIVOTAL POSITION (X,Y)	532600.000 6485700.000
X SPACING BETWEEN GRID POINTS	100.000
Y SPACING BETWEEN GRID POINTS	100.000
Z UNITS	nT
STARTING / ENDING COLUMNS	1 320
STARTING / ENDING ROW	1 512
DATA MEAN VALUE	-315.752
DATA MINIMUM	-456.230
DATA MAXIMUM	184.740

FIRST VERTICAL DERIVATIVE OF THE RESIDUAL MAGNETIC INTENSITY

INPUT GRID FILE NAME	**04430_1VD.GRD**
NUMBER OF ROWS & COLUMNS	512 320
PIVOTAL POSITION (X,Y)	532600.000 6485700.000
X SPACING BETWEEN GRID POINTS	100.000
Y SPACING BETWEEN GRID POINTS	100.000
Z UNITS	nT/m
STARTING / ENDING COLUMNS	1 320
STARTING / ENDING ROW	1 512
DATA MEAN VALUE	-0.005
DATA MINIMUM	-0.556
DATA MAXIMUM	0.344

APPARENT CONDUCTANCE DERIVED FROM DB/DT X AND Z COILS

INPUT GRID FILE NAME	**04430_COND_TS.GRD**
NUMBER OF ROWS & COLUMNS	512 320
PIVOTAL POSITION (X,Y)	532200.000 6485100.000
X SPACING BETWEEN GRID POINTS	100.000
Y SPACING BETWEEN GRID POINTS	100.000
Z UNITS	mS
STARTING / ENDING COLUMNS	1 320
STARTING / ENDING ROW	1 512
DATA MEAN VALUE	50.126
DATA MINIMUM	3.590
DATA MAXIMUM	229.720

3RD ORDER MOMENT CALCULATED FROM B FIELD X AND Z COILS

INPUT GRID FILE NAME	**04430_MOMXZ3.GRD**
NUMBER OF ROWS & COLUMNS	512 320
PIVOTAL POSITION (X,Y)	532200.000 6485100.000
X SPACING BETWEEN GRID POINTS	100.000
Y SPACING BETWEEN GRID POINTS	100.000
Z UNITS	ppm
STARTING / ENDING COLUMNS	1 320
STARTING / ENDING ROW	1 512
DATA MEAN VALUE	170.930
DATA MINIMUM	64.180
DATA MAXIMUM	1625.320

DECAY CONSTANT (TAU) CALCULATED FROM B FIELD Z COIL CHANNELS 12-20

INPUT GRID FILE NAME	**04430_TAUBZ12_20.GRD**
NUMBER OF ROWS & COLUMNS	512 320
PIVOTAL POSITION (X,Y)	532200.000 6485100.000
X SPACING BETWEEN GRID POINTS	100.000
Y SPACING BETWEEN GRID POINTS	100.000
Z UNITS	µsec
STARTING / ENDING COLUMNS	1 320
STARTING / ENDING ROW	1 512
DATA MEAN VALUE	997.004
DATA MINIMUM	558.860
DATA MAXIMUM	1440.730

APPENDIX 3
(in folder at back of report)

1:50,000 Scale Maps From Airborne Magnetic and MEGATEM Survey:

Map 1 – Flight Path
Map 2 – Residual Magnetic Intensity
Map 3 – First Vertical Derivative of the Residual Magnetic Intensity
Map 4 – Apparent Conductance derived from dB/dt X and Z Coils
Map 5 – 3rd Order Moment derived from B Field X and Z Coils
Map 6 – Decay Constant (Tau) derived from B Field Z Coil Channels 12-20
Map 7 – Basic EM Interpretation Map

APPENDIX 4

Report on Processing of MEGATEM II 90 Hz Data, Old Fort Bay Property, NE Alberta, Triex Minerals Corporation, April 2006

Condor Consulting, Inc.

REPORT ON PROCESSING OF MEGATEM II 90 Hz DATA

OLD FORT BAY PROPERTY

NE ALBERTA

TRIEX MINERALS CORPORATION

APRIL 2006

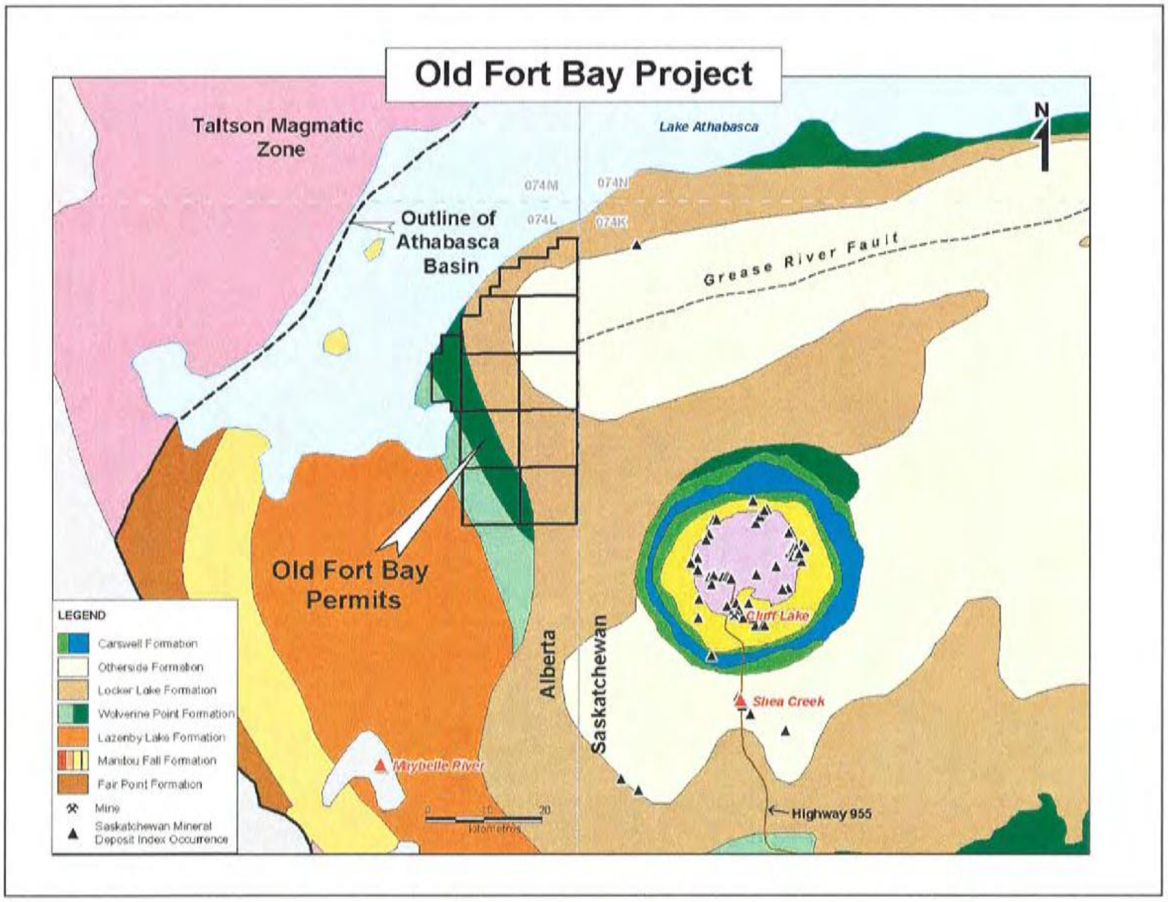

Condor Consulting
Lakewood Colorado
USA

Condor Consulting, Inc.

REPORT ON PROCESSING OF MEGATEM II 90 Hz DATA

OLD FORT BAY PROPERTY

NE ALBERTA

TRIEX MINERALS CORPORATION

APRIL 2006

CONTENTS

1.SUMMARY 2

2.INTRODUCTION & SURVEY DETAILS 3

3.PROCESSING & PRODUCTS 5
  PROCESSING 5
    EMFlow 5
    Layered-Earth Inversion 5
    Time Constant: AdTau 6
  PRODUCTS 7
    Table 3-1 Survey Products 7

4.DISCUSSION 9

5.REFERENCES 10

APPENDICES 11
  APPENDIX A INFORMATION ON EM PROCESSING 12
  APPENDIX B BACKGROUND PAPER ON AIRBORNE EM IN THE ATHABASCA BASIN 13
  APPENDIX C ARCHIVE DVD 14

1. SUMMARY

This report describes the processing of a MEGATEM® II 90 Hz EM data acquired over the Old Fort Bay property held by Triex Minerals Corporation. The property is located in NE Alberta along on the western side of the Athabasca Basin.

The processing of the EM data was undertaken using two codes; an imaging code EMFlow and a full layered-earth inversion code.

The outcomes are provided in profile and plan form in both hardcopy and digital formats to facilitate the client's use of the results. No interpretation of the outcomes has been provided.

Respectfully submitted

[redacted]

Ken Witherly

April 26, 2006

2. INTRODUCTION & SURVEY DETAILS

The location of the Old Fort Bay survey is shown in Figure 1. The outline of the processed MEGATEM EM survey results (a subset of a larger survey flown in November 2004) is shown below in Figure 2.

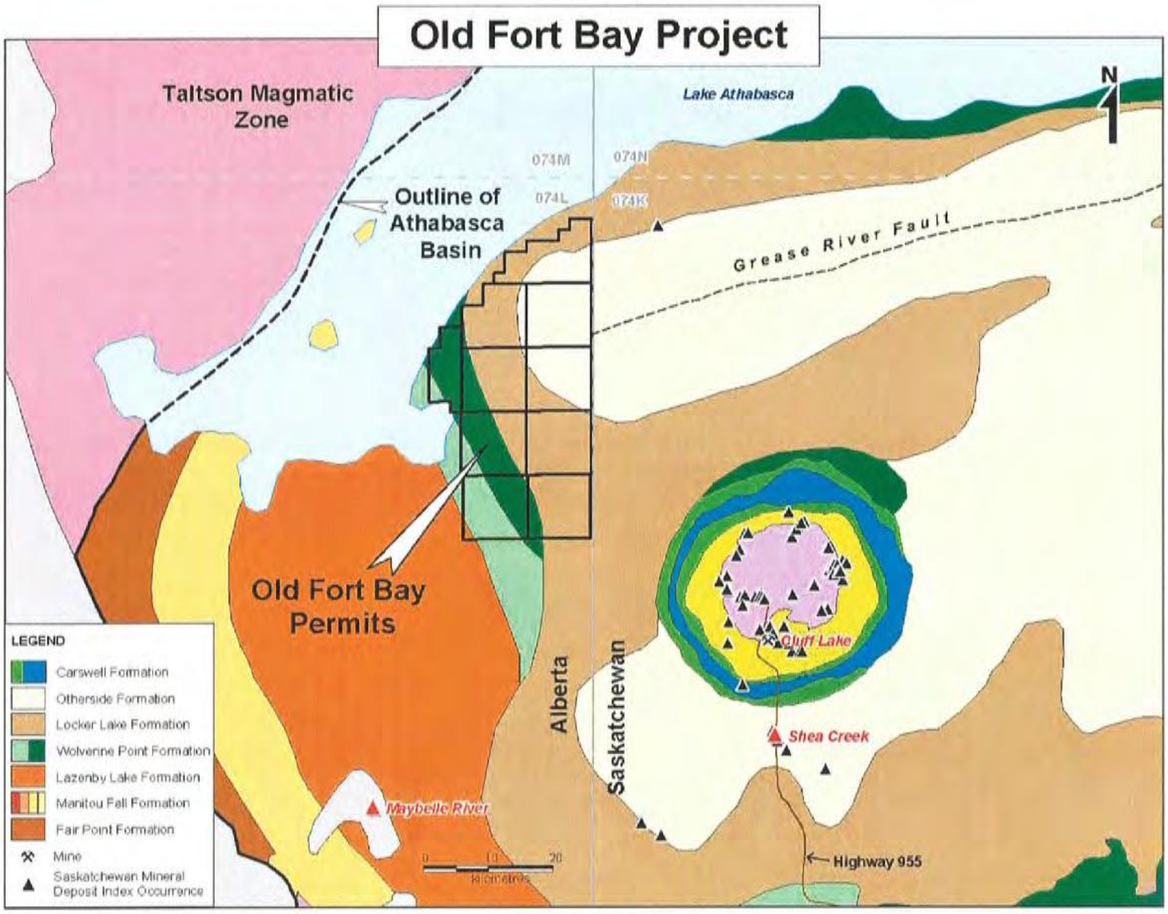

Figure 1: Location of Old Fort Bay survey

Background information on the property is provided below; this is drawn from the Triex web site-www.triexminerals.com.

The property was explored in the 1970's by several companies, including Esso Minerals. Reconnaissance-style lake water and lake sediment surveys, soil samples, and seismic and gravity surveys were completed in 1977. Data were integrated with regional airborne magnetic data to identify targets. A total of six drill holes were completed in successive programs in 1978 and 1979. Hole 08-78-2 is in the east-central part of the current property holding and was terminated prior to reaching the unconformity because of excessive caving. It targets a strong east-west feature on both magnetic and gravity maps which is believed to be the western terminus of the Grease River Shear Zone, a crustal-scale structural splay off the Snowbird Tectonic Zone in northern Saskatchewan. Holes 78-LAJV-002 and 004 are at the north end of the current property, near the south shore of

Lake Athabasca, and are believed to have intersected the southwestern extent of the Black Bay Shear Zone (Alberta Assess. Report 19780009), a major crustal feature that anchors mineral deposits in the Uranium City camp on the north shore of the lake. Core in Hole 004 is heavily fractured, and there is an east-west, multi-element soil anomaly associate with the surface projection of the fault. Basement samples from hole 002 at the unconformity are graphitic, chlorite-altered, and strongly sheared. Regolith at the unconformity is up to 6 metres thick and strongly hematitic. Core assays contain up to 292 ppm uranium and 0.08 oz/ton gold, as well as being enrichment in nickel, zinc and silver. A 1982 publication by the Geological Survey of Canada (Paper 81-20) discusses the positive mineral potential of the area based on the results from this historical drilling.

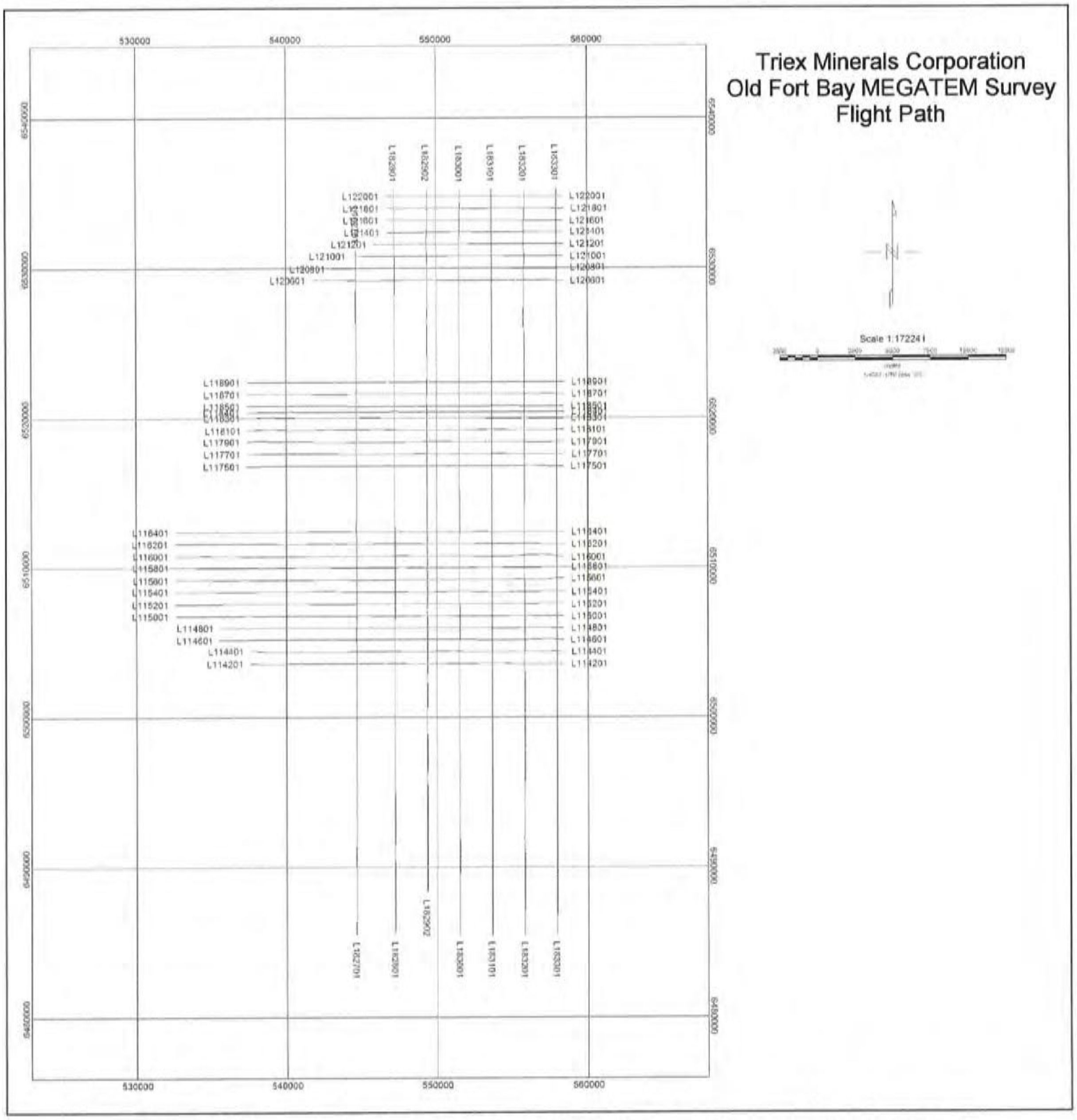

Figure 2: Location of MEGATEM flight lines processed by Condor

3. PROCESSING & PRODUCTS

PROCESSING

EMFlow

EMFlow is a software application that fits an approximate layered earth model to EM decay information on a fiducial by fiducial basis (Macnae et al 1998). The program creates conductivity-depth images and these outcomes are displayed as conductivity depth sections (CDS). Due to the nature of the algorithm, flat lying conductors are more likely to be imaged at their proper depth whereas steeply dipping conductors tend to be imaged deeper than their actual depth. Whenever possible, conductor depths on CDIs should be calibrated with local geological control.

Processing Parameters
Basis function: Tau Range 0.05 → 6 msec
Smoothing: 0.4

Plotting Parameters: On the CDSs, resistivities are in units of mS/m. The plotting range used was 0.5→50 mS/m (log ± 0.5).

Layered-Earth Inversion

The layered-earth inversion (LEI) algorithm models the EM data with a 28-layered earth model (Farquharson and Oldenburg, 1993, Ellis 1998) increasing in thickness from the surface to depth in an approximately logarithmic fashion. The first layer was 5m thick while the deepest was 232m thick. A starting model of 1,000 ohm-m (1 mS/m) was used, with a reference model of 10,000 ohm-m (0.1 m S/m). The reference model resistivity is what the program defaults to at depth when there is no longer enough information to further refine the inversion outcome.

The results of the inversion are presented in the form of a conductivity depth section (CDS).

Plotting Parameters: On the CDSs, resistivities are in units of mS/m. The plotting range used was 0.5→50 mS/m (log ± 0.5).

Additional information on EM data processing is provided in Appendix A.

Time Constant: AdTau

The AdTau program calculates the time constant (tau) from time domain decay data. The program is termed ***AdTau*** since rather than using a fixed suite of channels as commonly done, the user sets a noise level and depending on the local characteristics of the data, the program will then select the set of five channels above this noise level. In resistive areas, this means the calculation will favor earlier channels, whereas in conductive terrains the latest channels will more likely be above the noise floor. A typical decay fit; in this case, the last five channels are shown to the right in Figure 3.

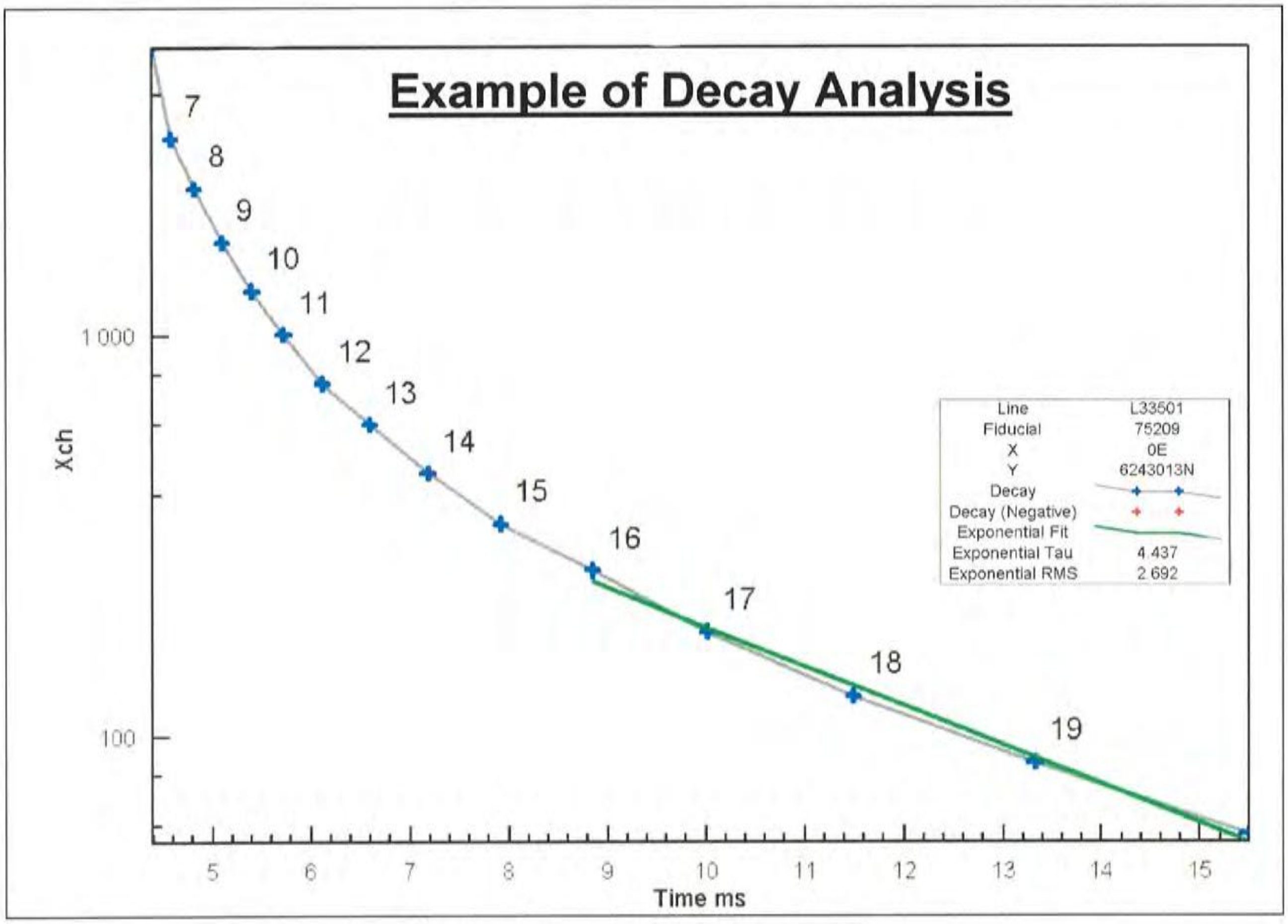

Figure 3: Example of AdTau decay

PRODUCTS

Table 3-1 lists the maps and products that are provided.

Base Maps: All maps are created using the following parameters:

Projection Description:

Datum:	NAD 83
Ellipsoid:	Clarke 1866
Projection:	UTM (Zone: 12N)
Central Meridian:	-111°W
False Northing:	0
False Easting:	500,000
Scale Factor:	0.9996

Table 3-1 Survey Products

Plates @ 1:50,000 (1 hard copy)

- TMI
- 1st Vertical Derivative of TMI
- EM Bfield Z Ch 8 amplitude
- AdTau Bfield Z (cut-off 1,000 fT)
- DTM

MultiPlots™ @ 1:50,000 (PDF + Profile Analyst session file)

Mini-Plates™ (located at the top of each MultiPlots™)- Flight line location map, TMI, 1st VD, EM Bfield Z Ch 8 amplitude, AdTau Bfield Z (cut-off 1,000 fT), DTM

- Profile-dB/dT X and Z Channels 6-20-profiles
- Profile-Bfield X and Z Channels 6-20-profiles
- Profile-TMI, 1stVD, Analytic Signal-profiles
- Profile-AdTau Z dB/dT (cut-off 1,000 pT/s) and Bfield-(cut-off 1,000 fT)
- CDS-Layered-Earth Inversion (results of Z dB/dT processing)+ system height
- CDS-EMFlow (results of Z dB/dT processing) + system height
- TrackMap: 1stVD + flight path

Processing Report (1 copy)

Archive DVD contains the following files: (Appendix C)

-Digital XYZ archive in Geosoft format

-Digital grid archives in Geosoft format

-Profile Analyst session file

-PDFs of Plates and MultiPlots™

-Processing report (PDF)

4. DISCUSSION

For both modeling applications, only the dB/dT outcomes were used as it has been our experience that the Bfield results are filtered in such a way (by Fugro) so as to distort the late-time decays, resulting in erroneous results appearing in the images.

For the EMFlow inversions, three runs were made as is provided for in the software; X, Z and X and Z together weighed 50/50. The Z-only results are displayed in the CDS but the other two outcomes are provided in the data bases.

For the LEI results, both X and Z were modeled; the Z result is displayed in the CDS but both outcomes are provided in the data bases.

In terms of outcomes, an example set of CDS are shown below in Figure 4. Both CDS appear to be showing the basically same conductivity structure. The EMFlow results appear 'sharper' however, and hence might be considered better as a result. This appearance is erroneous as the EMFlow program is designed to minimize layer thickness and as a result, will collapse conductivity structures even if geologically this is not actually the case. While the LEI results look more 'grainy' they are deemed to be more realistic with regards the likely geological structures being modeled. In using the outcomes, the EMFlow is useful to see features highlighted but the LEI outcomes are considered more quantitative with regards to depths and overall structure.

A background paper on the use of airborne EM in the Athabasca Basin (Irvine and Witherly 2006) is attached in Appendix B.

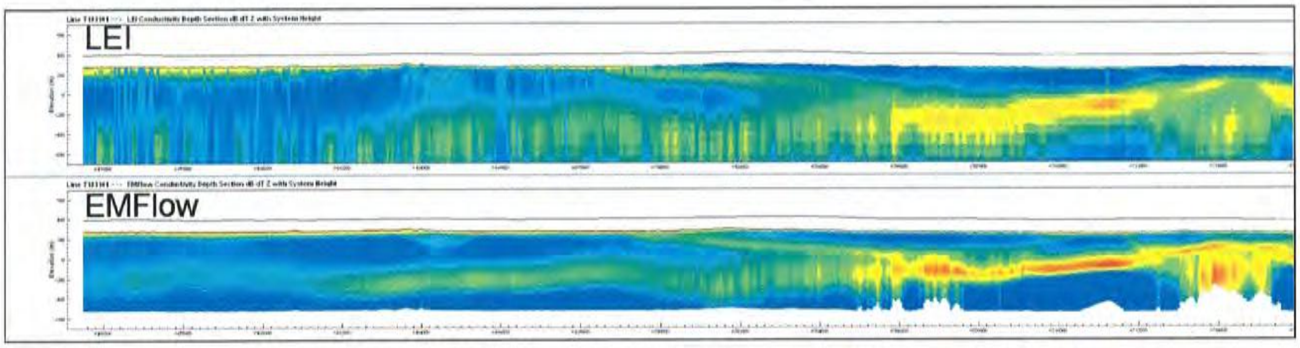

Figure 4: Example of CDS results; LEI and EMFlow-T183101

5. REFERENCES

Ellis, R. G., 1998, Inversion of airborne electromagnetic data, 68th Ann. Internat. Mtg: Soc. of Expl. Geophys., 2016-2019.

Farquharson, C.G. and Oldenburg, D.W., 1993, Inversion of time-domain EM data for a horizontally layered earth, Geophysical Journal International, Vol. 114, pp 433-441.

Macnae, J. King, A., Stolz, N., Osmakoff, A., Blaha, A. (1998) “Fast AEM data processing and inversion”, Exploration Geophysics, Vol. 29, pp 163-169.

APPENDICES

APPENDIX A INFORMATION ON EM PROCESSING

What is a CDI?

Condor Consulting, Inc.

The term CDI is short for **C**onductivity **D**epth **I**maging. The purpose of CDI processing is to convert multichannel EM data[1] into the equivalent conductivity distribution in the earth that would produce the observed EM response. While the program assumes the earth is layered (meaning all changes in conductivity are vertical), by processing many points along a line and then gridding the result, a two dimensional (or three dimensional if gridded again) approximation of the earth's conductivity can be obtained. The results of CDI processing are then displayed in a CDS, short for **C**onductivity **D**epth **S**ection (central image in the figure below).

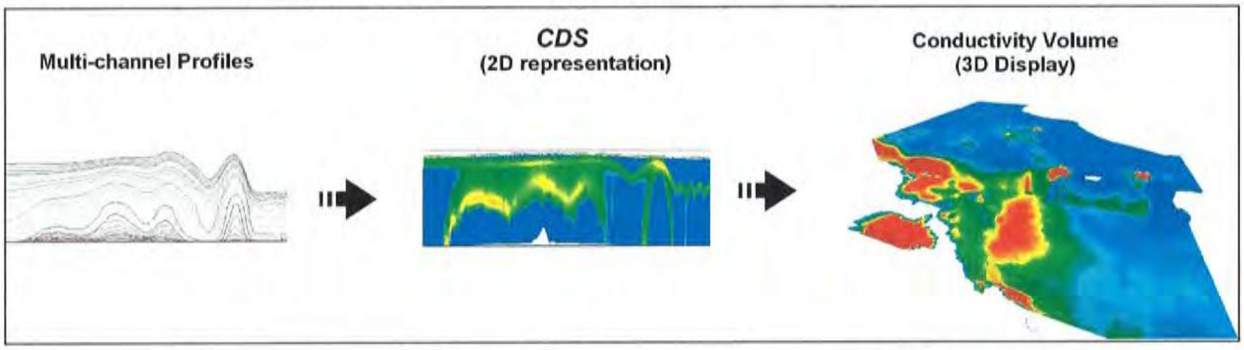

In what would be termed a simple conductivity environment where all conductors are expected to be steeply dipping in a resistive host rock, CDI processing will not likely add much new information when making target assessments. However, in many situations the target conductivity may be caused by a mixture of massive and disseminated sulfides and CDI processing will enhance the likelihood of being able to map the overall conductivity distribution much like IP surveying has been used historically in VMS exploration. Also, if the overburden is conductive and/or has a variable thickness, CDI processing helps to identify such changes and reduces the potential ambiguity of mistaking variations in the overburden for targets of interest in the bedrock.

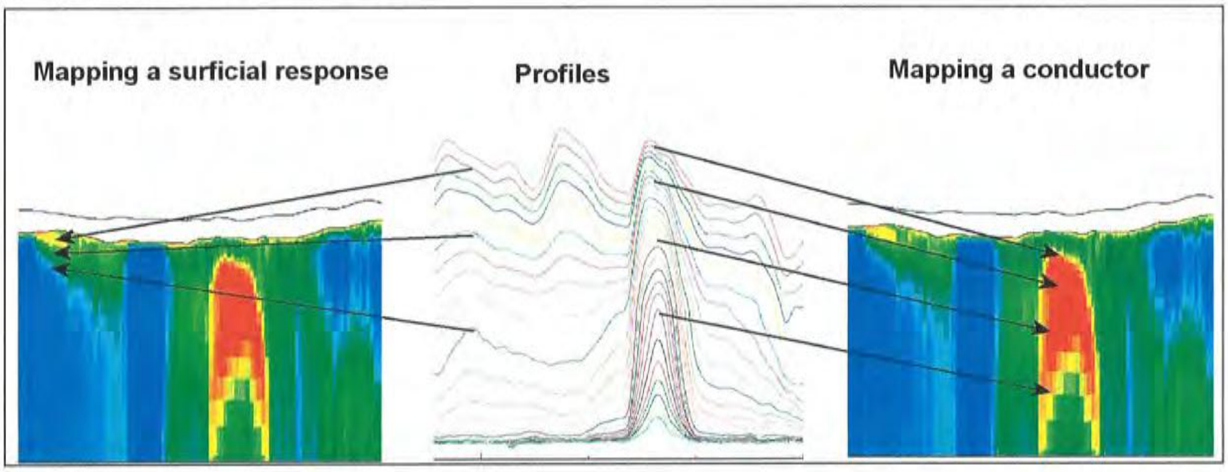

---

[1] Time domain CDIs are discussed here but the same process can as well be applied to frequency domain data as well, this is discussed under a companion Technical Note

APPENDIX B BACKGROUND PAPER ON AIRBORNE EM IN THE ATHABASCA BASIN

Advances in airborne EM acquisition and processing for uranium exploration in the Athabasca Basin, Canada.

Richard Irvine and Ken Witherly, Condor Consulting, Inc.*

Summary

Uranium deposits in the Athabasca Basin, northern Canada, are associated with graphitic metasediments and faults zones in the Archean basement and are often "blind", covered by hundreds of meters of resistive Proterozoic sandstones. Hence airborne electromagnetics (EM) is commonly used in initial exploration over large areas. In recent years new airborne EM systems have become commercially available which have the capability to detect large graphitic zones in or near the basement at depths approaching 1000 m, examples of which are in this paper. Conductivity depth inversions and forward modeling of graphitic conductors in a conductive half-space are important tools in interpretation as they provide quantitative confirmation that deep conductors are responsible for the observed responses.

Introduction

The Athabasca Basin straddles the Alberta-Saskatchewan border in Canada and occupies an area of about 100,000 sq km in northern Saskatchewan, accounting for approximately 30% of global primary uranium production.

The Basin is filled with the Proterozoic Athabasca Group consisting of relatively undeformed and flat-lying sedimentary rocks. The high-grade uranium deposits are loosely associated with the unconformity between these sandstones and underlying Archaean-Palaeoproterozoic metamorphic and igneous basement rocks. The deposits occupy a range of positions from wholly basement-hosted to wholly sediment-hosted, at structurally favorable sites in the interface between deeply weathered basement and overlying sandstones. In almost all cases the deposits appear to be structurally controlled by basement faults and fracture zones, which are localized in graphitic metapelitic gneisses that often flank structurally competent Archaean granitoid domes and may extend for up to 10 km or more. In some cases alteration zones associated with the fault zones and mineralization extend above the unconformity into the sandstone.

Electrical Characteristic Of Athabasca Basin

Figure 1 shows a geological cartoon for unconformity-style uranium deposits in the Athabasca Basin, while resistivity ranges for the different rock types are shown in Figure 2. The basement and overlying sandstones are generally very resistive, while the graphitic metapelite is relatively conductive (<1-50 ohm-m). Alteration zones in the sandstone have variable resistivity, ranging from 50-20,000 ohm-m. The regolith at the unconformity is generally not a significant conductor. Overburden and lake water may have relatively low resistivities, but are generally thin enough that they do not significantly hinder EM methods. Lake sediments have resistivities in the range 100-800 ohm-m and where thick may decrease the depth of penetration of EM systems.

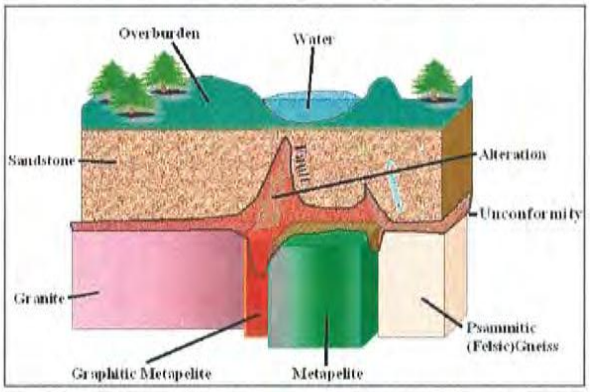

Figure 1: Geological cartoon for unconformity-style uranium deposits in the Athabasca region (courtesy Cogema Resources Inc.)

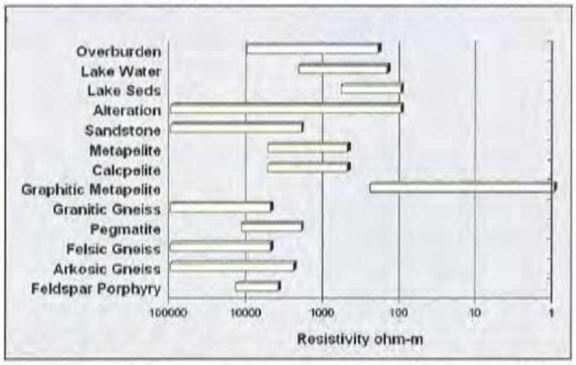

Figure 2: Resistivities of rock types in Athabasca Basin (modified from Cristall, 2006).

The depth to the unconformity between sandstone and basement varies from outcrop around the edges of the Basin to over 1500 m near the center. Initial exploration focused on the outer edges where the unconformity is

Note: This expanded abstract has been submitted for presentation at the Society of Exploration Geophysicists Meeting, October 2006. Until released by the SEG, Condor requests the recipient use the contained information for their personal use only.

shallow, but as the shallower deposits were discovered, it has moved increasingly into the deeper parts of the Basin.

Application of EM

With the major increase in uranium prices in the past two years, there has been a marked jump in exploration activity. Areas of the Athabasca basin with sandstone depths of 0.5-1.0 km are now being explored and this is presenting challenges to airborne EM acquisition and processing technology. In more mature exploration areas, the emphasis has moved from simple detection of basement graphitic faults to definition of alteration systems in the overlying sandstone in close proximity to these graphitic zones. Delineation of such poorer conductors in the vicinity of stronger conductors requires more sophisticated analysis such as layered earth inversions.

The most commonly used airborne systems in deep exploration in the Athabasca are time domain MEGATEM (Smith et al, 2003) and VTEM (Witherly et al, 2004), on the basis of their large dipole moment and relatively high signal/noise ratios.

Forward modeling and inversion technologies are useful for bridging the gap between geology and geophysics. Increased use is being made of 1D inversion software 2D/2.5D forward modeling/inversion of plates in a conductive, layered half-space and full 3D modeling.

Example 1

Figure 3 shows the VTEM response of a line over Cameco's O2 Next deposit along the Collins Bay Fault in the northeast of the basin where the depth to the unconformity is shallow (less than 30 m). LeroiAir (Raiche 1998) has been used to model the response of a plate conductor and water and overburden layers. The matching geological section has been added in the bottom of the figure. The fitted plate correlates well with the graphitic fault contact, as confirmed by drilling.

To obtain an appreciation of the depth of penetration of VTEM for a similar target, calculations were made for plates with the same physical parameters as those in Fig. 3, at depths of 400 and 800 m below ground, in a 50,000 ohm-m half-space (Figure 4). As expected the peak amplitude decreases with depth and the anomaly broadens and at 800 m depth the anomaly is basically a broad single high, with a half-width of more than 1 km. Peak amplitude decreases from approximately 0.9 at 61 m depth to 0.004 pV/Am^4 at 800 m depth. The VTEM noise level on recent surveys in the Athabasca has been approximately 0.001 pV/Am^4, so such an anomaly should be detectable.

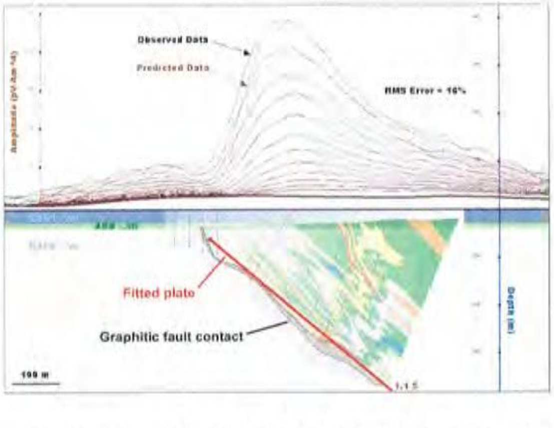

Figure 3: Observed and modeled VTEM responses for a line over the O2 deposit (top) and plate model and geology (bottom). (Modified from Cristall and Brisbin, 2006)

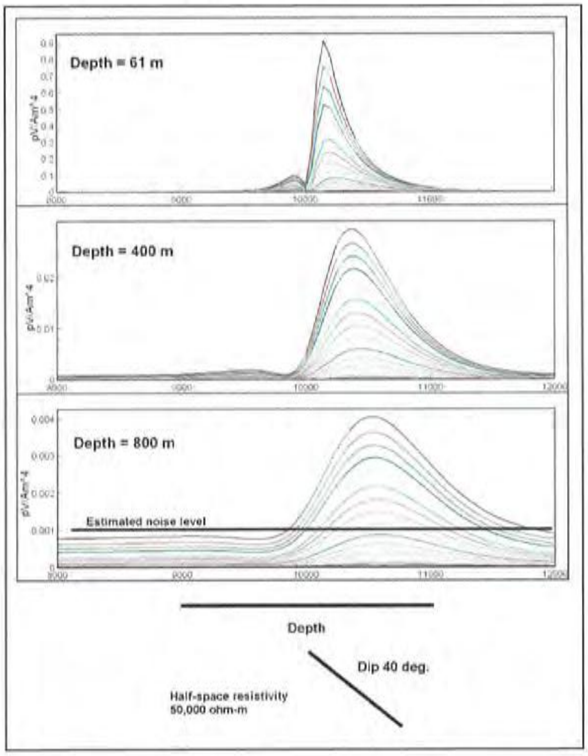

Figure 4: LeroiAir VTEM model responses for the plate shown in Fig. 3, at different depths.

Example 2

Figure 5 compares MEGATEM, VTEM and ground resistivity responses for a line in the Tucker Lake area, where drilling has defined the unconformity depth as approximately 650 m. The VTEM data has been laterally smoothed.

Layered earth inversions (LEI) which produce conductivity depth sections (CDS) are extremely useful in resolving the depth of conductors indicated on profiles, thus facilitating the differentiation of basement conductors probably due to graphite from conductors in the overlying sandstone which are probably due to alteration.

Relatively strong anomalies are observed for both systems and matching conductors are well defined on the CDS in this example. The tops of the strongest parts of the conductors lie at, or slightly above, the unconformity depth implying that these strong conductors lie mainly in the basement and thus are likely graphite.

Ground resistivity/IP and EM surveys are often carried out in the Basin in an effort to better resolve conductors observed in airborne EM surveys or as a primary exploration tool in brownfields exploration. The ground resistivity section on this line is similar to the CDS for VTEM, with the top of the strong conductor lying slightly above the unconformity - the extension of the conductor above the latter may indicate the presence of some alteration in the overlying sandstone. Thin conductors near the surface are likely due to lake sediments. Two other localized conductors within the sandstone are not reflected in the MEGATEM or VTEM EM profiles or CDSs and may be spurious.

Example 3

Fig. 6 compares MEGATEM, VTEM and ground resistivity data in an area where the unconformity is predicted to be approximately 800 m in depth. Anomalies are evident in the profiles for both the airborne systems and the peak amplitude of the VTEM is approximately 0.7 pV/Am^4, while the noise level for this line is less than 0.001 pV/Am^4. The extremely low background amplitude suggests that both the basement and sandstone resistivities in this area are high (greater than 50,000 ohm-m). The amplitude of the VTEM anomaly is almost double that of the modeled result for 800 m depth in Fig. 4, demonstrating that graphitic zones of a type associated with known economic uranium deposits can be detected to at least this depth.

Low resistivity zones are observed on the layered earth inversions, matching the profiles. The resistivity low is most pronounced below the unconformity (where it is interpreted to be due to graphite), but does extend for some distance above it. This could be due to lower resistivity alteration in the overlying sandstone or to an artifact in the inversion whereby the resistivity low has been "smeared" over greater than the true depth distribution.

The ground resistivity inversion is generally consistent with the airborne inversions, but the high resistivity zones in the upper part of the section are more erratic than for the MEGATEM and VTEM inversions. The resistivity low in the predicted basement is relatively strong, but a second low in the basement (to the left of the major low) and smaller lows closer to the surface have no matching signatures in either MEGATEM or VTEM profiles or CDS and appear dubious. The lateral and vertical resolution of the airborne systems appear superior to that of the ground resistivity survey in this example.

Conclusions

Advances in airborne EM systems in recent years have enabled conductive graphitic metasediments and faults in the basement associated with uranium deposits in the Athabasca Basin to be detected to depths approaching 1000 m. This is facilitated by the resistive overlying sandstone. 1D conductivity depth inversions and 2D/2.5D forward modeling/inversion are essential tools in delineating the conductivity distribution from the airborne survey data. Further developments will be directed towards differentiating poorly conductive alteration zones in the sandstone from underlying graphitic metasediments in the basement.

References

Cristall, J. and Brisbin, D., 2006, Geological sources of VTEM responses along the Collins Bay Fault, Athabasca Basin, Proceedings of the Giant Uranium Deposits Short Course, PDAC, 2006.

Raiche, A., 1998, Modelling the time-domain response of AEM systems, Exploration Geophysics 29, 103-106.

Smith, R., Fountain, D. and Allard, M., 2003, The MEGATEM fixed-wing transient EM system applied to mineral exploration: a discovery case history: First Break, 21, no. 7.

Witherly, K., Irvine, R. and Morrison, E., 2004, The Geotech VTEM time domain helicopter EM system, 74th Annual International Meeting, SEG, Expanded Abstracts.

Acknowledgments

Daniel Sattel processed the data shown in Figure 5. Jamin Cristall of Cameco Corporation provided useful advice in running modeling software.

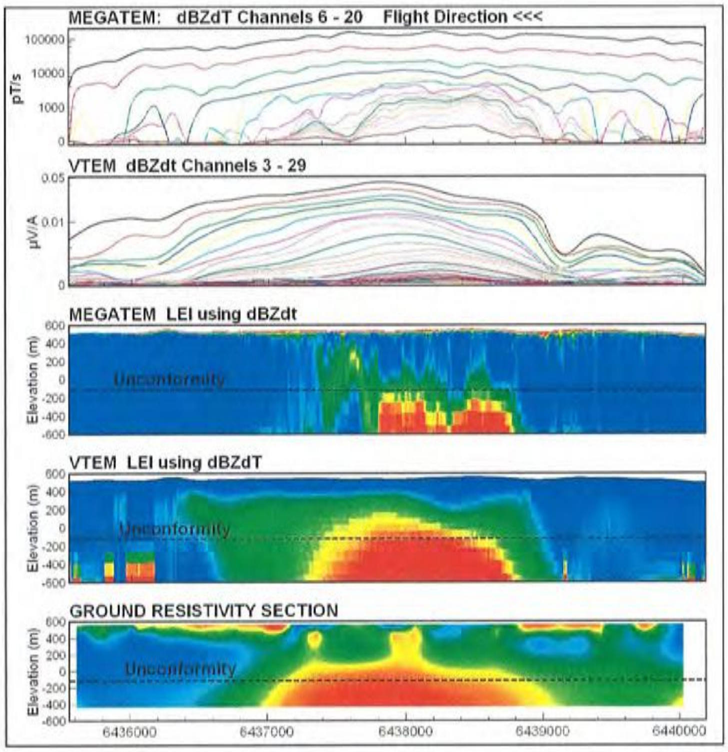

Figure 5: Comparison of MEGATEM and VTEM profiles and CDS with ground resistivity for one line in the Tucker Lake area, Athabasca Basin. (Red is conductive, blue resistive). The ground resistivity section was obtained by inverting pole-pole pole electrode array with a spacing of 200 m and "n" values up to 18. (Data courtesy of Cogema Resources Inc. and Geotech Ltd.)

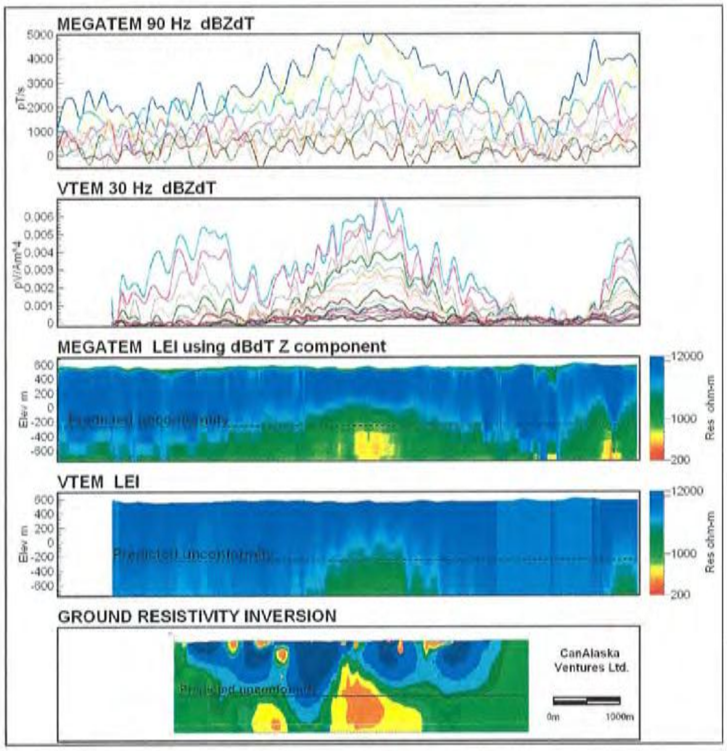

Figure 6: Comparison of MEGATEM and VTEM profiles and CDS with ground resistivity for one line in the Athabasca Basin. (Orange-yellow is conductive, blue resistive). The ground resistivity section was obtained by inverting pole-pole pole electrode array with a spacing of 200 m and "n" values up to 18. (Data used with permission of CanAlaska Ventures Ltd. The ground resisistivity section was modified from an image produced by SJ Geophysics).

APPENDIX C ARCHIVE DVD

APPENDIX 5
(in folder at back of report)

1:50,000 Scale Maps From Processing of MEGATEM II 90 Hz Data:

Map 8 – TMI
Map 9 – 1st Vertical Derivative of TMI
Map 10 – EM Bfield Z Ch 8 amplitude
Map 11 – AdTau Bfield Z (cut-off 1,000 fT)
Map 12 – DTM

APPENDIX 6

Summary Interpretation of Time Domain Electromagnetic Data
from a
Fugro MEGATEM Survey
Carried Out During the Period October 20 and November 12, 2004
on
Permits 9305010842 through 9305010851
in the
Western Athabasca Basin Region Saskatchewan
NTS 74 L/9, & 16

OLD FORT BAY PROJECT

Summary Interpretation of Time Domain Electromagnetic Data

from a
Fugro MEGATEM Survey
Carried Out During the Period October 20th and November 12th, 2004

on
Permits 9305010842 through 9305010851

in the
Western Athabasca Basin Region, Saskatchewan
NTS 74 L/9, & 16

For

Triex Minerals Corporation
and
Roughrider Uranium Corp.

By
Edwin R. Rockel
Interpretex Resources Ltd.
March 20, 2007

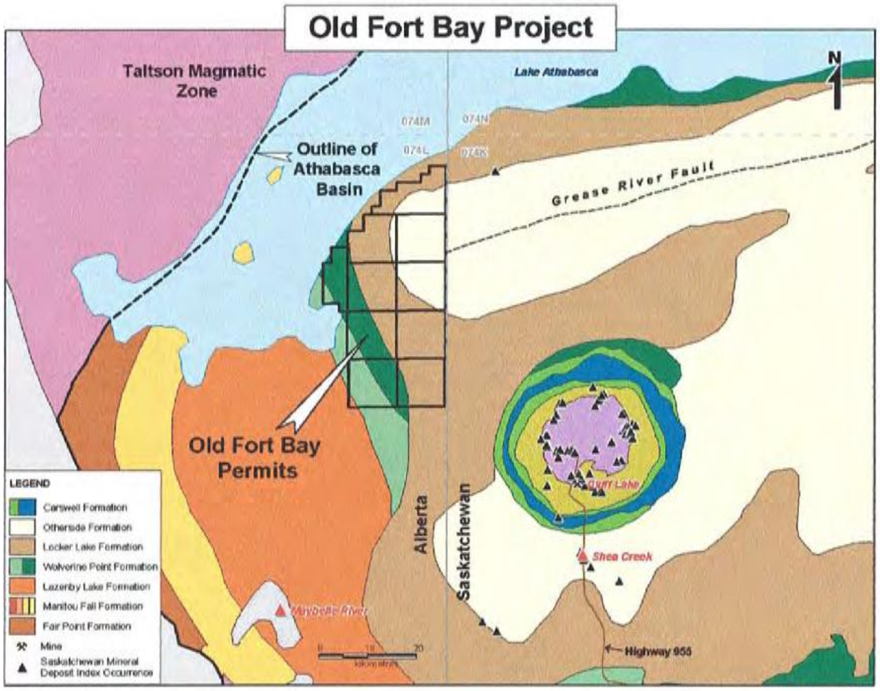

Table of Contents

1. INTRODUCTION 3
1.1 Fugro 3
1.2 Condor Processing 4

2. DISCUSSION 5

3. CONCLUSIONS AND RECOMMENDATIONS 11

APPENDIX I - Statement of Qualifications 12

APPENDIX II - Full Map Images of Maps Used in this Report 13

1. INTRODUCTION

This summary interpretation refers to reports;

Interpretation report
of the
Old Fort Bay Property MEGATEM survey
Western Athabasca Basin
for
Triex Minerals Corp. and Roughrider Uranium Corp.
by
Yuri Kroupoderov
Senior Geophysicist,
Brian Schacht
Consulting Geophysicist
and
Jean Lemieux
Chief Geophysicist,
Fugro Airborne Surveys
Interpretation & Consulting Services,
Ottawa.
March 17, 2005

and;

REPORT ON PROCESSING OF MEGATEM II 90 Hz DATA
OLD FORT BAY PROPERTY
NE ALBERTA
TRIEX MINERALS CORPORATION
APRIL 2006
by
Ken Witherly,
Condor Consulting, Inc.
April 26, 2006

This report uses various diagrams from these reports and images or parts of (cropped) images from the data CD supplied to Triex Minerals Corp. by the above contractors. Excerpts taken from these reports are in Italic font.

1.1 Fugro Data

Between October 20th and November 12th, 2004 Fugro Airborne Surveys conducted a MEGATEM® electromagnetic and magnetic survey of the Old Fort Bay Property on behalf of Triex Minerals Corp. and Roughrider Uranium Corp. Using Fort McMurray, Alberta as the base of operations, a total of 2924 line kilometres of data was collected using a Dash 7 modified aircraft. (Fugro)

The purpose of the survey was to obtain information about the subsurface magnetic and conductive environment within the permits, that may reflect zones of significant alteration and mineralization within bedrock at or near the basement rock interface.

Data were processed and interpreted by Fugro and presented in a report by Lemieux, et al. The report correctly points out that high frequency magnetic anomalies found in this survey are likely due to detrital (glacial) material. With previous drilling indicating basement depths at 800 meters or more throughout the survey area only the broad (deep) magnetic anomalies are considered important. The Fugro interpretation report also indicates that only two basement structures were defined, one in the SW corner of the area *and the E-W structure extending westward across the centre of the block from the eastern margin.* The present interpretation explores the possibility of additional deep-seated structures in the area.

Electromagnetic results were displayed, by Fugro, using "Apparent Conductance", "Response from dB/dt Z-channel 8", "3rd Order Moment" and "Decay Constant (TAU) from B-Field" maps (not included here). Fugro's conclusions were that *in this dataset, we have not been able to identify EM responses that could be attributed to deep graphitic horizons. The only "sub-surface" conductive horizon identified, which shows some structural control from the basement, is the NW – SE conductive band in the southern part of the survey area, but this is quite broad (~ 12 km) and is more likely assumed to reflect some other intrasedimentary conductive layer within the Athabasca Formation (clay layers, mudstones, etc.).*

Other possible conductive implications are examined in the present interpretation.

1.2 Condor Processing

In an effort to extract more information out of the data using a different point of view, Condor Consultants Inc. were contracted to re-process some of the data however no interpretation of the results was provided. Results of the Condor re-processing were similar to Fugro's work.
The following survey lines and tie lines were processed by Condor;

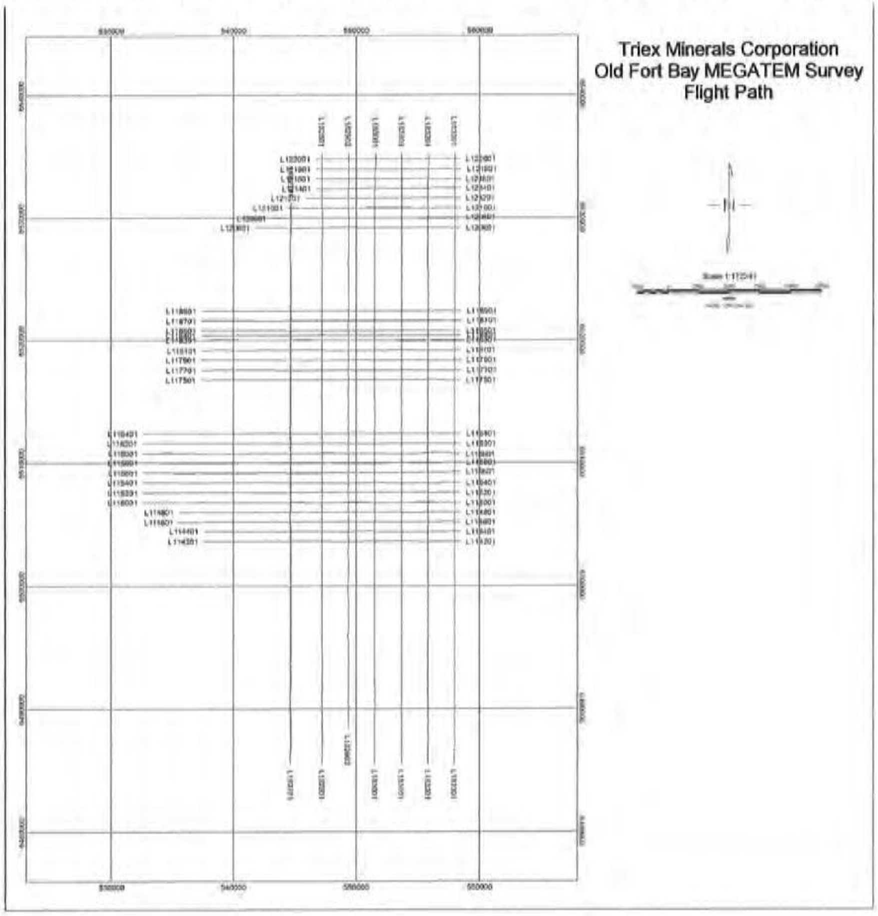

total of 911 line km of survey data were processed by Condor.

Survey	Tie
114201	182701
114401	182801
114601	182902
114801	183001
115001	183101
115201	183201
115401	183301
115601	
115801	
116001	
116201	
116401	
117501	
117701	
117901	
118101	
118301	
118401	
118501	
118701	
118901	
120601	
120801	
121001	
121201	
121401	
121601	
121801	
122001	

2. DISCUSSION

A good summary of the few deep drill holes within the area boundaries is provided by Condor. The summary states that *a total of six drill holes were completed in successive programs in 1978 and 1979. Hole 08-78-2 is in the east-central part of the current property holding and was terminated prior to reaching the unconformity because of excessive caving. It targets a strong east-west feature on both magnetic and gravity maps which is believed to be the western terminus of the Grease River Shear Zone, a crustal-scale structural splay off the Snowbird Tectonic Zone in northern Saskatchewan. Holes 78-LAJV-002 and 004 are at the north end of the current property, near the south shore of Lake Athabasca, and are believed to have intersected the southwestern extent of the Black Bay Shear Zone (Alberta Assess. Report 19780009), a major crustal feature that anchors mineral deposits in the Uranium City camp on the north shore of the lake. Core in Hole 004 is heavily fractured, and there is an east-west, multielement soil anomaly associate with the surface projection of the fault. Basement samples from hole 002 at the unconformity are graphitic, chlorite-altered, and strongly sheared. Regolith at the unconformity is up to 6 metres thick and strongly hematitic. Core assays contain up to 292 ppm uranium and 0.08 oz/ton gold, as well as being enrichment in nickel, zinc and silver.*

Note that the hole designations quoted by Witherly are not the same as the AGS hole IDs available to the writer. Assuming that the northern holes 78-ALJV-002 and 004 are part of the cluster of holes with AGS ID from FC-001 through 006 (at the northern area boundary) and that hole 08-78-2 is the same as AGS hole FC-069 then the summary of these deep drill holes indicates three significant facts, 1) the "strong east-west magnetic feature" (central-east part of the area) remains unexplained 2) graphite, alteration and uranium mineralization all occur at the bottom of deep hole 78-LAJV-002 near the northern area boundary, apparently associated with faults or shear zones and 3) the *multielement soil anomaly associated with the surface projection of the fault* suggests that some faults may continue to near surface and may have a near surface geochemical and then perhaps a geophysical signature. Thus the "strong east-west magnetic feature", possibly related to deep structure, is still prospective and if other structural features can be predicted, they may also be targets for deep exploration for uranium mineralization. Both Fugro and Condor have presented concise descriptions of the geological model for the area and the expected mineralization scenarios so only relevant geological descriptions will be given here. Both company's manipulations and Fugro's interpretation resulted in no specific conductors defined that were considered to be related to deep basement graphitic faults.

As described by Richard Irvine and Ken Witherly of Condor Consulting Inc., in their paper "Advances in airborne EM acquisition and processing for uranium exploration in the Athabasca Basin, Canada", most uranium deposits in the deep basin environment *appear to be structurally controlled by basement faults and fracture zones, which are localized in graphitic metapelitic gneisses that often flank structurally competent Archean granitoid domes and may extend for up to 10 km or more. In some cases alteration zones extend above the unconformity into the sandstone* as seen in the cartoon (Figure 1 to the right) taken from Irvine and Witherly's paper. A graphic summary of the structural history of the Athabasca Basin and unconformity uranium mineralization at the NRCAN website

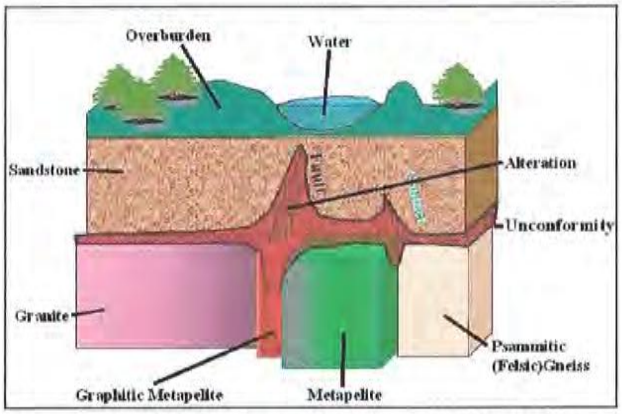

Figure 1: Geological cartoon for unconformity-style uranium deposits in the Athabasca region (courtesy Cogema Resources Inc.)

http://ess.nrcan.gc.ca/2002_2006/nrd/wchurchill/pdf/project8_2_pres_20.pdf indicates that uranium was emplaced by long-lasting hydrothermal systems that were focused in repeatedly reactivated basement faults over 500 Ma during development of the Athabasca basin. These faults can continue into the overlying sediments and will flatten and splay. With this in mind an attempt was made in the present interpretation to see if any deep structures, that may have continued into the Athabasca sediments and perhaps near surface, could be delineated using the present survey magnetic and electromagnetic data.

Condor's inverted "conductivity depth sections" and Fugro's "conductivity depth transform" sections (essentially the same thing with different names and using different methods) all show horizontally layered conductive and non-conductive zones throughout the area.

Fugro "Conductivity Depth Transform" Sections on Plan Map

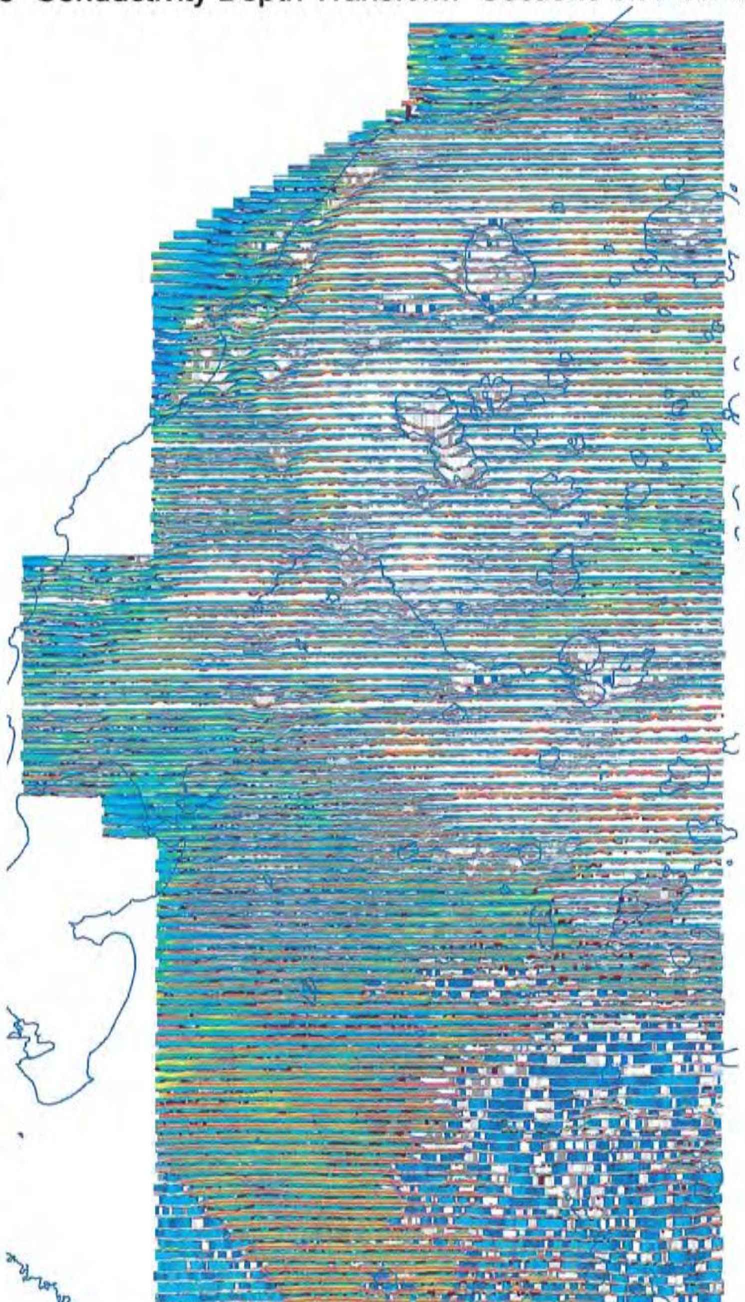

A display of Fugro's conductivity sections stacked onto a plan map (to the right) shows how the subsurface conductive layers change in depth and conductivity throughout the survey area. It is immediately obvious that the widespread horizontal conductive layer or layers that exist throughout the survey area are not always at the same calculated depth. Many abrupt changes in layer depths form linear trends. Some of these trends coincide with Fugro's fault interpretation (from magnetic data) suggesting that abrupt changes in the depth of various horizontal conductive layers may indicate the location of basement structures that have continued into the sandstone and produced a relative uplift or down-drop of parts of the widespread horizontal conductive layers. Further interpretation of magnetic data by the writer, for the present report, produced magnetic lineaments interpreted as additional possible faults, both deep and shallow (using residual magnetic intensity, first vertical derivative and tilt derivative maps).

Below, the same image of stacked CDT's and an image of filtered residual magnetic intensity (RMI), both faded to 60%, were overlain by possible "deep" faults or structures interpreted from the filtered residual magnetic intensity data.

Stacked CDT's with Interpreted Deep Faults

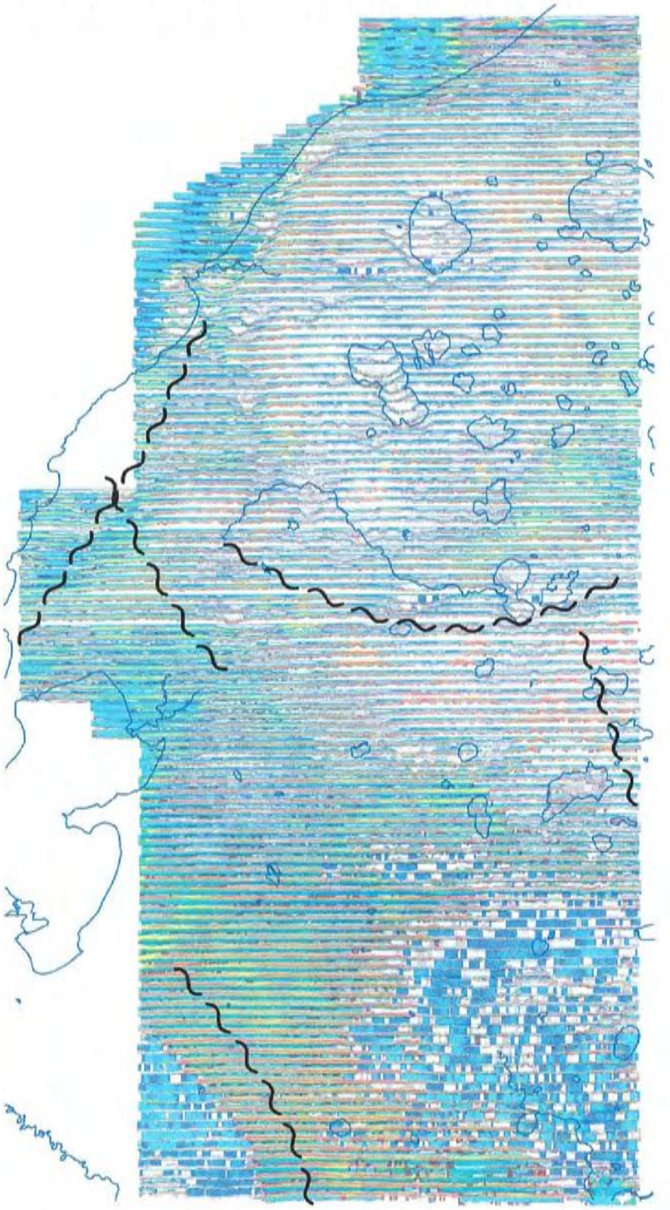

Filtered RMI with Interpreted Deep Faults

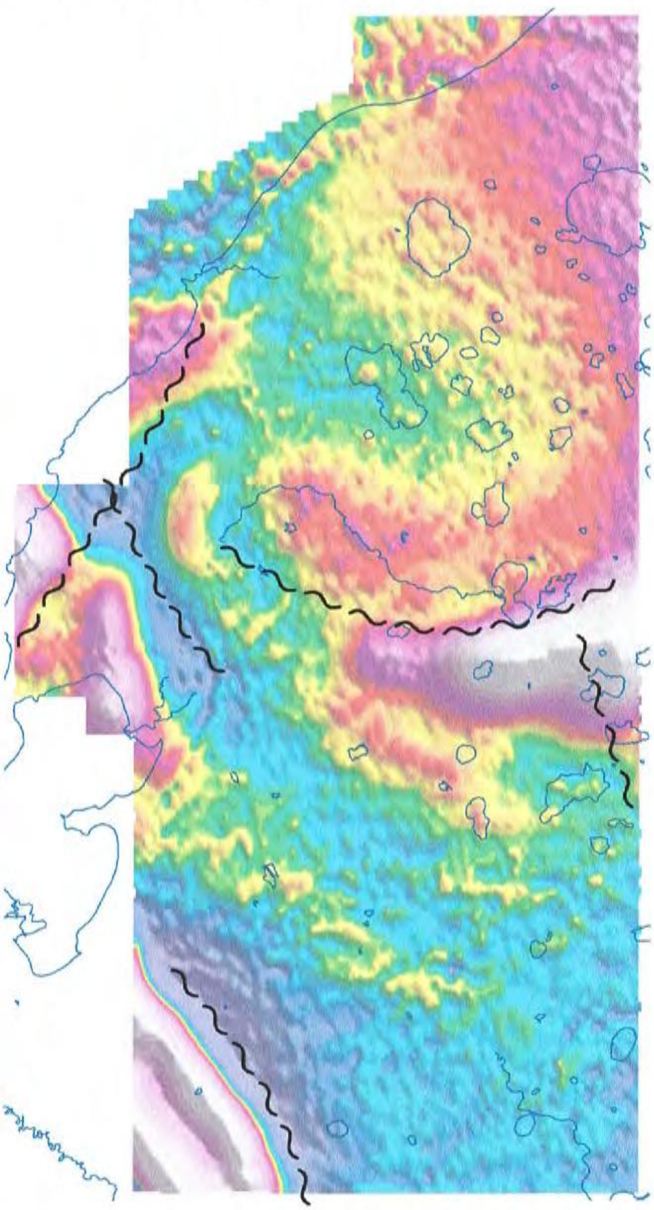

The interpretation shown in these two displays predicts the approximate locations of edges or changes to long wavelength magnetic features that are believed to represent basement structure.

In the next two maps Fugro's fault interpretation in the northern third of the survey area has been added. The first map is the same faded CDT map and the second is Fugro's first vertical derivative map with previous deep drill locations (using AGS hole ID designations) added as well.

Faded CDT's & Deep Faults plus Fugro Faults

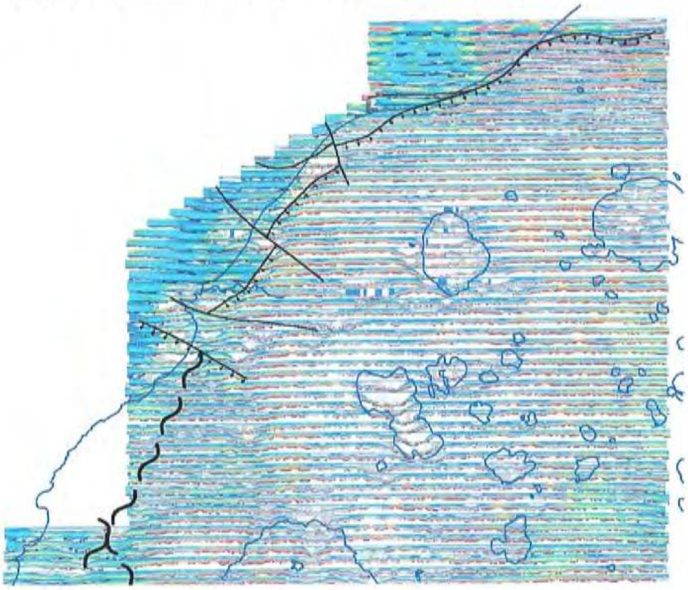

1st VD & Deep Faults plus Fugro Faults

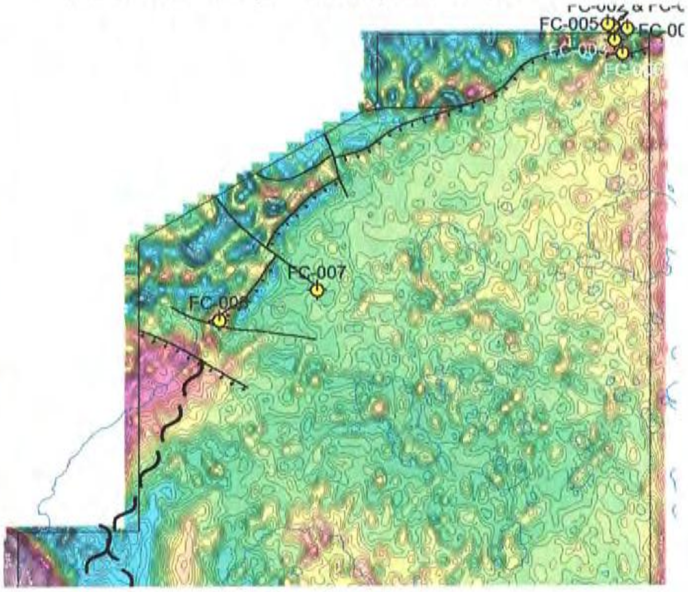

Below the same images have the "abrupt linear changes in conductor depth and/or strength" (in red) added to show how some correlate with Fugro's interpreted faults.

Faded CDT's, Deep, Fugro & EM Faults

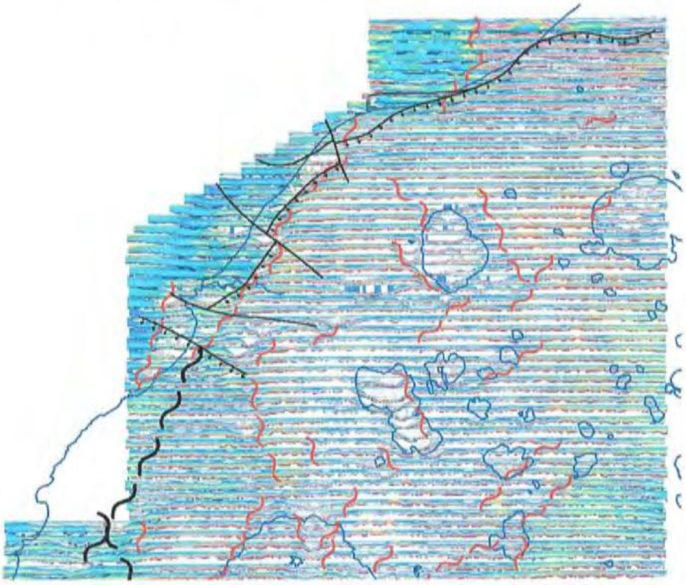

1st VD, Deep, Fugro & EM Faults

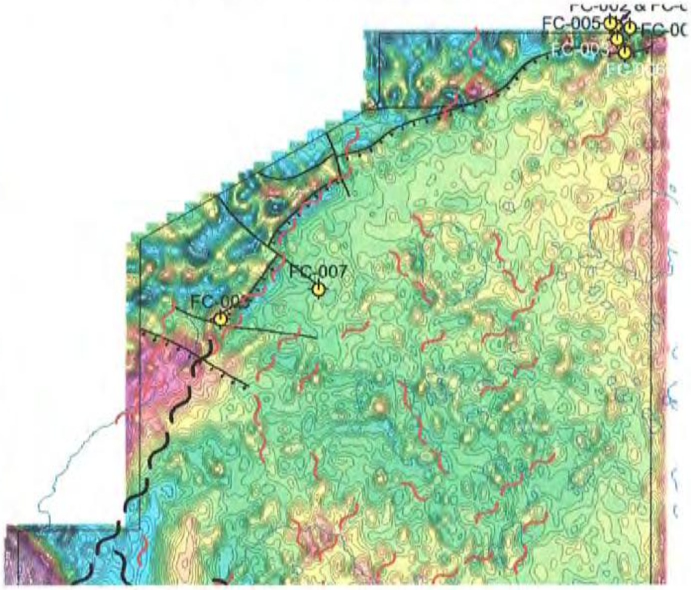

Note that most of the interpreted EM "abrupt linear changes" trend either northeast or northwest. At this point it is important to mention that the horizontal conductive layer that pervades the area *does not*, as pointed out by Fugro, *reflect a surface glacial feature but an intrasedimentary lithological unit with some fault control from the basement*. Thus the abrupt linear changes in depth and conductivity of the layer are believed to represent subsurface changes and not changes in glacial or other conductive overburden.

The following maps show the complete area with the same information as above.

Faded CDT's, Deep, Fugro & EM Faults

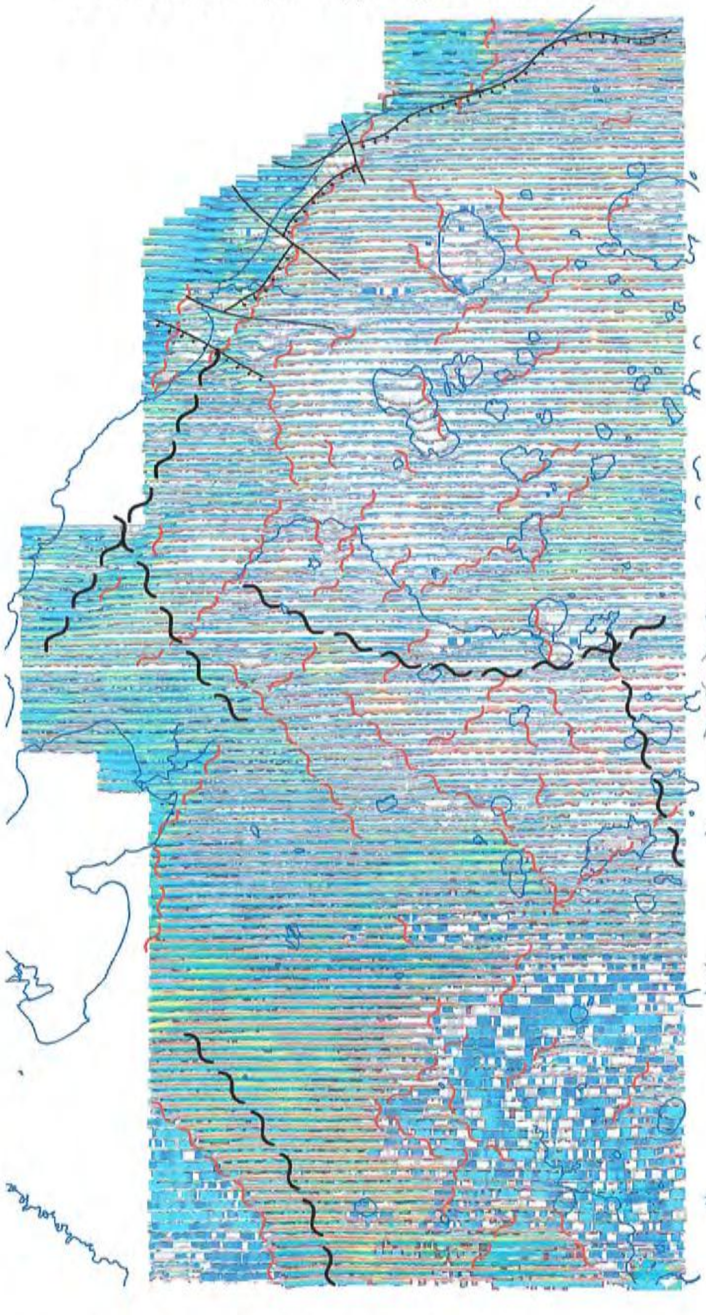

1st VD, Deep, Fugro & EM Faults

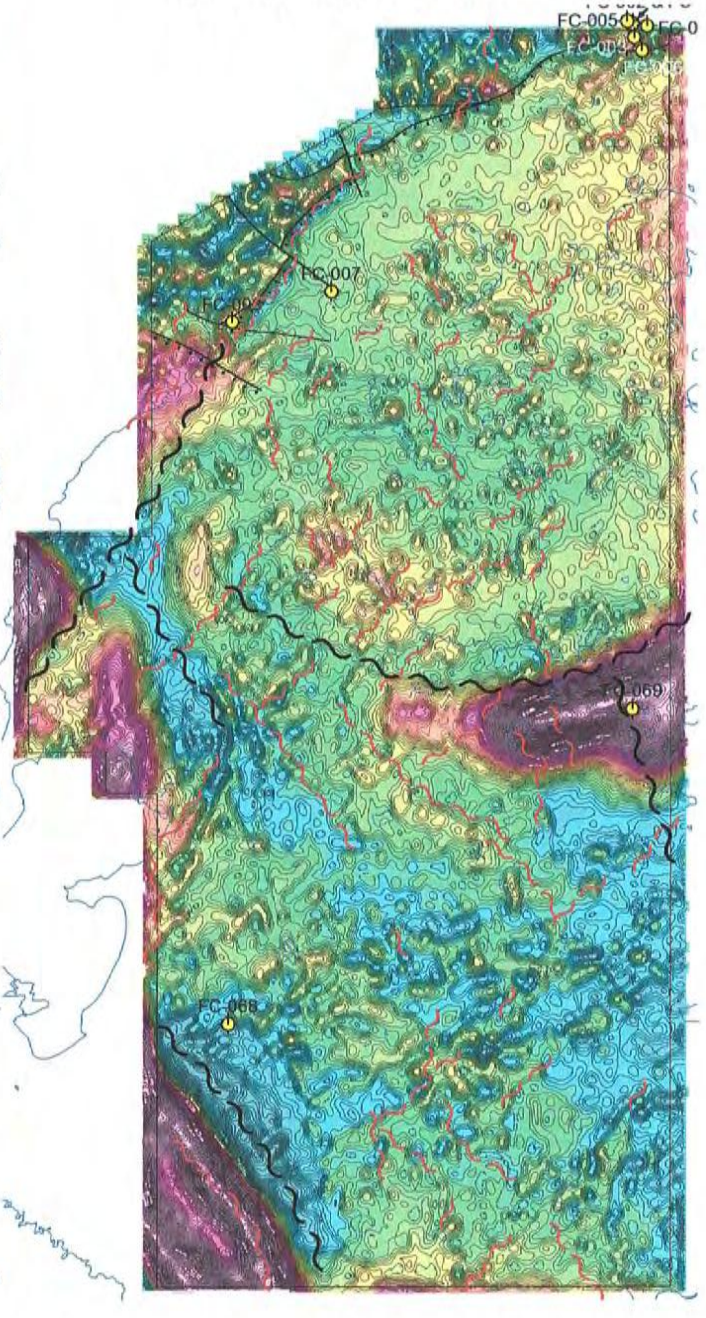

Once again most of the abrupt linear changes in the conductive layer can be seen to trend either northeast or northwest throughout the area. The question is, could these directions indicate a general structural "fabric" in the Atabasca sediments related to basement structure? The next two maps below may shed some light on this question.

These maps, again the same CDT and first vertical derivative maps, now have structure interpreted from first vertical derivative and tilt derivative maps (shown at the end of the report in Appendix II).

Faded CDT's, Deep, Fugro, EM & 1VD Faults

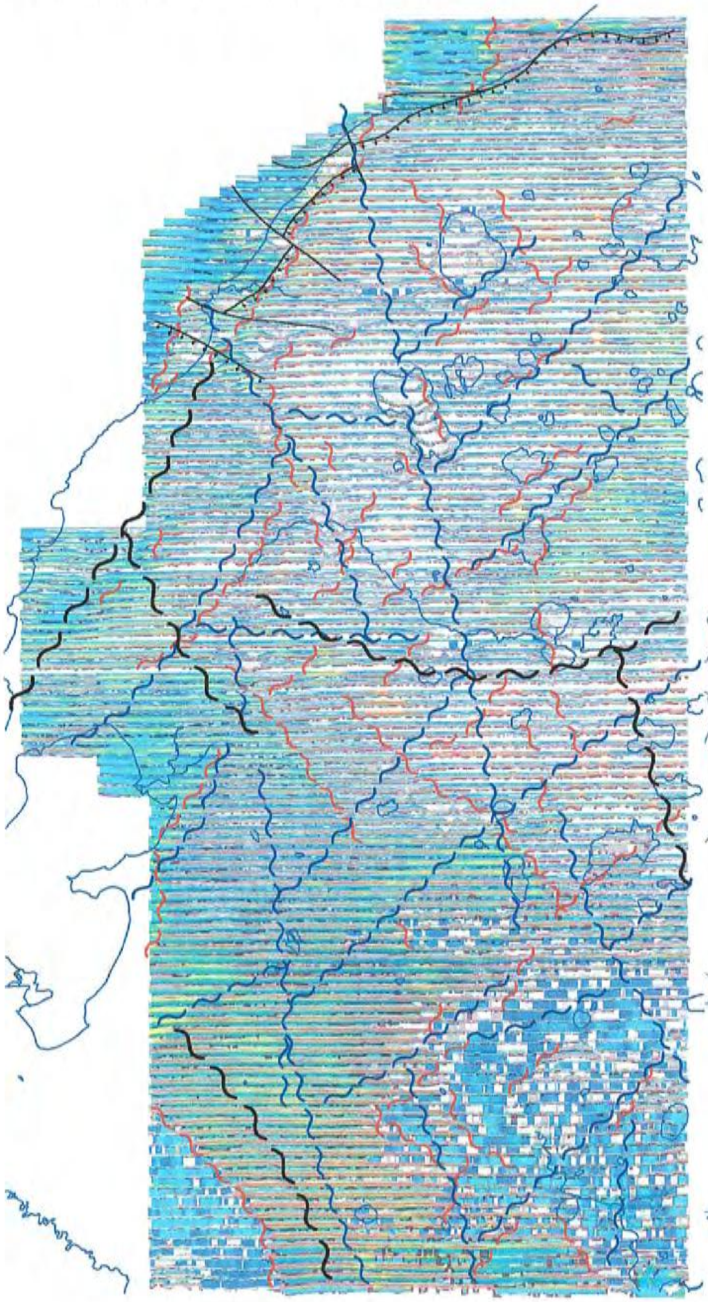

1st VD, Deep, Fugro, EM & 1VD Faults

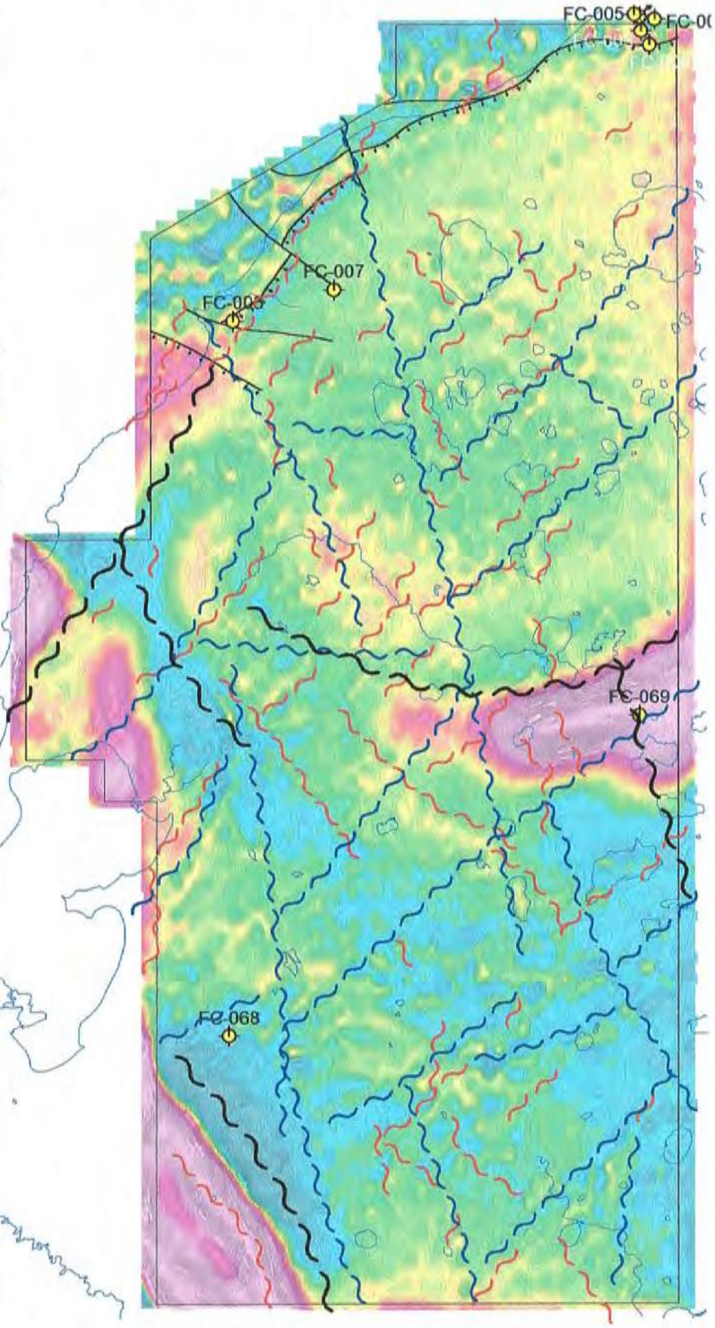

Now we see that most of the structural trend directions interpreted (independent of the EM data) from first vertical and tilt derivative maps are also northeast and northwest. Furthermore some correspond with or are flanked by the abrupt linear changes ("EM faults") in the conductive layer (interpreted from the CDT stacked section map). It is interesting to note that the deep drill hole (AGS ID) FC-069 targeting the "strong east-west magnetic feature" in the central-east part of the area coincides with a predicted deep fault as well as an intersection with a northeast fault interpreted from the derivative maps. This is consistent with a dilation zone occurring within the Athabasca sediments resulting in the "excessive caving" and loss of the hole "prior to reaching the unconformity" (described by Condor in their processing report).

3. CONCLUSIONS AND RECOMMENDATIONS

Although no bona fide conductors that may represent basement graphitic structures were found that would satisfy the classic target scenario in the deep basin, it is believed that the airborne (MEGATEM) survey was successful in defining non-traditional zones of interest within the survey area. These zones of interest are where lineaments interpreted from magnetic and electromagnetic data coincide to form what may be complex structural environments conducive to fluid flow and mineral precipitation.

RMI with Interpreted Faults and Zones of Interest

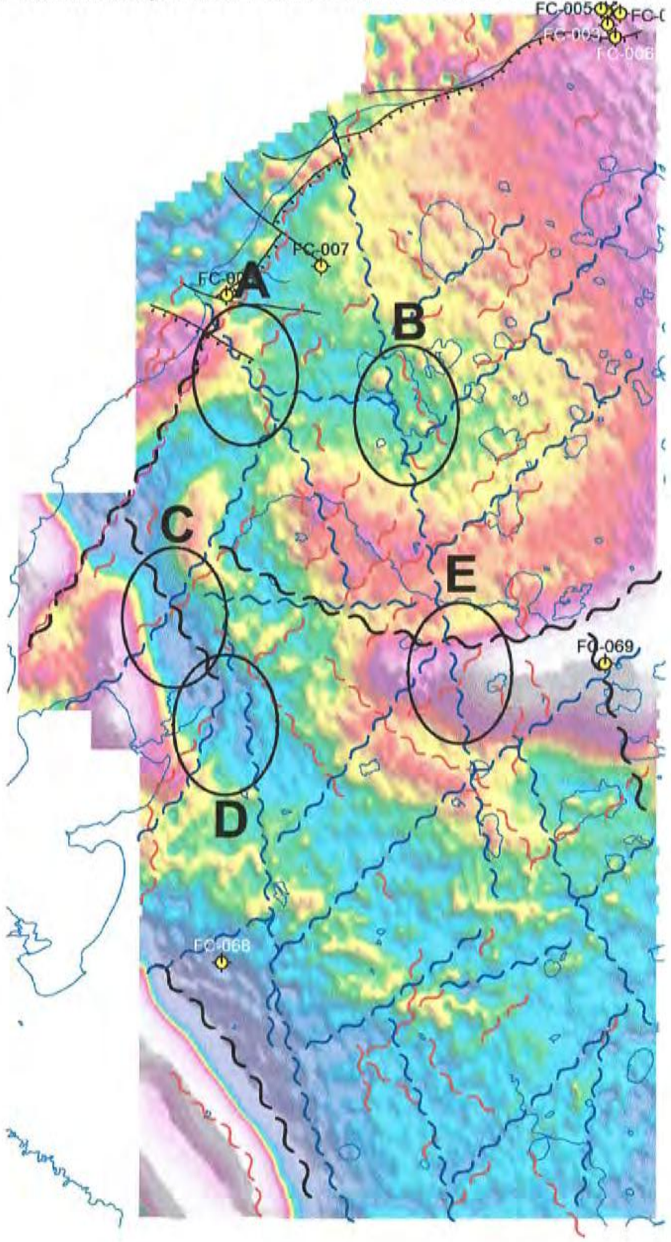

Five zones of interest, "A" through "E", have been suggested for follow-up on the ground. With the exception of "B" all are in the vicinity of interpreted deep structure and are thought to have the best potential for the discovery of deep faulting and alteration. Area "B" is interesting because the complex (interpreted) structural environment coincides with an unusually strong (surface) conductive lake oriented northwest and with a broad rounded magnetic low region.

Within these five zones a ground exploration program is recommended to more accurately establish targets for additional exploration. Since there seems to be evidence for surface multi-element soil anomalies some consideration could be given to widely spaced geochemical and/or radon gas surveys to test for indications of small amounts of indicator elements emanating from deep structural sources. In addition a deep penetrating ground geophysical survey method such as magnetotellurics (MT) is suggested in order to help define changes in deep subsurface electrical properties that can indicate alteration zones and possible associated uranium mineralization as targets for drill testing.

Respctfully Submitted

E. R. ROCKEL

Edwin R. Rockel, B.Sc., P.Geo.

Appendix I

Statement of Qualifications

STATEMENT OF QUALIFICATIONS - E. R. Rockel

I, Edwin Ross Rockel, of the city of Surrey, Province of British Columbia, hereby certify that:

- I received a B.Sc. degree in Geophysics from the University of British Columbia in 1966.
- I currently reside at 13000 54A Avenue, in the City of Surrey, in the Province of British Columbia.
- I have been practising my profession since graduation.
- I am a Professional Geoscientist registered in the Province of British Columbia.
- I am a Professional Geoscientist registered in the Northwest Territories.
- This report may be used for the development of the property, provided that no portion will be used out of context in such a manner as to convey meanings different from that set out in the whole.
- Consent is hereby given to the company for which this report was prepared to reproduce the report or any part of it for the purposes of development of the property, or facts relating to the raising of funds by way of a prospectus and/or statement of material facts.

Dated 20 March, 2007 **Signed**

E. R. Rockel, B.Sc., P.Geo.

E. R. ROCKEL

Appendix II

Full Map Images of Maps Used in this Report

(Note: The "Stacked Fugro Conductivity Depth Transforms" map and the "First Vertical Derivative of Residual Magnetic Intensity" are Fugro products that have been modified by the writer for the purposes of this report. The "Residual Magnetic Intensity Contours & Interpretation" map and "Tilt Derivative of RMI & Interpretation" map, created by the writer, contain a Map Index copied from the Fugro production maps. The Fugro "Flight Path, Permits and Interpretation Map" is the Fugro "Flight Path" production map modified by the writer to include permit boundaries and labels and the present geophysical interpretation. All maps in this Appendix are also presented as E-size hard copy maps at a scale of 1:50,000.

Stacked Fugro Conductivity Depth Transforms

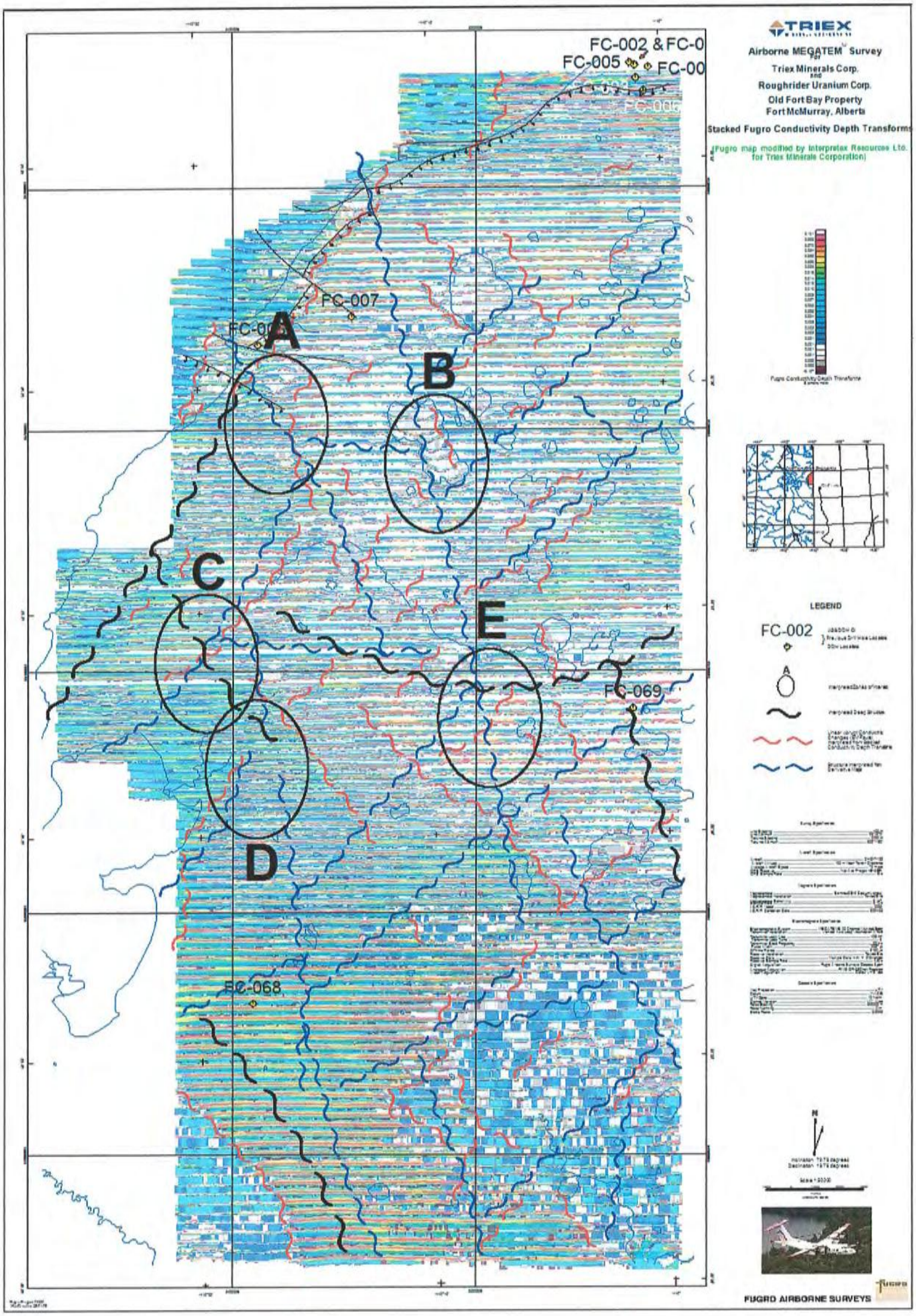

Residual Magnetic Intensity Contours & Interpretation

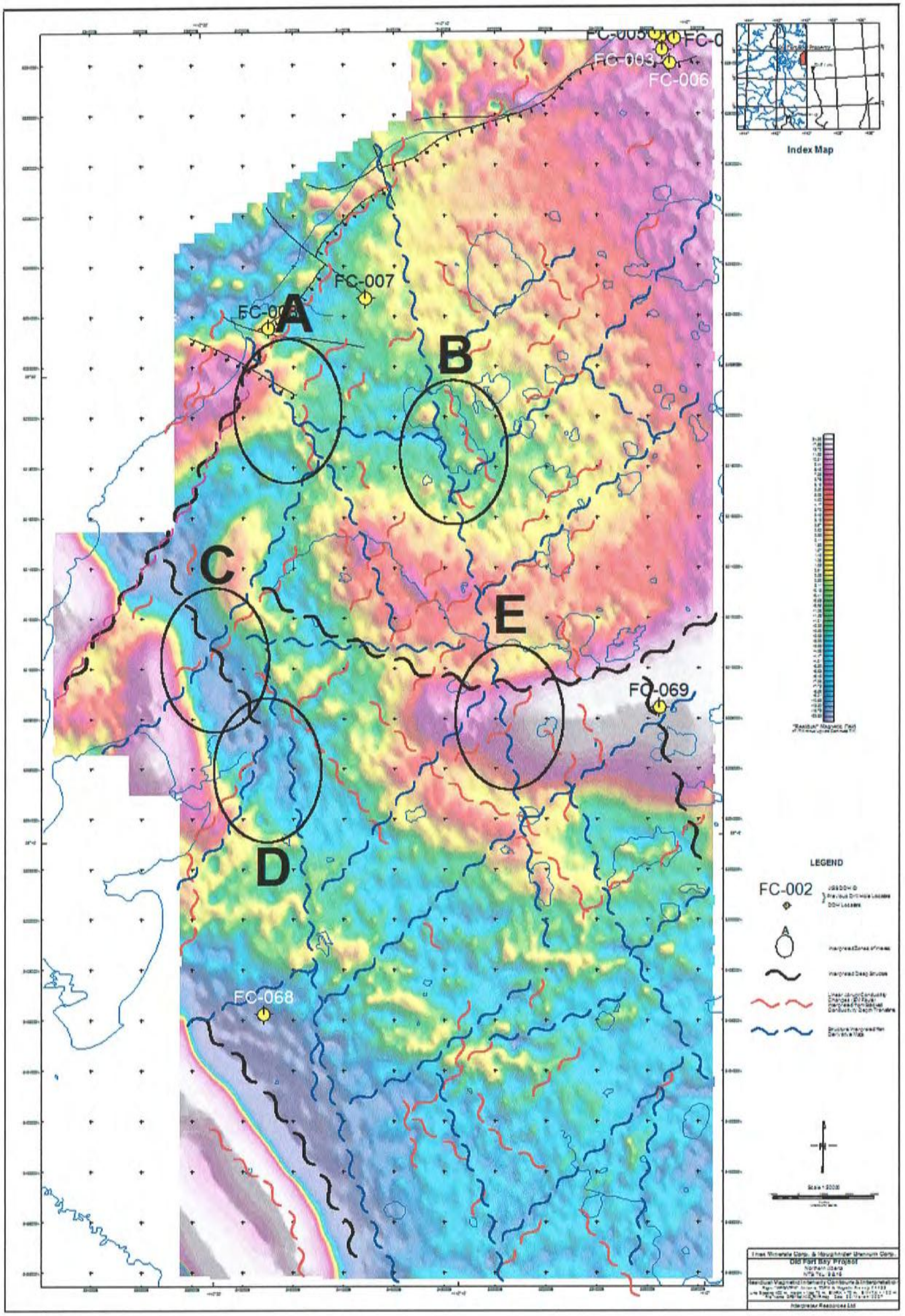

First Vertical Derivative of Residual Magnetic Intensity

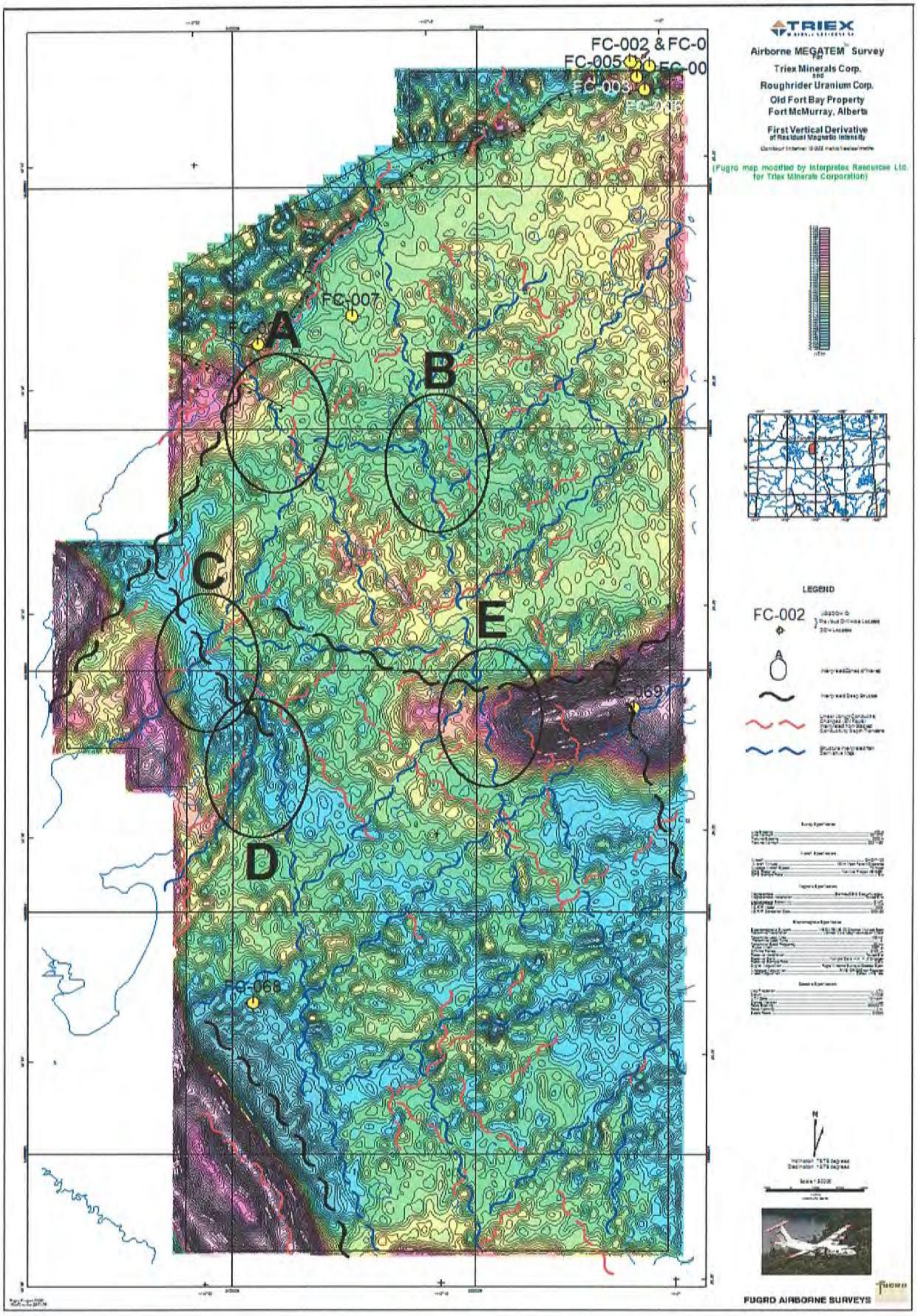

Tilt Derivative of RMI & Interpretation

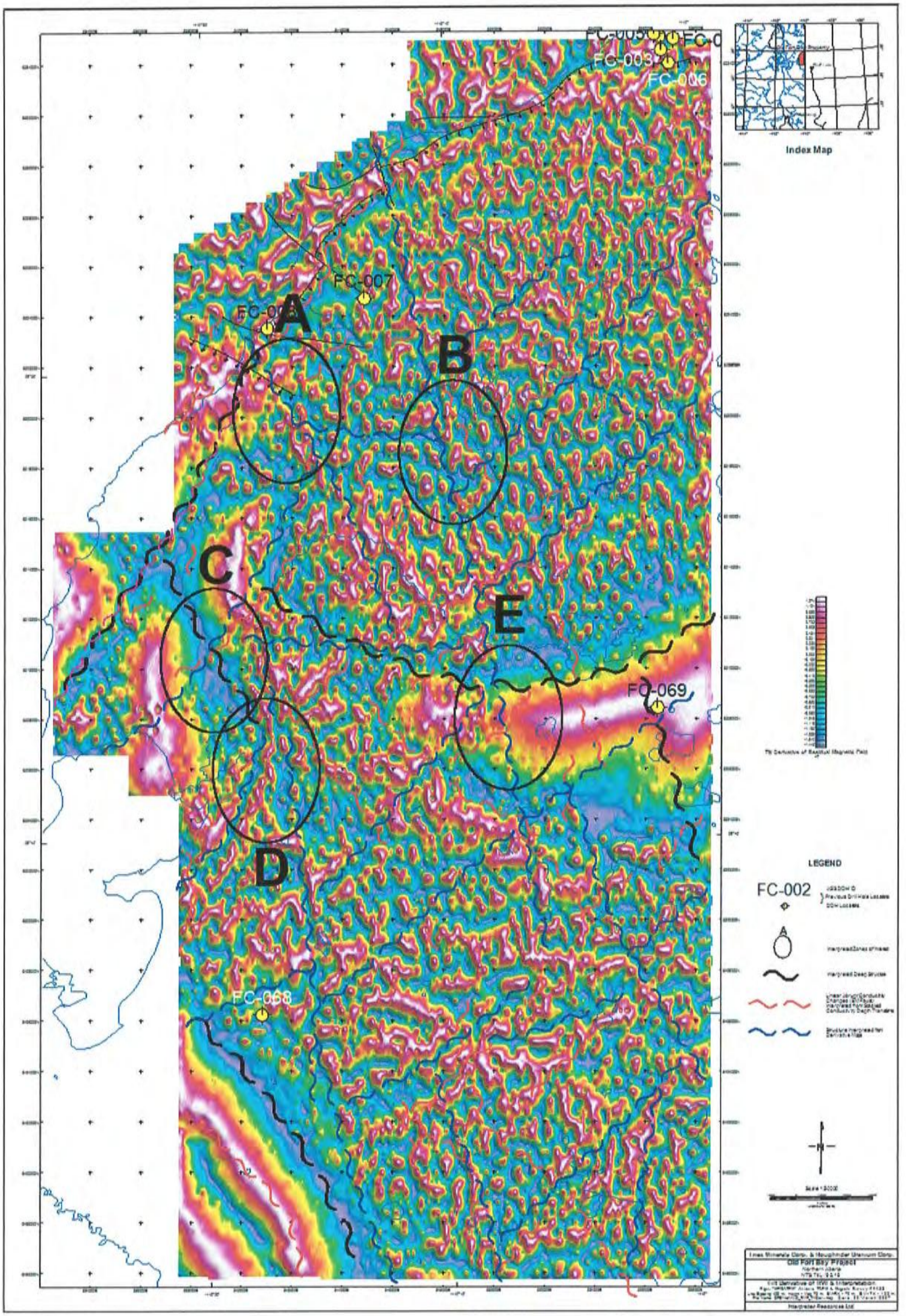

Flight Path, Permits and Interpretation Map

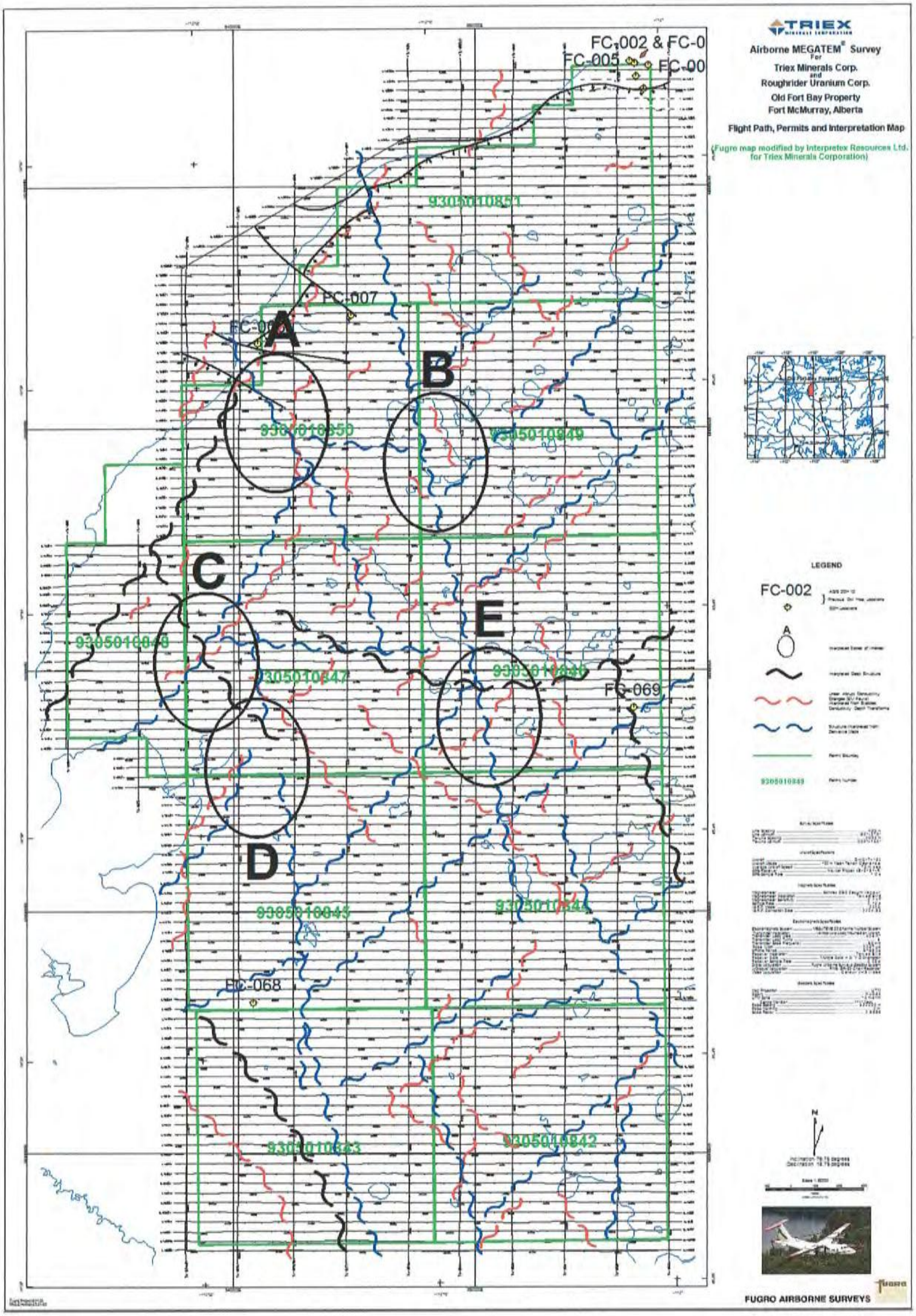

APPENDIX 7
(in folder at back of report)

1:50,000 Scale Maps from Interpretex Resources Ltd.

- **Map 13 - Stacked Fugro Conductivity Depth Transforms**
- **Map 14 - Residual Magnetic Intensity Contours & Interpretation**
- **Map 15 - First Vertical Derivative of Residual Magnetic Intensity**
- **Map 16 - Tilt Derivative of RMI & Interpretation**
- **Map 17 - Flight Path, Permits and Interpretation Map**

20070005

TRIEX MINERALS CORPORATION

Airborne MEGATEM® Survey
For
Triex Minerals Corp.
and
Roughrider Uranium Corp.

Old Fort Bay Property
Fort McMurray, Alberta

Flight Path

APPENDIX 3

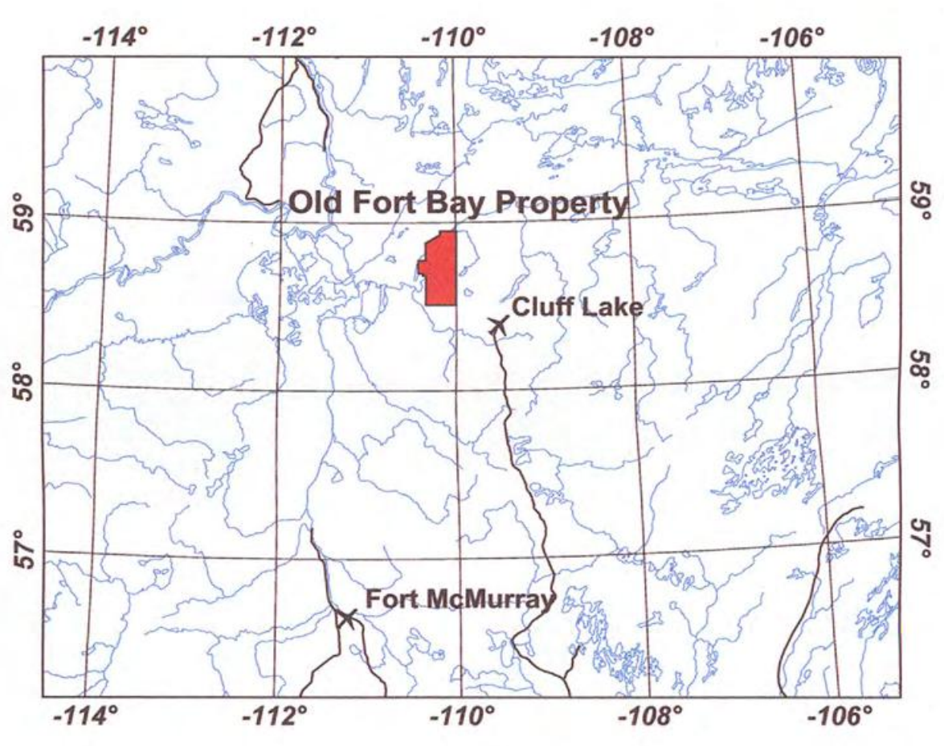

Survey Specifications

Line Spacing	400 m
Line Azimuth	90°-270°
Tie-Line Spacing	2000 m
Tie-Line Azimuth	000°-180°

Aircraft Specifications

Aircraft	DHC-7-102
Aircraft Altitude	120 m Mean Terrain Clearance
Average Aircraft Speed	70 m/sec
GPS Receiver	NovAtel Propak 4E-3151-R
GPS Sample Rate	1.0 s

Magnetic Specifications

Magnetometer	Scintrex CS-2 Cesium Vapour
Magnetometer Installation	Towed Bird
Magnetometer Sensitivity	0.1 nT
Sample Rate	0.10 s
I.G.R.F. Model	2003
I.G.R.F. Correction Date	2004.95

Electromagnetic Specifications

Electromagnetic System	MEGATEM® 20 Channel Multicoil System
Transmitter Installation	Vertical Axis Loop Mounted on Aircraft
Transmitter Loop Area	406 m²
Transmitter Loop Turns	6
Transmitter Base Frequency	90 Hz
Pulse Width	2287 µs
Off-time Period	3169 µs
Receiver Installation	Towed Bird
Receiver Coils	Multiple Coils in X, Y, Z Orientation
Receiver Sample Rate	0.25 s
Digital Acquisition	Fugro Airborne Surveys Geodas System
Analogue Acquisition	RMS GR-33 Chart Recorder
Video Acquisition	Colour VHS Video

Geodetic Specifications

Map Projection	UTM
Datum	NAD83
UTM Zone	12 North
Central Meridian	111° West
False Easting	500000 m
False Northing	0 m
Scale Factor	0.9996

Inclination 79.76 degrees
Declination 18.79 degrees

Scale 1:50000

1000 0 1000 2000 3000
metres
NAD83 / UTM zone 12N

Fugro Project 04430
Map Creation 25.01.05

FUGRO AIRBORNE SURVEYS

20070005

Fugro Project 04430
Map Creation 25.01.05

TRIEX MINERALS CORPORATION

Airborne MEGATEM® Survey
For
Triex Minerals Corp.
and
Roughrider Uranium Corp.

Old Fort Bay Property
Fort McMurray, Alberta

Residual Magnetic Intensity

Contour Interval 2 nanoTeslas

181
68
20
-44
-110
-156
-180
-196
-214
-232
-244
-254
-262
-270
-278
-286
-294
-302
-310
-318
-326
-334
-342
-350
-358
-366
-374
-382
-390
-398
-406
-414
-422
-430
-450
nT

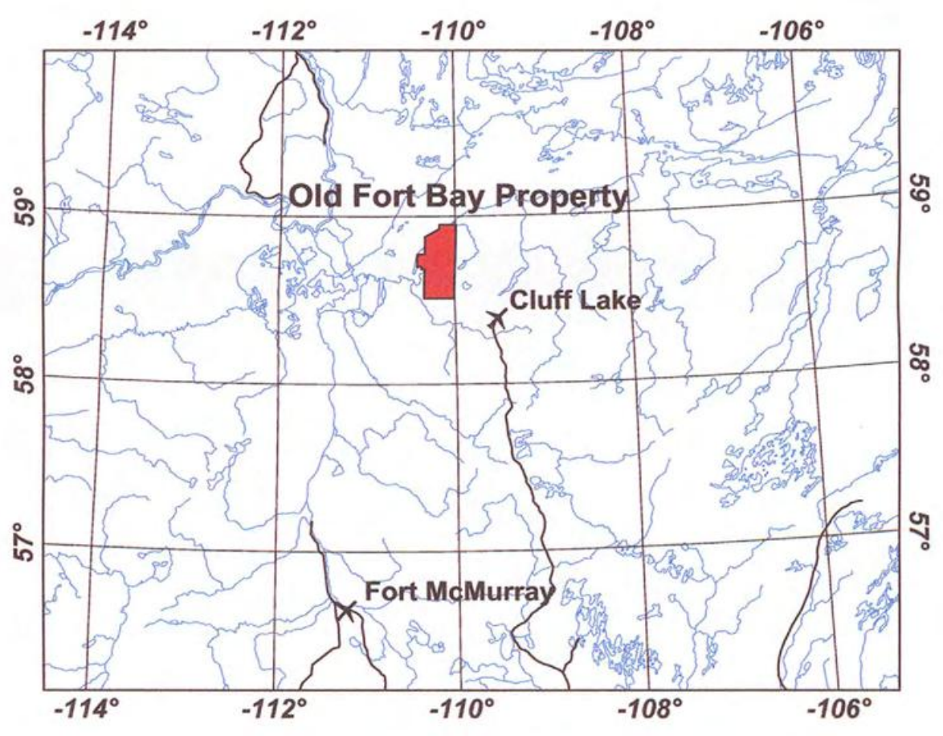

Survey Specifications

Line Spacing	400 m
Line Azimuth	90°-270°
Tie-Line Spacing	2000 m
Tie-Line Azimuth	000°-180°

Aircraft Specifications

Aircraft	DHC-7-102
Aircraft Altitude	120 m Mean Terrain Clearance
Average Aircraft Speed	70 m/sec
GPS Receiver	NovAtel Propak 4E-3151-R
GPS Sample Rate	1.0 s

Magnetic Specifications

Magnetometer	Scintrex CS-2 Cesium Vapour
Magnetometer Installation	Towed Bird
Magnetometer Sensitivity	0.1 nT
Sample Rate	0.10 s
I.G.R.F. Model	2003
I.G.R.F. Correction Date	2004.95

Electromagnetic Specifications

Electromagnetic System	MEGATEM® 20 Channel Multicoil System
Transmitter Installation	Vertical Axis Loop Mounted on Aircraft
Transmitter Loop Area	406 m²
Transmitter Loop Turns	6
Transmitter Base Frequency	90 Hz
Pulse Width	2287 µs
Off-time Period	3169 µs
Receiver Installation	Towed Bird
Receiver Coils	Multiple Coils in X, Y, Z Orientation
Receiver Sample Rate	0.25 s
Digital Acquisition	Fugro Airborne Surveys Geodas System
Analogue Acquisition	RMS GR-33 Chart Recorder
Video Acquisition	Colour VHS Video

Geodetic Specifications

Map Projection	UTM
Datum	NAD83
UTM Zone	12 North
Central Meridian	111° West
False Easting	500000 m
False Northing	0 m
Scale Factor	0.9996

N

Inclination 79.76 degrees
Declination 18.79 degrees

Scale 1:50000
1000 0 1000 2000 3000
metres
NAD83 / UTM zone 12N

FUGRO AIRBORNE SURVEYS

20070005

TRIEX
MINERALS CORPORATION

Airborne MEGATEM® Survey
For
Triex Minerals Corp.
and
Roughrider Uranium Corp.

Old Fort Bay Property
Fort McMurray, Alberta

First Vertical Derivative
of Residual Magnetic Intensity
Contour Interval 0.002 nanoTeslas/metre

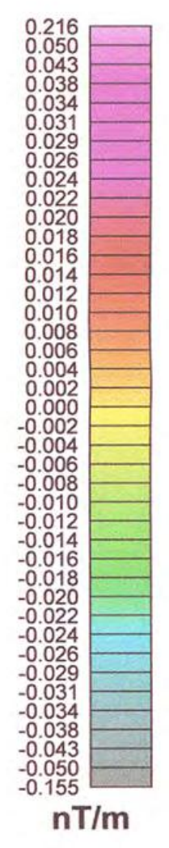

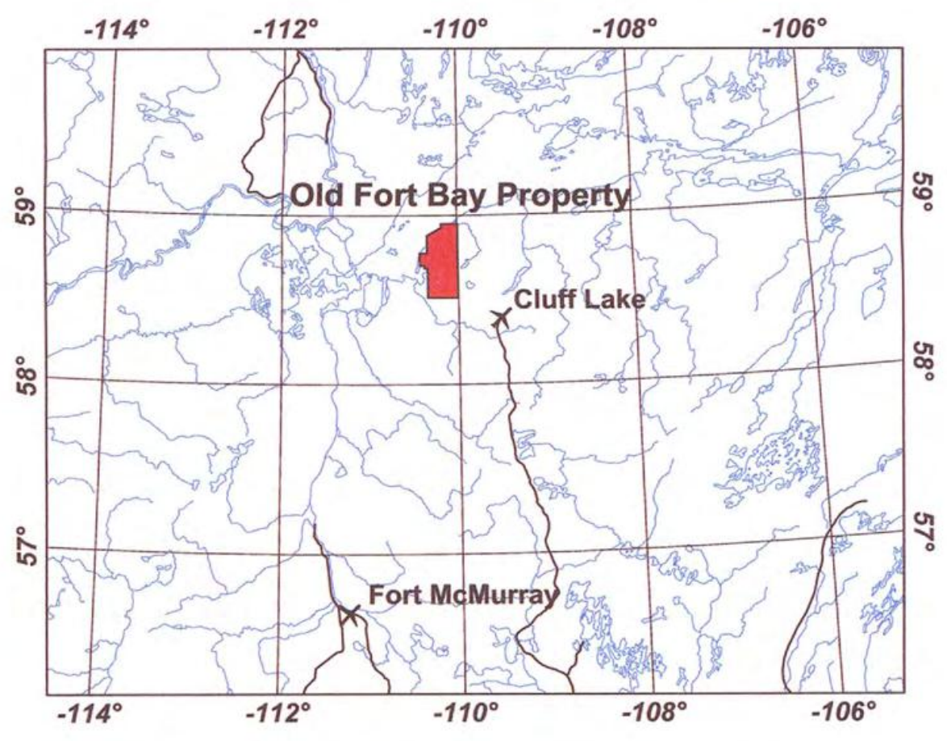

Survey Specifications

Line Spacing	400 m
Line Azimuth	90°-270°
Tie-Line Spacing	2000 m
Tie-Line Azimuth	000°-180°

Aircraft Specifications

Aircraft	DHC-7-102
Aircraft Altitude	120 m Mean Terrain Clearance
Average Aircraft Speed	70 m/sec
GPS Receiver	NovAtel Propak 4E-3151-R
GPS Sample Rate	1.0 s

Magnetic Specifications

Magnetometer	Scintrex CS-2 Cesium Vapour
Magnetometer Installation	Towed Bird
Magnetometer Sensitivity	0.1 nT
Sample Rate	0.10 s
I.G.R.F. Model	2003
I.G.R.F. Correction Date	2004.95

Electromagnetic Specifications

Electromagnetic System	MEGATEM® 20 Channel Multicoil System
Transmitter Installation	Vertical Axis Loop Mounted on Aircraft
Transmitter Loop Area	406 m²
Transmitter Loop Turns	6
Transmitter Base Frequency	90 Hz
Pulse Width	2287 μs
Off-time Period	3169 μs
Receiver Installation	Towed Bird
Receiver Coils	Multiple Coils in X, Y, Z Orientation
Receiver Sample Rate	0.25 s
Digital Acquisition	Fugro Airborne Surveys Geodas System
Analogue Acquisition	RMS GR-33 Chart Recorder
Video Acquisition	Colour VHS Video

Geodetic Specifications

Map Projection	UTM
Datum	NAD83
UTM Zone	12 North
Central Meridian	111° West
False Easting	500000 m
False Northing	0 m
Scale Factor	0.9996

Inclination 79.76 degrees
Declination 18.79 degrees

Scale 1:50000

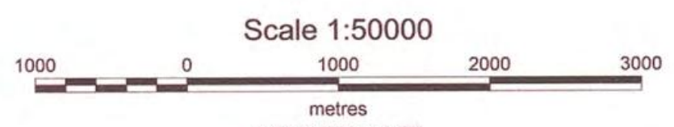

FUGRO AIRBORNE SURVEYS

Fugro Project 04430
Map Creation 25.01.05

20070005

TRIEX MINERALS CORPORATION

Airborne MEGATEM® Survey
For
Triex Minerals Corp.
and
Roughrider Uranium Corp.

Old Fort Bay Property
Fort McMurray, Alberta

Apparent Conductance
Derived from dB/dt X and Z Coils
Contour Interval 2 milliSiemens

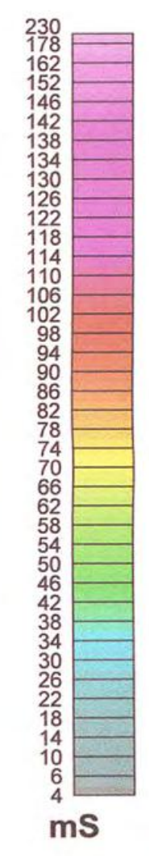

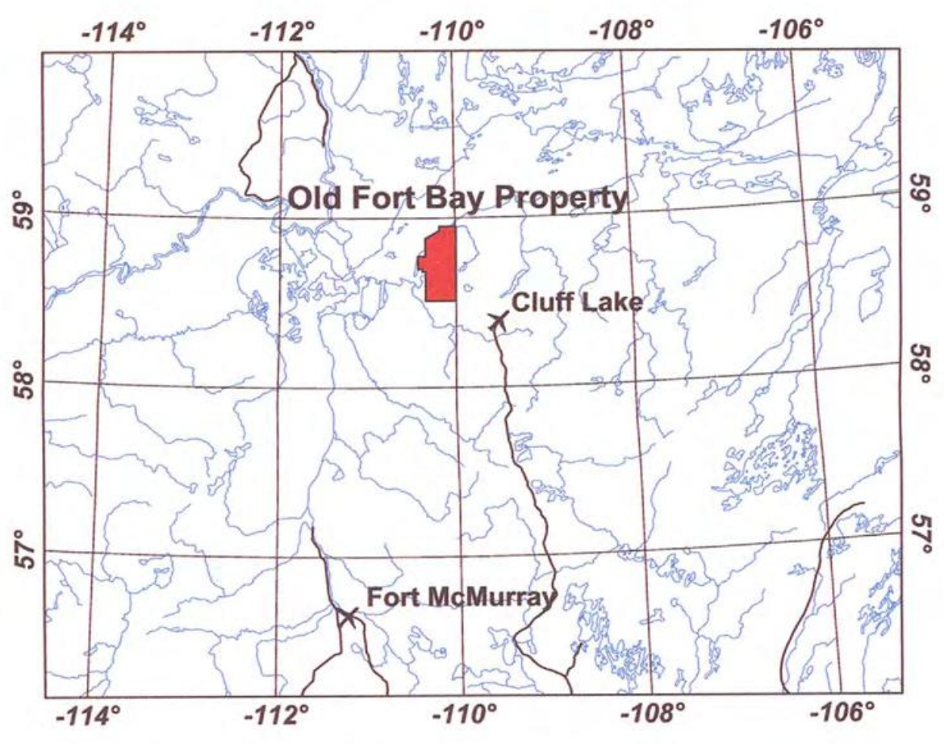

Survey Specifications

Line Spacing	400 m
Line Azimuth	90°-270°
Tie-Line Spacing	2000 m
Tie-Line Azimuth	000°-180°

Aircraft Specifications

Aircraft	DHC-7-102
Aircraft Altitude	120 m Mean Terrain Clearance
Average Aircraft Speed	70 m/sec
GPS Receiver	NovAtel Propak 4E-3151-R
GPS Sample Rate	1.0 s

Magnetic Specifications

Magnetometer	Scintrex CS-2 Cesium Vapour
Magnetometer Installation	Towed Bird
Magnetometer Sensitivity	0.1 nT
Sample Rate	0.10 s
I.G.R.F. Model	2003
I.G.R.F. Correction Date	2004.95

Electromagnetic Specifications

Electromagnetic System	MEGATEM® 20 Channel Multicoil System
Transmitter Installation	Vertical Axis Loop Mounted on Aircraft
Transmitter Loop Area	406 m²
Transmitter Loop Turns	6
Transmitter Base Frequency	90 Hz
Pulse Width	2287 µs
Off-time Period	3169 µs
Receiver Installation	Towed Bird
Receiver Coils	Multiple Coils in X, Y, Z Orientation
Receiver Sample Rate	0.25 s
Digital Acquisition	Fugro Airborne Surveys Geodas System
Analogue Acquisition	RMS GR-33 Chart Recorder
Video Acquisition	Colour VHS Video

Geodetic Specifications

Map Projection	UTM
Datum	NAD83
UTM Zone	12 North
Central Meridian	111° West
False Easting	500000 m
False Northing	0 m
Scale Factor	0.9996

Inclination 79.76 degrees
Declination 18.79 degrees

Scale 1:50000

metres
NAD83 / UTM zone 12N

Fugro Project 04430
Map Creation 25.01.05

FUGRO AIRBORNE SURVEYS

20070005

TRIEX
MINERALS CORPORATION

Airborne MEGATEM® Survey
For
Triex Minerals Corp.
and
Roughrider Uranium Corp.

Old Fort Bay Property
Fort McMurray, Alberta

3rd Order Moment
Derived from B Field X and Z Coils
Contour Interval 2 parts-per-million

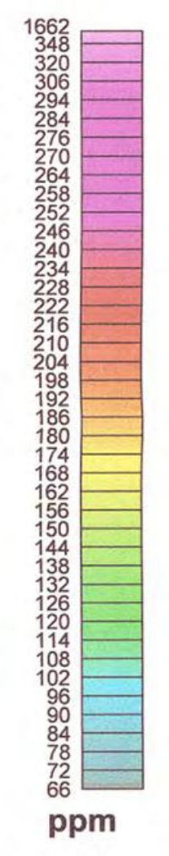

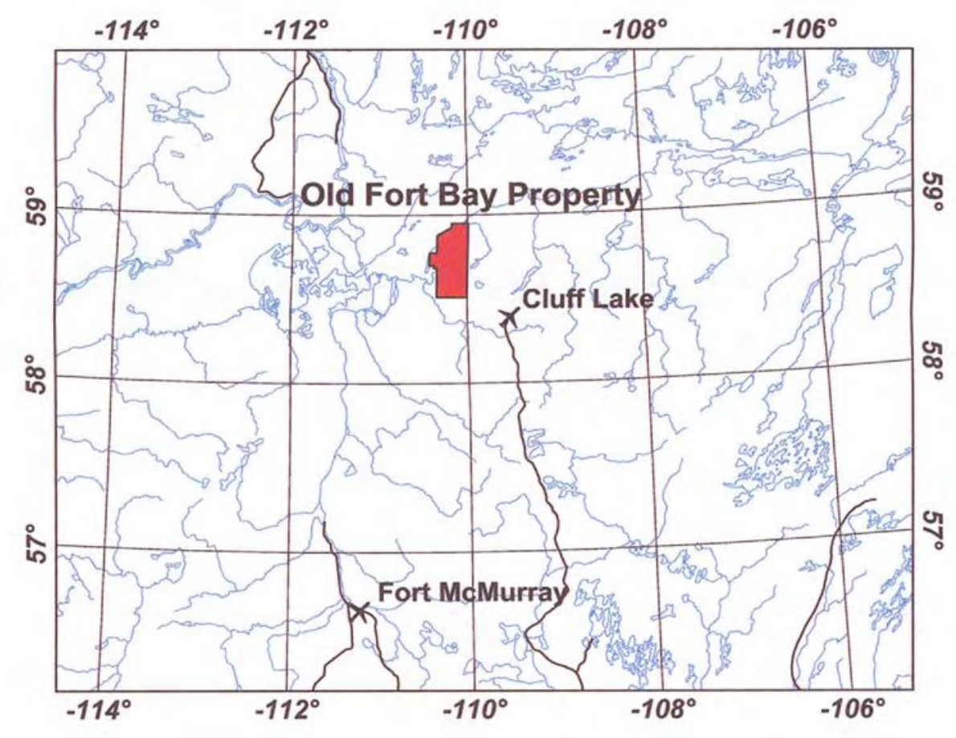

Survey Specifications

Line Spacing .... 400 m
Line Azimuth .... 90°-270°
Tie-Line Spacing .... 2000 m
Tie-Line Azimuth .... 000°-180°

Aircraft Specifications

Aircraft DHC-7-102
Aircraft Altitude .... 120 m Mean Terrain Clearance
Average Aircraft Speed .... 70 m/sec
GPS Receiver .... NovAtel Propak 4E-3151-R
GPS Sample Rate .... 1.0 s

Magnetic Specifications

Magnetometer .... Scintrex CS-2 Cesium Vapour
Magnetometer Installation .... Towed Bird
Magnetometer Sensitivity .... 0.1 nT
Sample Rate .... 0.10 s
I.G.R.F. Model 2003
I.G.R.F. Correction Date 2004.95

Electromagnetic Specifications

Electromagnetic System .... MEGATEM® 20 Channel Multicoil System
Transmitter Installation .... Vertical Axis Loop Mounted on Aircraft
Transmitter Loop Area .... 406 m²
Transmitter Loop Turns 6
Transmitter Base Frequency .... 90 Hz
Pulse Width .... 2287 µs
Off-time Period.......... 3169 µs
Receiver Installation .... Towed Bird
Receiver Coils .... Multiple Coils in X, Y, Z Orientation
Receiver Sample Rate .... 0.25 s
Digital Acquisition .... Fugro Airborne Surveys Geodas System
Analogue Acquisition .... RMS GR-33 Chart Recorder
Video Acquisition .... Colour VHS Video

Geodetic Specifications

Map Projection .... UTM
Datum NAD83
UTM Zone .... 12 North
Central Meridian .... 111° West
False Easting .... 500000 m
False Northing .... 0 m
Scale Factor 0.9996

Inclination 79.76 degrees
Declination 18.79 degrees

Scale 1:50000

metres
NAD83 / UTM zone 12N

FUGRO AIRBORNE SURVEYS

Fugro Project 04430
Map Creation 25.01.05

20070005

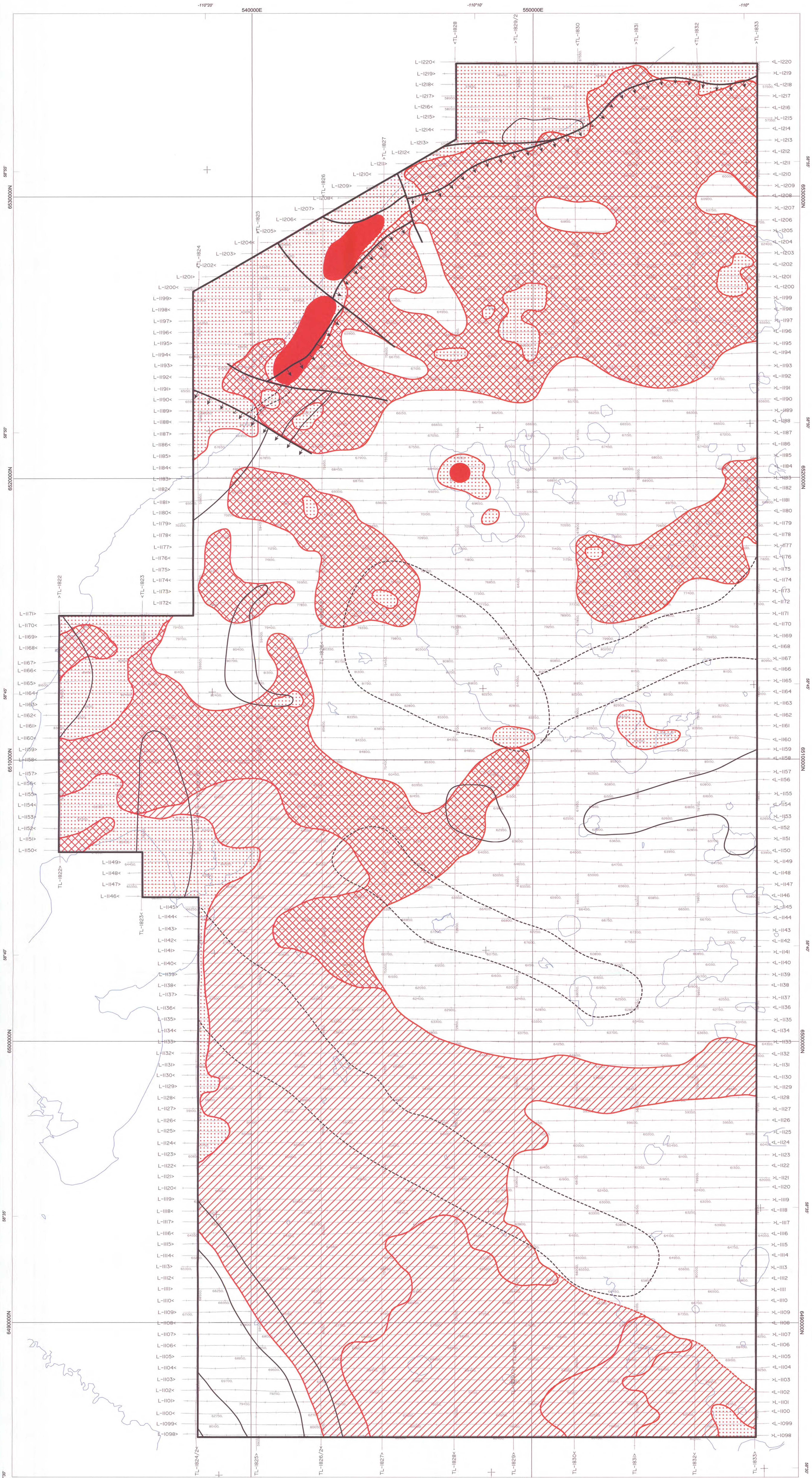

TRIEX
MINERALS CORPORATION

Airborne MEGATEM® Survey
For
Triex Minerals Corp.
and
Roughrider Uranium Corp.

Old Fort Bay Property
Fort McMurray, Alberta

Basic EM Interpretation Map

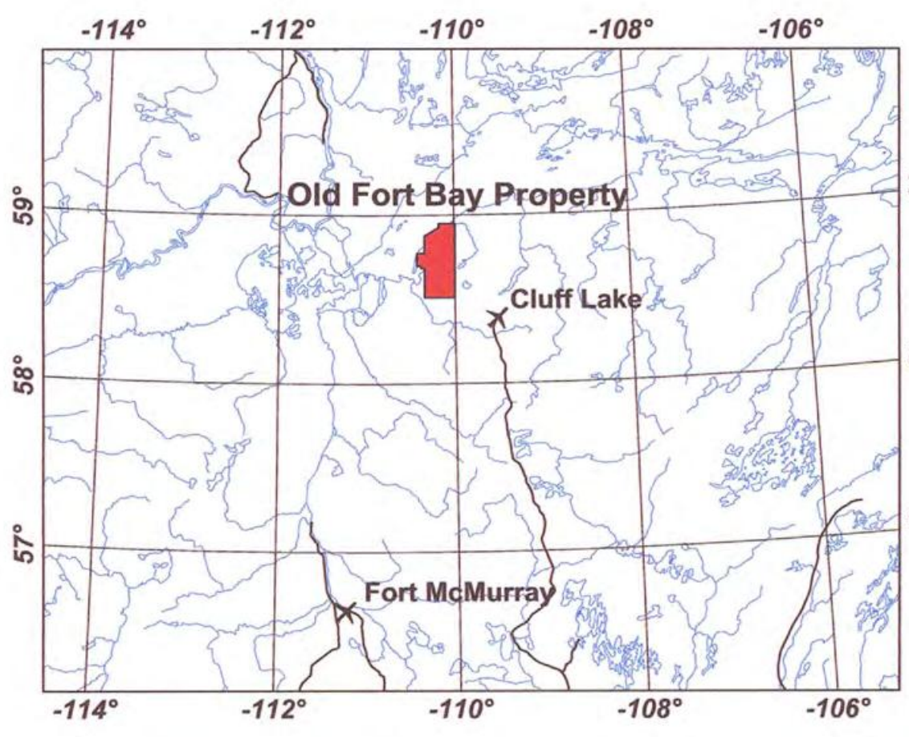

Interpretation Legend

∴	Surface conductive response (lake bottom sediments, marches, alluvium)
▨	Subsurface (intrasedimentary) conductive layer response
▩	Zones of stronger late-time response
●	Zones of B-field enhanced response
═	EM zone boundary (solid line-defined, dashed line-assumed)
╱	Tectonic Faults Interpreted from the Survey Magnetics (arrows show dip-slip direction)
╌	Archean Magnetic/Lithological Boundary (solid line-defined, dashed line-assumed)

Survey Specifications

Line Spacing	400 m
Line Azimuth	90°-270°
Tie-Line Spacing	2000 m
Tie-Line Azimuth	000°-180°

Aircraft Specifications

Aircraft	DHC-7-102
Aircraft Altitude	120 m Mean Terrain Clearance
Average Aircraft Speed	70 m/sec
GPS Receiver	NovAtel Propak 4E-3151-R
GPS Sample Rate	1.0 s

Magnetic Specifications

Magnetometer	Scintrex CS-2 Cesium Vapour
Magnetometer Installation	Towed Bird
Magnetometer Sensitivity	0.1 nT
Sample Rate	0.10 s
I.G.R.F. Model	2003
I.G.R.F. Correction Date	2004.95

Electromagnetic Specifications

Electromagnetic System	MEGATEM® 20 Channel Multicoil System
Transmitter Installation	Vertical Axis Loop Mounted on Aircraft
Transmitter Loop Area	406 m²
Transmitter Loop Turns	6
Transmitter Base Frequency	90 Hz
Pulse Width	2287 µs
Off-time Period	3169 µs
Receiver Installation	Towed Bird
Receiver Coils	Multiple Coils in X, Y, Z Orientation
Receiver Sample Rate	0.25 s
Digital Acquisition	Fugro Airborne Surveys Geodas System
Analogue Acquisition	RMS GR-33 Chart Recorder
Video Acquisition	Colour VHS Video

Geodetic Specifications

Map Projection	UTM
Datum	NAD83
UTM Zone	12 North
Central Meridian	111° West
False Easting	500000 m
False Northing	0 m
Scale Factor	0.9996

Inclination 79.76 degrees
Declination 18.79 degrees

Scale 1:50000
1000 0 1000 2000 3000
metres
NAD83 / UTM zone 12N

FUGRO AIRBORNE SURVEYS

Fugro Project 04430
Map Creation 11.03.05

20070005

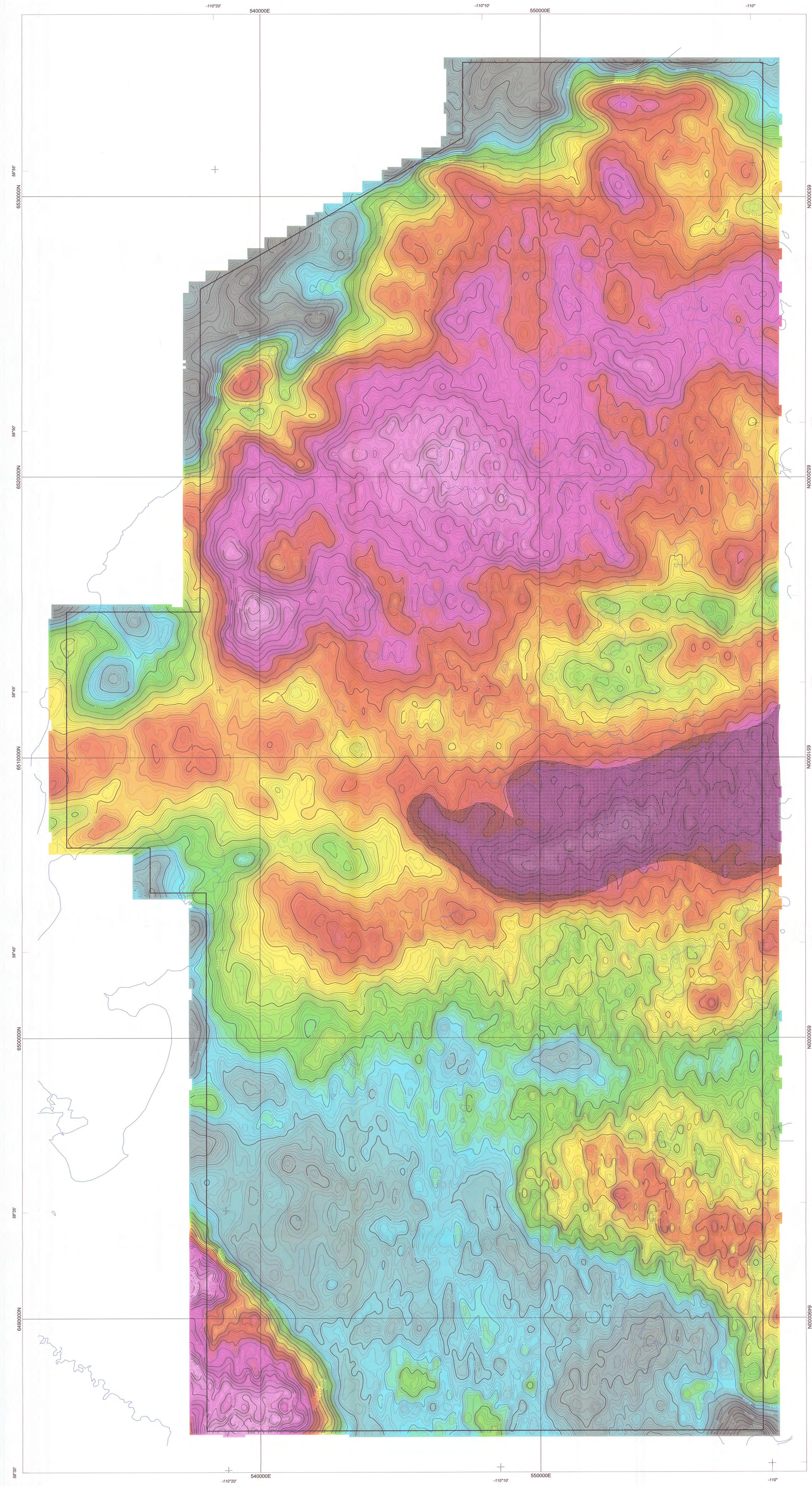

TRIEX MINERALS CORPORATION

Airborne MEGATEM® Survey
For
Triex Minerals Corp.
and
Roughrider Uranium Corp.

Old Fort Bay Property
Fort McMurray, Alberta

Decay Constant (Tau)
Derived from B Field Z Coil Channels 12-20

Contour Interval 5 microseconds

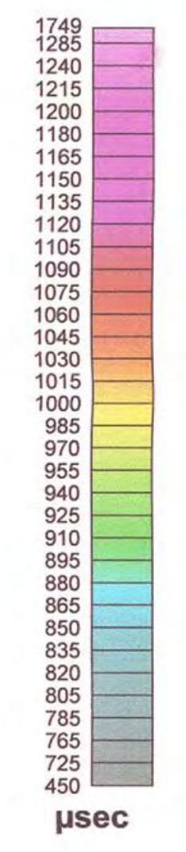

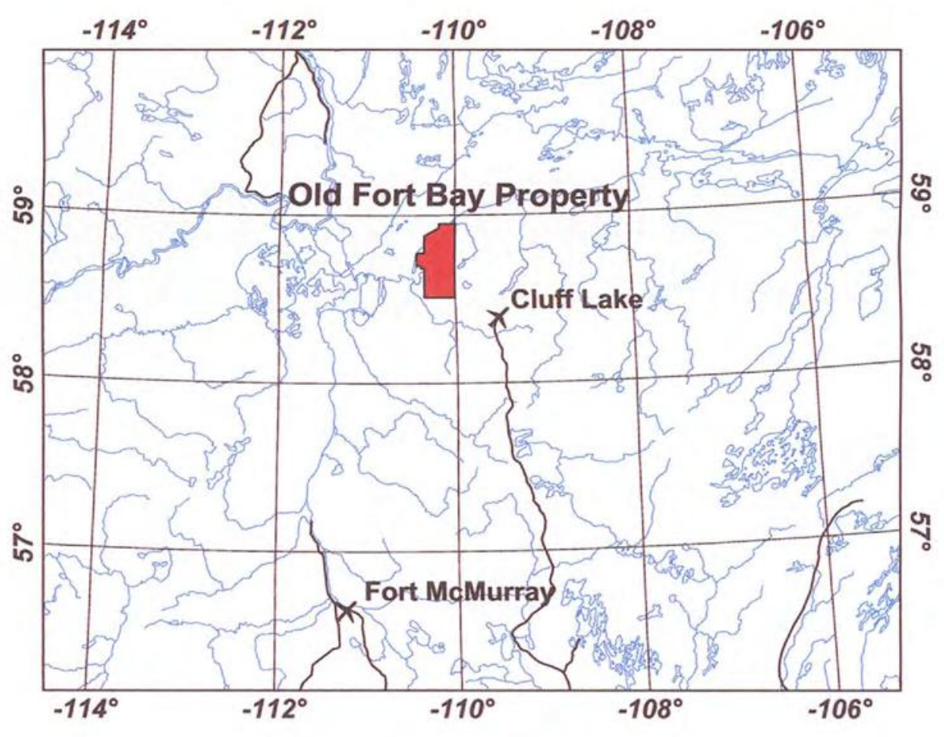

Survey Specifications

Line Spacing	400 m
Line Azimuth	90°-270°
Tie-Line Spacing	2000 m
Tie-Line Azimuth	000°-180°

Aircraft Specifications

Aircraft	DHC-7-102
Aircraft Altitude	120 m Mean Terrain Clearance
Average Aircraft Speed	70 m/sec
GPS Receiver	NovAtel Propak 4E-3151-R
GPS Sample Rate	1.0 s

Magnetic Specifications

Magnetometer	Scintrex CS-2 Cesium Vapour
Magnetometer Installation	Towed Bird
Magnetometer Sensitivity	0.1 nT
Sample Rate	0.10 s
I.G.R.F. Model	2003
I.G.R.F. Correction Date	2004.95

Electromagnetic Specifications

Electromagnetic System	MEGATEM® 20 Channel Multicoil System
Transmitter Installation	Vertical Axis Loop Mounted on Aircraft
Transmitter Loop Area	406 m²
Transmitter Loop Turns	6
Transmitter Base Frequency	90 Hz
Pulse Width	2287 µs
Off-time Period	3169 µs
Receiver Installation	Towed Bird
Receiver Coils	Multiple Coils in X, Y, Z Orientation
Receiver Sample Rate	0.25 s
Digital Acquisition	Fugro Airborne Surveys Geodas System
Analogue Acquisition	RMS GR-33 Chart Recorder
Video Acquisition	Colour VHS Video

Geodetic Specifications

Map Projection	UTM
Datum	NAD83
UTM Zone	12 North
Central Meridian	111° West
False Easting	500000 m
False Northing	0 m
Scale Factor	0.9996

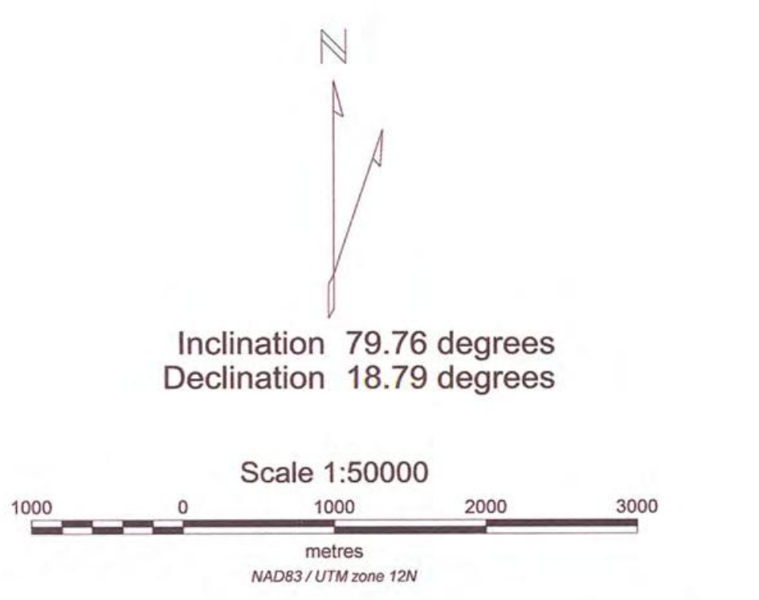

Inclination 79.76 degrees
Declination 18.79 degrees

Scale 1:50000

Fugro Project 04430
Map Creation 25.01.05

FUGRO AIRBORNE SURVEYS

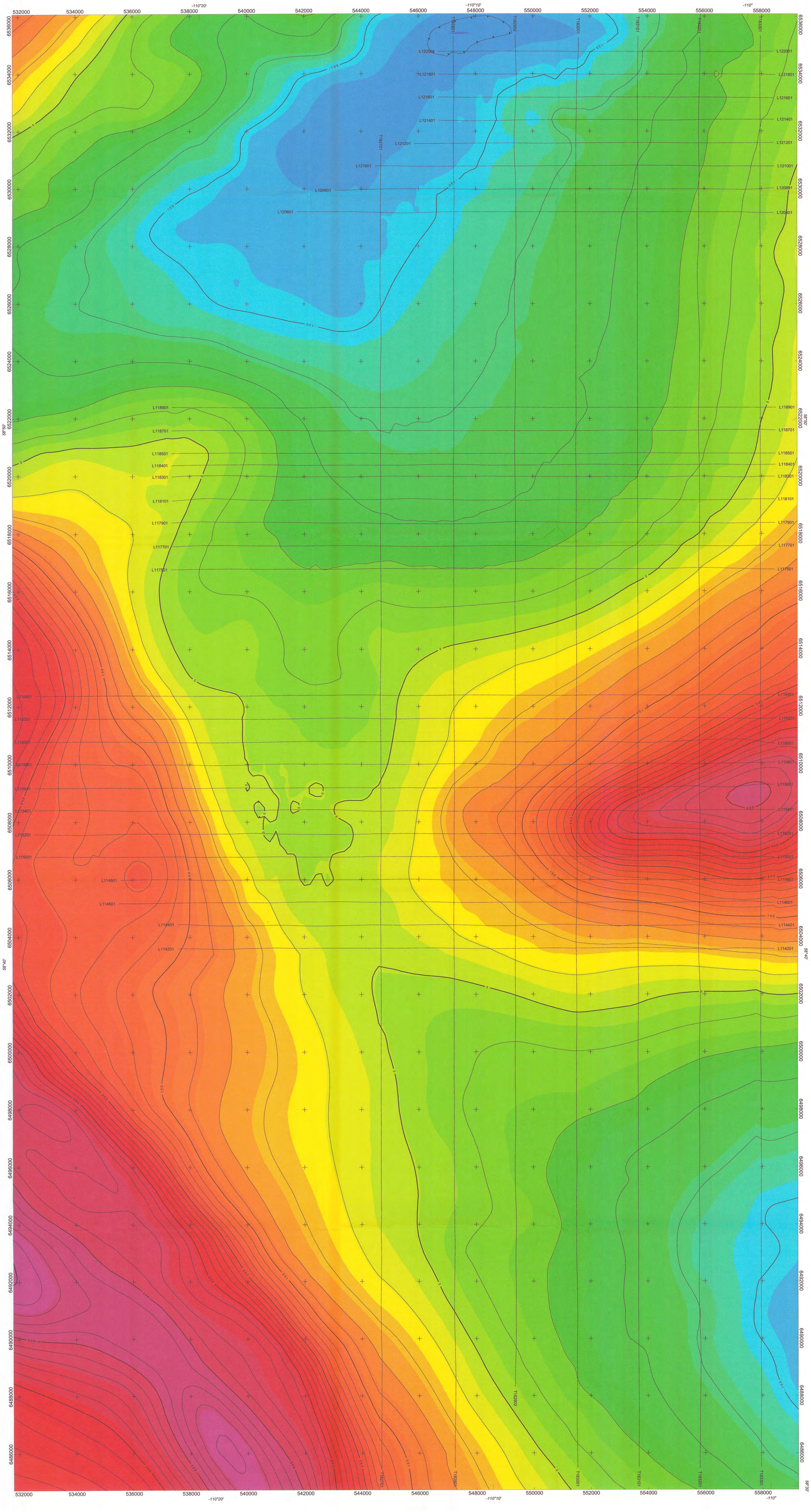

Triex Minerals Corporation

Old Fort Bay Project

Alberta

MEGATEM® Survey

Residual Magnetic Intensity

(stitched with 200m GDR Magnetics)

Flown: July 2005
Processed: April 2006

APPENDIX 5

Condor Consulting Inc.
Lakewood, Colorado

20070005

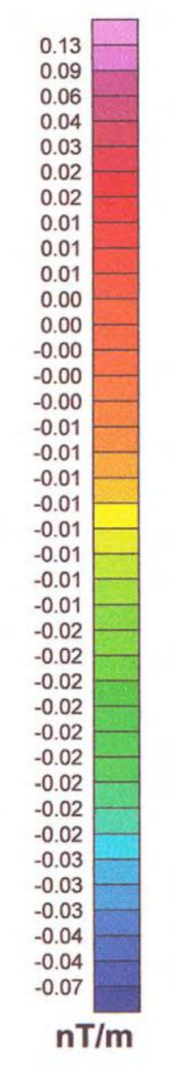

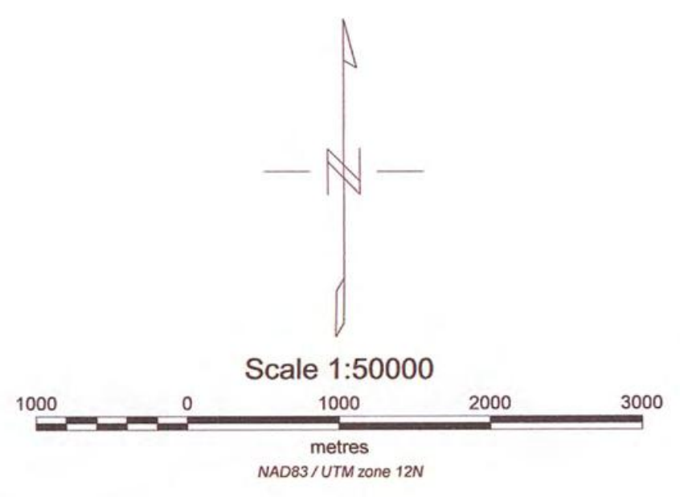

Triex Minerals Corporation

Old Fort Bay Project

Alberta

MEGATEM® Survey

1st Vertical Magnetic Derivative

(stitched with 200m GDR Magnetics)

Flown: July 2005
Processed: April 2006

Condor Consulting Inc.
Lakewood, Colorado

20070005

Triex Minerals Corporation

Old Fort Bay Project
Alberta

MEGATEM® Survey

EM B-field Z Channel 8

Flown: July 2005
Processed: April 2006

Condor Consulting Inc.
Lakewood, Colorado

20070005

Triex Minerals Corporation

Old Fort Bay Project

Alberta

MEGATEM® Survey

AdTau Bfield Z

using 1000 fT cutoff

Flown: July 2005
Processed: April 2006

Condor Consulting Inc.
Lakewood, Colorado

20070005

Triex Minerals Corporation

Old Fort Bay Project
Alberta

MEGATEM® Survey

Digital Terrain Model

Flown: July 2005
Processed: April 2006

Condor Consulting Inc.
Lakewood, Colorado

20070005

20070005

TRIEX
MINERALS CORPORATION

Airborne MEGATEM® Survey
For
Triex Minerals Corp.
and
Roughrider Uranium Corp.

Old Fort Bay Property
Fort McMurray, Alberta

Stacked Fugro Conductivity Depth Transforms

(Fugro map modified by Interpretex Resources Ltd.
for Triex Minerals Corporation)

APPENDIX 7

0.121
0.090
0.070
0.054
0.039
0.029
0.022
0.018
0.014
0.012
0.010
0.008
0.007
0.006
0.005
0.004
0.003
0.002
0.002
0.001
0.001
0.001
0.001
0.000
0.000
-0.127

Fugro Conductivity Depth Transforms
Siemens/meter

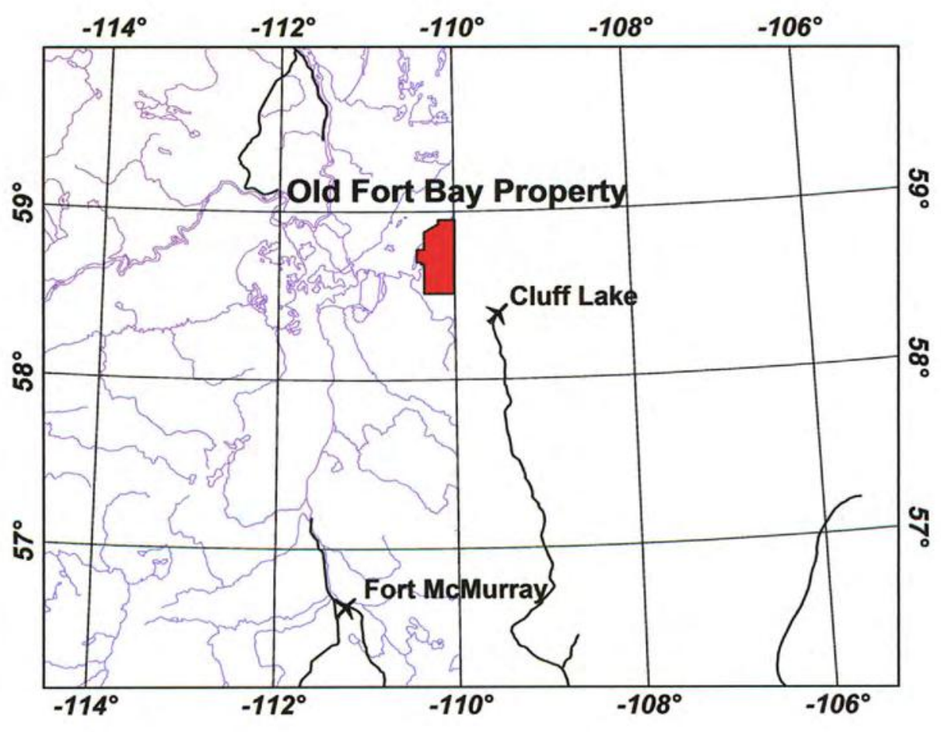

LEGEND

FC-002	AGS DDH ID } Previous Drill Hole Locations
⊕	DDH Locations
A ○	Interpreted Zones of Interest
∼∼	Interpreted Deep Structure
∼∼∼	Linear Abrupt Conductivity Changes (EM Faults) Interpreted from Stacked Conductivity Depth Transforms
∼∼∼	Structure Interpreted from Derivative Maps

Survey Specifications

Line Spacing	400 m
Line Azimuth	90°-270°
Tie-Line Spacing	2000 m
Tie-Line Azimuth	000°-180°

Aircraft Specifications

Aircraft	DHC-7-102
Aircraft Altitude	120 m Mean Terrain Clearance
Average Aircraft Speed	70 m/sec
GPS Receiver	NovAtel Propak 4E-3151-R
GPS Sample Rate	1.0 s

Magnetic Specifications

Magnetometer	Scintrex CS-2 Cesium Vapour
Magnetometer Installation	Towed Bird
Magnetometer Sensitivity	0.1 nT
Sample Rate	0.10 s
I.G.R.F. Model	2003
I.G.R.F. Correction Date	2004.95

Electromagnetic Specifications

Electromagnetic System	MEGATEM® 20 Channel Multicoil System
Transmitter Installation	Vertical Axis Loop Mounted on Aircraft
Transmitter Loop Area	406 m²
Transmitter Loop Turns	6
Transmitter Base Frequency	90 Hz
Pulse Width	2287 µs
Off-time Period	3169 µs
Receiver Installation	Towed Bird
Receiver Coils	Multiple Coils in X, Y, Z Orientation
Receiver Sample Rate	0.25 s
Digital Acquisition	Fugro Airborne Surveys Geodas System
Analogue Acquisition	RMS GR-33 Chart Recorder
Video Acquisition	Colour VHS Video

Geodetic Specifications

Map Projection	UTM
Datum	NAD83
UTM Zone	12 North
Central Meridian	111° West
False Easting	500000 m
False Northing	0 m
Scale Factor	0.9996

N

Inclination 79.76 degrees
Declination 18.79 degrees

Scale 1:50000
1000 0 1000 2000 3000
metres
NAD83 / UTM zone 12N

Fugro Project 04430
Map Creation 25.01.05

FUGRO AIRBORNE SURVEYS

Triex Minerals Corp. & Roughrider Uranium Corp.

Old Fort Bay Project

Northern Alberta
NTS: 74L / 9 & 16

Residual Magnetic Intensity Contours & Interpretation

Fugro "MEGATEM" Airborne TDEM & Magnetic Survey 04422
Line Spacing 400 m., Height - Mag 73 m., EM-RX - 70 m., EM-TX - 120 m.
File Name: OFBfinalMAG_RMF.map, Date: 20/March/2007

Interpretex Resources Ltd.

20070005

20070005

TRIEX MINERALS CORPORATION

Airborne MEGATEM® Survey
For
Triex Minerals Corp.
and
Roughrider Uranium Corp.

Old Fort Bay Property
Fort McMurray, Alberta

First Vertical Derivative
of Residual Magnetic Intensity
Contour Interval 0.002 nanoTeslas/metre

(Fugro map modified by Interpretex Resources Ltd.
for Triex Minerals Corporation)

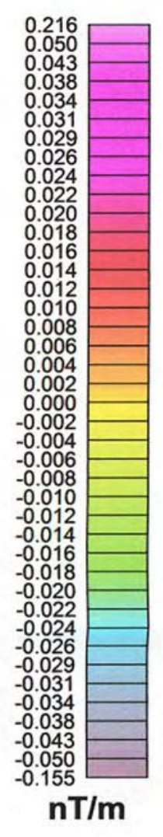

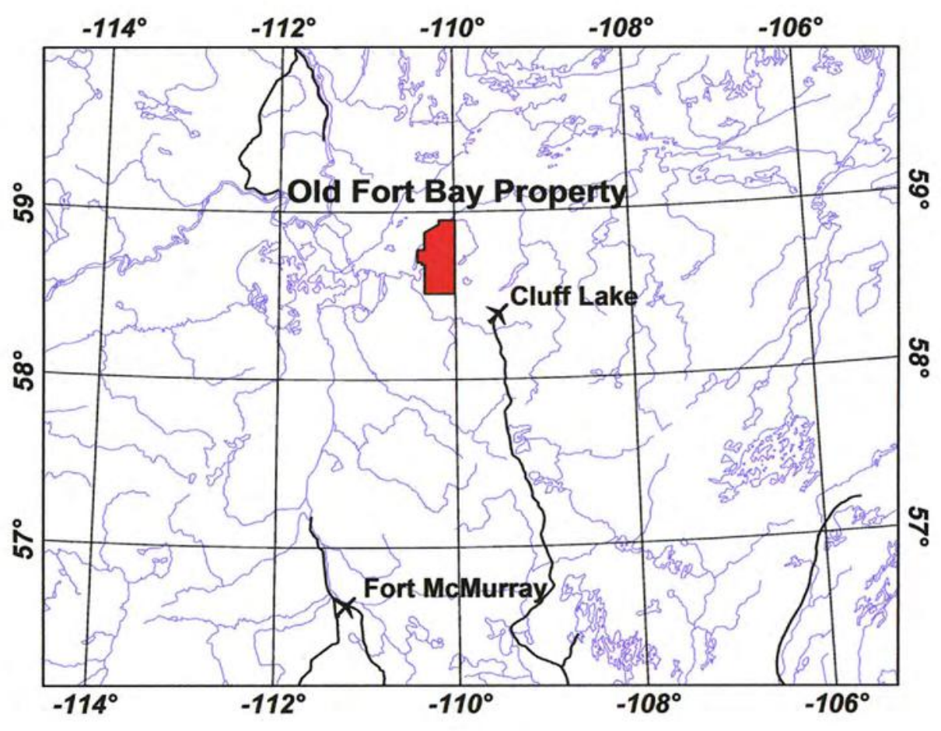

LEGEND

FC-002	AGS DDH ID } Previous Drill Hole Locations
●	DDH Locations
A ◯	Interpreted Zones of Interest
〰	Interpreted Deep Structure
〰	Linear Abrupt Conductivity Changes (EM Faults) Interpreted from Stacked Conductivity Depth Transforms
〰	Structure Interpreted from Derivative Maps

Survey Specifications

Line Spacing	400 m
Line Azimuth	90°-270°
Tie-Line Spacing	2000 m
Tie-Line Azimuth	000°-180°

Aircraft Specifications

Aircraft	DHC-7-102
Aircraft Altitude	120 m Mean Terrain Clearance
Average Aircraft Speed	70 m/sec
GPS Receiver	NovAtel Propak 4E-3151-R
GPS Sample Rate	1.0 s

Magnetic Specifications

Magnetometer	Scintrex CS-2 Cesium Vapour
Magnetometer Installation	Towed Bird
Magnetometer Sensitivity	0.1 nT
Sample Rate	0.10 s
I.G.R.F. Model	2003
I.G.R.F. Correction Date	2004.95

Electromagnetic Specifications

Electromagnetic System	MEGATEM® 20 Channel Multicoil System
Transmitter Installation	Vertical Axis Loop Mounted on Aircraft
Transmitter Loop Area	406 m²
Transmitter Loop Turns	6
Transmitter Base Frequency	90 Hz
Pulse Width	2287 µs
Off-time Period	3169 µs
Receiver Installation	Towed Bird
Receiver Coils	Multiple Coils in X, Y, Z Orientation
Receiver Sample Rate	0.25 s
Digital Acquisition	Fugro Airborne Surveys Geodas System
Analogue Acquisition	RMS GR-33 Chart Recorder
Video Acquisition	Colour VHS Video

Geodetic Specifications

Map Projection	UTM
Datum	NAD83
UTM Zone	12 North
Central Meridian	111° West
False Easting	500000 m
False Northing	0 m
Scale Factor	0.9996

Inclination 79.76 degrees
Declination 18.79 degrees

Scale 1:50000
1000 0 1000 2000 3000
metres
NAD83 / UTM zone 12N

FUGRO AIRBORNE SURVEYS

Fugro Project 04430
Map Creation 25.01.05

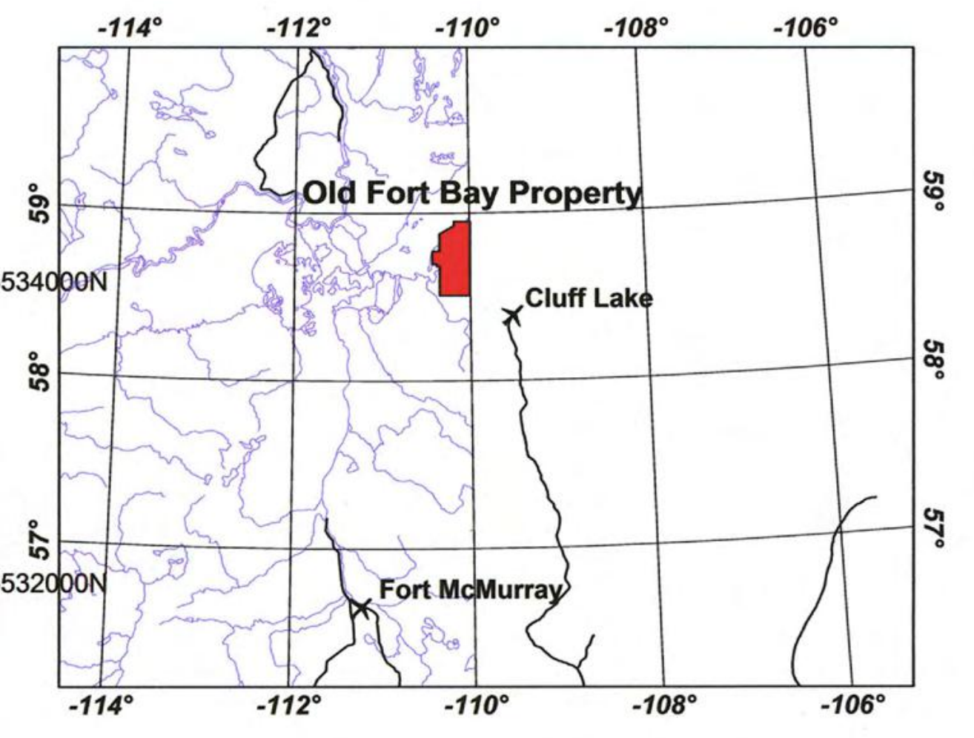

Index Map

1.274
1.124
0.989
0.859
0.733
0.608
0.484
0.361
0.239
0.120
0.005
-0.109
-0.220
-0.322
-0.418
-0.509
-0.599
-0.683
-0.763
-0.839
-0.912
-0.982
-1.048
-1.118
-1.185
-1.259
-1.340
-1.445

Tilt Derivative of Residual Magnetic Field
nT

LEGEND

FC-002	AGS DDH ID } Previous Drill Hole Locations
●	DDH Locations
A ○	Interpreted Zones of Interest
∼ ∼	Interpreted Deep Structure
∼ ∼ ∼	Linear Abrupt Conductivity Changes (EM Faults) Interpreted from Stacked Conductivity Depth Transforms
∼ ∼ ∼	Structure Interpreted from Derivative Maps

Scale 1:50000
1000 0 1000 2000 3000
metres
NAD83 / UTM zone 12N

Triex Minerals Corp. & Roughrider Uranium Corp.

Old Fort Bay Project
Northern Alberta
NTS: 74L / 9 & 16

Tilt Derivative of RMI & Interpretation
Fugro "MEGATEM" Airborne TDEM & Magnetic Survey 04422
Line Spacing 400 m., Height - Mag 73 m., EM-RX - 70 m., EM-TX - 120 m.
File Name: OFBfinalMAG_RMF_TiltDeriv.map, Date: 20/March/2007

Interpretex Resources Ltd.

20070005

20070005

Fugro Project 04430
Map Creation 25.01.05

TRIEX
MINERALS CORPORATION

Airborne MEGATEM® Survey
For
Triex Minerals Corp.
and
Roughrider Uranium Corp.
Old Fort Bay Property
Fort McMurray, Alberta

Flight Path, Permits and Interpretation Map

(Fugro map modified by Interpretex Resources Ltd. for Triex Minerals Corporation)

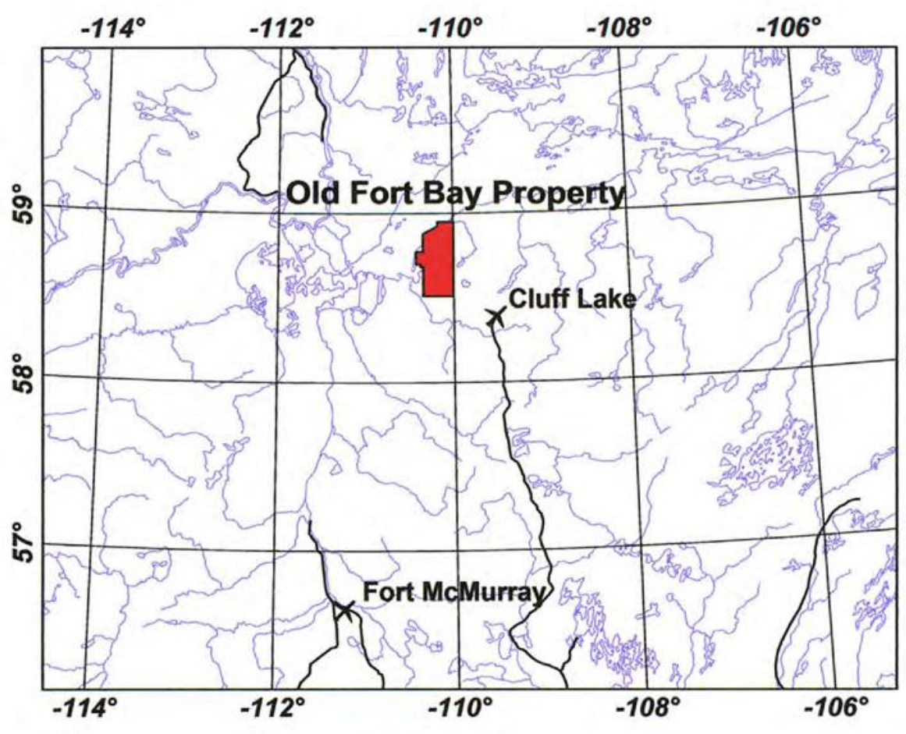

LEGEND

FC-002 AGS DDH ID
} Previous Drill Hole Locations
DDH Locations

A Interpreted Zones of Interest

Interpreted Deep Structure

Linear Abrupt Conductivity Changes (EM Faults) Interpreted from Stacked Conductivity Depth Transforms

Structure Interpreted from Derivative Maps

Permit Bounday

9305010849 Permit Number

Survey Specifications

Line Spacing	400 m
Line Azimuth	90°-270°
Tie-Line Spacing	2000 m
Tie-Line Azimuth	000°-180°

Aircraft Specifications

Aircraft	DHC-7-102
Aircraft Altitude	120 m Mean Terrain Clearance
Average Aircraft Speed	70 m/sec
GPS Receiver	NovAtel Propak 4E-3151-R
GPS Sample Rate	1.0 s

Magnetic Specifications

Magnetometer	Scintrex CS-2 Cesium Vapour
Magnetometer Installation	Towed Bird
Magnetometer Sensitivity	0.1 nT
Sample Rate	0.10 s
I.G.R.F. Model	2003
I.G.R.F. Correction Date	2004.95

Electromagnetic Specifications

Electromagnetic System	MEGATEM® 20 Channel Multicoil System
Transmitter Installation	Vertical Axis Loop Mounted on Aircraft
Transmitter Loop Area	406 m²
Transmitter Loop Turns	6
Transmitter Base Frequency	90 Hz
Pulse Width	2287 µs
Off-time Period	3169 µs
Receiver Installation	Towed Bird
Receiver Coils	Multiple Coils in X, Y, Z Orientation
Receiver Sample Rate	0.25 s
Digital Acquisition	Fugro Airborne Surveys Geodas System
Analogue Acquisition	RMS GR-33 Chart Recorder
Video Acquisition	Colour VHS Video

Geodetic Specifications

Map Projection	UTM
Datum	NAD83
UTM Zone	12 North
Central Meridian	111° West
False Easting	500000 m
False Northing	0 m
Scale Factor	0.9996

Inclination 79.76 degrees
Declination 18.79 degrees

Scale 1:50000
1000 0 1000 2000 3000
metres
NAD83 / UTM zone 12N

FUGRO AIRBORNE SURVEYS